Master Thesis

TVVR21/5007

Modeling wind-induced currents in lake Bolmen, Sweden, using TELEMAC 2D

Prasanjaya Ekanayake

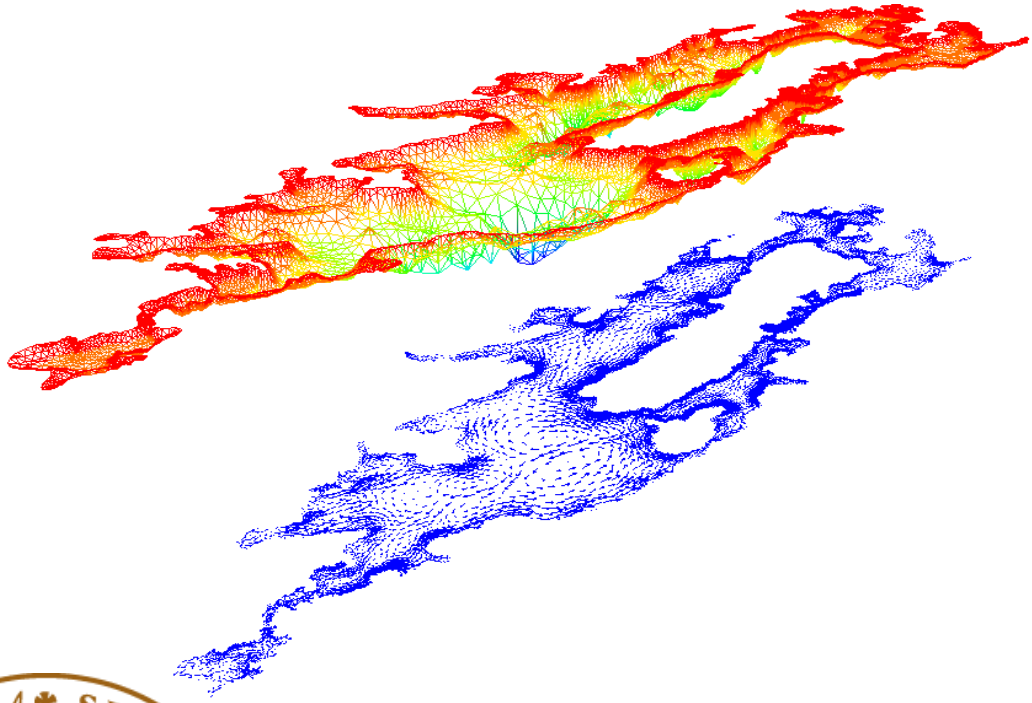

Division of Water Resources Engineering
Department of Building and Environmental Technology
Lund University

Modeling wind-Induced currents in lake Bolmen, Sweden, using TELEMAC 2D

By : Prasanjaya Ekanayake

Master Thesis

Division of Water Resources Engineering
Department of Building and Environmental Technology
Lund University
Box 118
221 00 Lund, Sweden

Water Resources Engineering
TVVR21/5007
ISSN 1101-9824
Lund 2021
www.tvrllth.se

Master Thesis
Division of Water Resources Engineering
Department of Building and Environmental Technology
Lund University

Title :	Modelling Wind-Induced Currents In Lake Bolmen, Sweden, Using TELEMAC 2D
Author :	Prasanjaya Ekanayake
Supervisor :	Clemens Klante
Asst Supervisor :	Professor Magnus Larson
Examiner :	Dr. Rolf Larsson
Language :	English
Year :	2021
Keywords :	Bolmen , TELEMAC 2D , Wind induced currents , QGIS , Blue Kenue

ACKNOWLEDGEMENT

I wish to thank the supervisor Clemens Klante who was more than generous with his expertise and precious time. A special thanks to Clemens Klante for being my supervisor and dedicating his countless hours of reflecting, reading, encouraging, and most of all patients throughout the entire process.

I would thank the assistant supervisor, Professor Magnus Larsson, for suggesting me the research area and allowing me to work under his guidance. Your expertise was indispensable in formulating the research questions and methodology. Your insightful feedback pushed me to sharpen my thinking and brought my work to a higher level.

Thank you, Dr. Rolf Larsson, for accepting to be the examiner for my Master thesis work. I would like to acknowledge and thank the administration of Lund University for enabling me to conduct my study and for offering any support that was needed.

My heartfelt gratitude goes to the SI Institute for providing me with a scholarship to study and complete my thesis at Lund University in Sweden.

POPULAR SUMMARY

Lake Bolmen serves as the primary source of water for the majority of Skåne's areas. Understanding how this water source is influenced by changes in climate, weather, and land use is becoming more crucial in ensuring that Lake Bolmen remains a stable water supply in the future. Lately, Bolmen has been noticed with watercolor shifting (brownification). Hence, numerous researches have been performed on biological, chemical, and environmental aspects. However, no reported information was found on wind-induced water currents and how they affect mixing and material transportation in Lake Bolmen. As a result, this study was undertaken in order to study various configurations of wind effect on lake currents and to further explore the mixing phenomenon caused by wind-driven currents. To accomplish this task, a two-dimensional numerical model of Bolmen Lake was created using the TELEMAC-MASCARET computer software system. Several simulations were run by changing the magnitude and direction of the wind in the specified two-dimensional settings. Identifying any unique characteristics of wind-induced currents and observations will be examined. Ultimately, the goal of this research is to better understand the relationship involving wind-induced currents and hydrodynamic behavior in Lake Bolmen.

ABSTRACT

Transport and material intermixing within lake systems have a significant impact on lake water quality. However, since researchers are primarily concerned with biological, environmental, and ecological aspects, physics and hydrodynamic behavior in lake water currents frequently receive less attention.

The results of several wind-induced current circulation scenarios in Lake Bolmen with its complicated bathymetry are presented. The significance of various physical parameters influencing the circulation pattern owing to wind force acting on the lake, as well as the prediction of how physical changes can modify the circulation pattern, were explored. Herein a two-dimensional mathematical model for Bolmen Lake in Sweden was analyzed by TELEMAC-MASCARET Software. QGIS and Blue Kenue software were used to processing and visualize the data and results. Simulation conducted for steady winds, stratified water condition, and actual wind data. Wind intensity and direction affect the lake's ultimate hydrodynamic circulation. In steady-state simulations, stable circulation vector graphs displaying water current movements were achieved after two days. The tracer was included in a lake model to assess the effects of instantaneous solute transmission via advection and diffusion processes. Tracer time-series graphs and velocity maps were also employed to understand the mixing process within the lake.

Vorticity patterns of the velocity field and the tracer analysis were the key indicators used to identify the hydrodynamic circulation governed by wind force. Vorticity patterns and magnitude of velocity fields change within the lake area and were distinguished with the changing wind direction and magnitude. In each simulation clear patterns observed distinguishable from the rest of the simulations carried out. Also, noticeable tracer detection times were observed in each simulation. Stratification seems to have minimal impact on water currents and their characteristics. The study can be further improved by accommodating three-dimensional modeling, water inflow and outflow to the lake, and calibrating with water level data.

Keywords: Bolmen Lake, TELEMAC 2D , Wind induced currents ,QGIS ,Blue Kenue

CONTENTS

LIST OF TABLES

LIST OF FIGURES

LIST OF ABBREVIATIONS AND ACRONYMS

ζ	Surface shear stress
SBL	Surface Boundary Layer
N	North ,
Nm^{-2}	Newton per Square meter
g	Gravity
HS	Humic Substances
TOC	Total Organic Carbon
Cd -	The Drag coefficient
ρ_{air}	Density of Air
ρ	Density of Water
U_{10}	Wind velocity at 10 m above the sea level

LIST OF APPENDICES

1 INTRODUCTION

1.1 Background

Many Lakes and rivers have become more susceptible to water color changes in recent years, which have also become disadvantages for water treatment, recreational activities increased presences of algae and cyanobacteria, loss of ecosystem services etc. Dissolved organic matter and iron, which leach from the soil and are introduced into waterways may cause a rise in color. However, the occurrence of the brownification and its relationships to local ecosystems are not fully researched and analyzed. This 'brownification' process is associated with an increase in yellow-brown color of lake and stream water that strongly absorbs solar radiation in the short wavelength part of the visible spectrum (Graneli, 2012).

Although the mechanism of brownification is not well known, it is widely assumed that water and materials from the catchment area are subjected to a variety of processes such as sedimentation, resuspension, chemical reactions, biological interactions, and so on. Water circulation, turbulence within the water body, diffusion, and dispersion levels all contribute to differing mixing characteristics in the water body. As a result, researching hydrodynamics, transport, and mixing characteristics of water sources may provides a greater understanding of the spatial and temporal differences in water color (Liu, 2018)

The study focuses on Lake Bolmen, which is located in the municipalities of Gislaved, Hylte, Ljungby, and Värnamo in the Swedish province of Småland. Water browning has had a major impact on Lake Bolmen, which has seen a significant rise in color over the last few decades (Borgström, 2020). As a result, this research focuses on defining the hydrodynamic characteristics of the lake Bolmen that are influenced by wind. The research ideology is to simulate wind-induced water currents in order to see how they generate water currents and influence water mixing, which may have an impact on water color changing leading to brownification. Since Lake Bolmen is one of the key drinking water sources for this region, understanding the brownification will help to improve the drinking water production. Effective purification mechanisms or brownification mitigation techniques can be adopted in order to reduce the production

of drinking water cost. Eventually which support to provide Drinking water for nearly 600,000 people in the southern-most part of Sweden.

Water color changes or the brownification effect has studied in the lake Bolmen against various parameters. Such as Secchi depth, pH, alkalinity, color, turbidity and TOC (Borgström, 2020).However none of these parameters provide direct relationship with Lake Hydrodynamic behaviors. The ability of a lake's stream and diffusion system to maintain its water quality is determined by the lake's stream capacity and diffusion system. According to Bengtsson (1978), water motions in a lake are caused by wind, which then transfers its energy to the lake. Lake morphometric, shore configuration, backside conditions, wind expositions, general climatic circumstances, relative location of inlet and outlet, rotation of the earth density stratification, and other factors all influence water flow in the Lake.

As per the Bengtsson(1978) wind causes the major influence in Hydrodynamic behavior in the Lake systems. Accurate forecasts of wind-induced currents are critical for a variety of research and operational applications because they can regulate the transport of sediments and pollutants. Since measurements of such currents are usually missing, computational models can assist in achieving the above goals and have become important resources for scientists and engineers. In this study the numerical model in two dimensions has been constructed to observe the currents generated due to the wind effects.

The best technique to investigate the wind impacts on Bolmen Lake is to conduct in-situ measurements of water currents against the winds. However, this procedure may result in time-consuming and arduous work. With the study's allocated time and resources, this is not a realistic option. Furthermore, unique wind effects cannot be reproduced in reality again and over again for testing purposes. However, no such experimental data were found to be released. To see the impacts of wind on water currents, the best method is to create a numerical model and simulate it using computer software. TELEMAC 2D soft wear and Blue Kenue were employed in this study to achieve this goal.

1.2 Objectives

The primary aim of this study is to investigate the water circulation in Lake Bolmen due to wind-induced currents and these currents' effects on transport and mixing of materials in the lake.

Detailed outlined of the objectives identified:

I. Construct a two dimensional geometrical model with the assistance of computer soft wears Blue Kenue and QGIS.

II. Using TELEMAC 2D to simulate a 2D model for the selected wind configurations and acquire the results.

III. Determine the effect of generated currents on material mixing and the hydrodynamic behavior of the lake.

1.3 Procedure

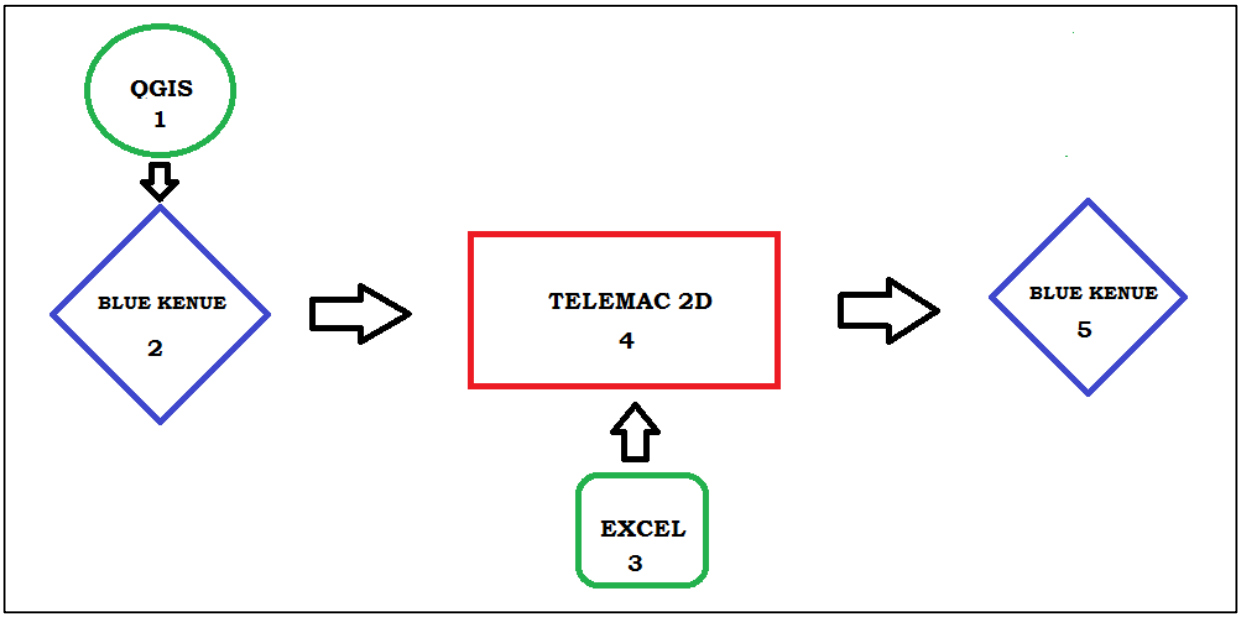

Figure 1-1 Schematic diagram of data processing tools involved

Overview of each tools and steps mention in the Figure 1.1 can be summarized as below

1. QGIS- Preparation of Bathymetric raster file from field survey data
2. Blue Kenue – Preparation of 2D model, Define Boundaries, Geometry and Mesh creation
3. EXCEL – Modify wind data received from SMHI to TELEMAC support configuration
4. TELEMAC- Solving the differential equations in the numerical model to get the solutions to the equations
5. Blue Kenue – Visualize the results obtained from the TLEMAC results files.

The procedure followed in this study can be summarized as below, for detailed content reader requested to follow the respective chapters.

Step : 1 Constructing the two-dimension Lake model can be commenced with the help of Blue Kenue and QGIS software. To continue with this task, lake bathymetric data must be collected and modified using QGIS software until it is appropriate for input into the Blue Kenue soft wear for mesh generation. Normally, the lake bottom elevations are transformed to a raster file and sent to the Blue Kenue program following the appropriate QGIS work.

Step : 2 In this stage, the geometric conditions of the Lake need to be defined using the outside boundary of the lake, inside boundaries of islands, and imported bathymetry data. Then the triangular mesh can be generated using the Blue Kenue. The mesh needs to be assigned for respective boundaries conditions (eg: liquid boundary, fixed boundary) before commencing simulating with TELEMAC.

Step : 3 Using the TELEMAC steering file commonly called CAS file, the user can define and assign the parameters such as Frictional coefficient of Bottom, Initial water depth of the lake, Wind directions, Water density, output parameters, etc. Assigning tracer parameters locations, computational time steps, Duration of the simulation are also some of the parameters that needed to be defined.

Step : 4 Having successfully developed geometry files and Boundary condition files using the Blue Kenue and CAS file in TELEMAC the model without errors

can be commenced for the computational stage. The computation will last according to the user-defined input in CAS fie. Until computation is completed results file will not be generated,

Step : 5 The TELEMAC-generated results files can be viewed in Blue Kenue. The output parameters defined in the CAS file in procedure step 3 are contained in the results files. Various characteristics, such as velocity and water depth, can be extracted as time-series analyses or cross-section analyses, depending on the user's needs. Blue Kenue has a variety of supporting tools for analyzing the outputs.

Step : 6 Number of simulation configurations needed to be executed as explained in section 6.3 Simulation using TELEMAC.

Step : 7 Finally, the accumulated observational findings from the TELEMAC simulation required to be processed to obtain more thorough and reasonably logical conclusions. Having accurate results will assist in the formulation of the physics behind material mixing and the lake's hydrodynamic behavior.

2 THEORETICAL BACKGROUND

Lake formation and evolution involve physical, chemical, and biological processes. These factors govern the meteorological constraints surrounding the lakes. Lake geomorphology determines lake inflow, drainage, and nutrient fluxes. Dissolved gases, lake ecosystems, and nutrients ultimately determine the metabolism in freshwater (Hutchinson, 1941), which is mostly determined by the geomorphology of the lake basin. The cross-sectional form of the basin, which is typically U or V-shaped, always has an effect on lake metabolism. (Wetzel, 2001). Finally, the lake basin has a substantial influence on the physical, chemical, and biological processes that occur in the lake. The lake bathymetric map is the simplest approach to display morphological characteristics. Bathymetric maps are often produced using a variety of approaches. Standard survey procedures were used to survey the shorelines. Aerial imaging can be useful in some situations. Finally, a series of depths comprising Lake Bottom elevations are plotted and contours are produced. Nowadays Sonar transects, are being used to collect high-accuracy data. Some of the key terms associated with lake morphometric parameters include maximum length (effective length in two most distant points inshore without land interruption), maximum width (longest distance right-angled to mas length), area, volume, max depth, mean depth, relative depth, and shoreline (intersection of terrain with water level), and so on.

Lake basins in freshwater systems are typically circular to elliptical in form (Wetzel, 2001). A lake's average depth may varies by few meters to many, with the deepest point being located distant from the shoreline. Wind-generated waves acting on lake water damage the shoreline. With this phenomenon, lake water might be low or high turbid. Flushing rates are relatively lengthy and range from one to several years. Inflow to the lakes might be caused by runoff from tributaries or diffusive groundwater sources.

It is widely acknowledged that the water quality level in a lake is determined by the degree of water circulation and the diffusion capacity of the lake. (Starosolszky, 1974) The water transport mechanism in a lake is based on

1. Momentum transferred from the wind
2. Through flow
3. The thermal stratifications caused density differences

The Morphology of the basin, Shore geometry & configuration, Bottom sediment characteristics, Wind exposures, Climate conditions, inflow and outflow of the lake, Coriolis effect due to ti rotations of the earth and their causes, density , and thermal stratification effects all play a role in lake circulation. When it comes to lake water circulation, the wind is the most important factor. According to Starosolszky(1974) Wind-induced lake currents are classified into two types.

1. Wind-induced Direct currents
2. Wind induced Surface oscillations (Standing Waves /Seich currents-When the wind stops suddenly blowing, the water level alterations appear in the form of oscillations known as standing waves, seiches.)

The method for transferring momentum must be accurate to see the water motion-induced due to wind. The wind force that causes the frictional force on water determines the velocity of the water molecules (Bengtsson, 1978). Therefore, the frictional drag must play a significant role in this explanation. Aside from wind speed, the roughness of the lake's water layer and thermal stability have a considerable influence. The molecular characteristics of the wind and water interphase influence how heat or solar radiation is absorbed and the momentum drag caused by wind forces (Bengtsson, 1978). The basic formulation of wind drag is written as Eq 2.1

$$\tau = \rho_{air} C_d (W - U_0)^2 \qquad Eq\ 2.1$$

τ - Wind shear acting on water surface

ρ_{air} - Air Density

C_d - The Drag coefficient between the air and water molecules

W - Wind speed at a given height overs the surface of the water

U_0 - Surface velocity

The drag coefficient, which is controlled by the roughness of the lake water (Attar and Li, 2012). The typical roughness is constantly determined by wind speed, lake shape, and fetch area, as well as wind turbulence. The drag coefficient must be calculated using observable field measurement data. With this approach, if the wind speed is known, the wind stress acting on water may be simply calculated (Bengtsson, Hellström and Rakoczi, 1990). However, because lakes vary in form and might have a larger surface area, the drag coefficient may range between zones within the same lake. Some basin regions may have a smooth water surface, while others may have a rough surface. As a result, there may be noticeable stress change caused by variations in the roughness coefficient.

The ratio of 2 to 4% between surface current speed and wind speed is commonly used by limnological scientists and researchers(Bengtsson, 1978). However, some argue that this percentage might be significantly lower than that. Wind shear directly affects the flow magnitudes rather than the patterns. The high wind velocity causes a lot of turbulence. The wind also creates horizontal eddies and lower-depth horizontal eddies. These gyre patterns vary with the wind intensity. Previous research discovered that horizontal turbulence decreases as one moves from the top to the bottom of the lake. Furthermore, the significance is limited to the coastline areas and only after achieving the steady-state configuration. It has been discovered that the horizontal dispersion of inertia works to smooth out the strong local currents(Bengtsson, 1978).

2.1 **Wind Forces and Lake Currents**

It is undeniable that the sun is the primary source of energy that generates winds in the atmosphere. The heat created by solar radiation warms up and rises the atmosphere (a layer of air composed of different gases closer to the earth's surface). As heated air expands, it creates a low density and low-pressure zone. As a result, the relatively cooler air in the high-pressure zones is flowing towards the low-pressure zones, causing wind. If the ensuing pressure difference is large, the resulting winds will be strong owing to the force provided by the large pressure differential (Parker, 2003). As a result, the wind is formed on the earth's surface.

The air blows across the topography of the earth's surface from higher pressure zone to lower pressure zones. Water particles in the air-water interphase are inclined to flow in the direction of the momentum of the wind. Thus, the wind blowing from a high-pressure zone to a low-pressure zone causes a water current in water bodies on the earth's surface. Moreover, Surface water current patterns are influenced by wind direction, Coriolis forces due to the Earth's rotation, and the morphological features that interact with the currents(Wetzel 2001). Currents may also be induced by temperature (thermal) and salinity (haline) fluctuations in water masses, a process is known as thermohaline circulation (Toggweiler & Key, 2001). However, in this study, the wind-induced currents on lakes are going to be discussed. This should be noted that wind-induced currents in larger oceans and relatively smaller Lakes might have significant differences in their respective hydrodynamics behaviors. Because the forces affecting the motion of fluid movements are varying. Such as inflow and outflow of the lake, and tidal movements in ocean currents.

Currents are non-periodic water motions that tend to flow downstream in a water stream and are caused by external factors (Wetzel 2001). When dealing with the lake context Wind, gradients in air pressures, water density gradients owing to thermal effects, and concentration of dissolved elements are some well-known examples of external forces. Currents have a strong influence on the lake's ecology. They have the ability to erode Lake Bottom deposits. Also have capacity to transport sediments from one position and deposit them in another. If the predominant winds or the strongest winds blow in one direction, currents will continue to carry sediments in that direction.

Wind-generated surface currents are heavily influenced by wave height (Prandle and Matthews, 1990). Water sped up in the uppermost layer will accelerate with the wind until it reaches critical velocity. When it goes over the critical velocity, the velocity decreases. After then, the wind factor takes on a nonlinear value. However, no recorded information on critical wind velocity experimental data was discovered in the Bolmen. According to research, water currents in larger lakes are more likely to exhibit the behavior of Gyrals/Swirls (Witten and Thomas, 1976). However, many of the other influencing factors listed above, such as Coriolis (geostrophic rotations), Standing waves, and so on, can affect these Gyrals.

The frictional drag that causes currents has the potential to generate moving surface waves with oscillatory movements. These progressive waves can cause slight movement in the lakes' deeper areas. If there are short surface waves, they will attempt to travel in smaller circular orbits perpendicular to the lake water surface. These are, however, relatively weak movements with small translation velocities.

Langmuir circulations are another type of wind-induced motion that can cause surface water movement. Langmuir (1938) introduced the phenomena of vertical helical water currents at the upper layers of the water flow in turbulent flow conditions. Convection forces generate long lines due to the Langmuir effects, which are put up parallel to the wind direction see the Figure 2.1 . However, the causes and behavior of the Langumuire circulations are not fully understood (Harris and Lott, 1973). Aside from the aforementioned surface currents, surface progression waves, and Langmuir circulations, there are several more surface layer movements caused by various sources, such as surface seiches, interior seiches, and long surface and internal waves. However, because it is beyond the scope of the study, these will not be elaborated.

.

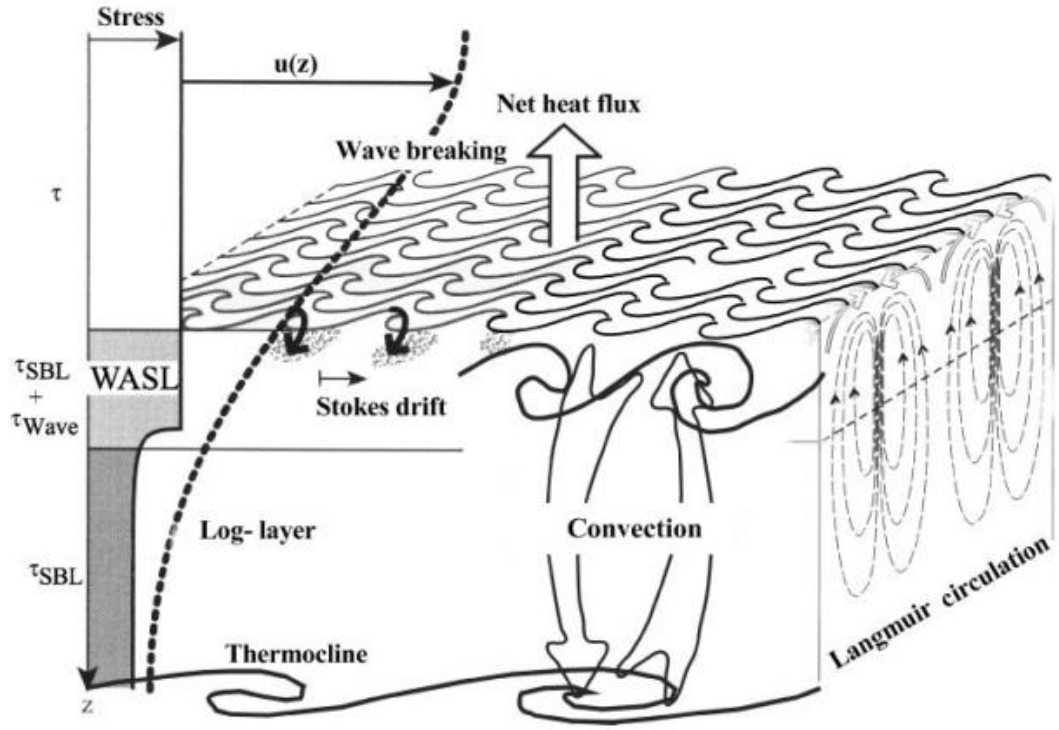

Figure 2-1 Three dimensional cross section view of Water and Atmosphere Interaction in Surface boundary layer (SBL). (Source Wüest, 2003)

The surface shear stress ζ [Nm^{-2}] , the force per unit area acting on the surface as a result of the wind, is the most important parameter determining the wind-driven domain. The downward eddy-transport of horizontal momentum from the atmospheric winds might be understood as the cause of this stress. The idea of "continuous stress" would need the same Reynolds flux ζ_{SBL} , the underlying water, where U,W (u,w) are the horizontal and vertical velocities of air (water) [m s^{-1}], ρ_{air} (p) is the density of air (water) [kg m^{-3}], and (prime) signifies variations. The "constant stress" assumption applies for quite some height in the atmosphere and over a portion of the SBL, it is momentum conservation that is important at the interface (Wüst, 2003).

The momentum flux into the SBL, ζ_{SBL},, is lower than the applied stress from the air due to the existence of waves (Figure 2-1). A portion of is consumed by wave acceleration and maintenance (so-called wave stress), while the remaining momentum flux SBL is driving the SBL water underneath the waves (Anis, 1995). Because

momentum is conserved at the interface, the two momentum fluxes on the water side contribute to the overall wind stress. See Eq 2.2

$$\zeta = \zeta_{SBL} + {}_{WAVE} \qquad \text{Eq 2.2}$$

This concept implies that waves serve as a secondary conduit for the transfer of matter to water. As a result, the wind stress, this is often parameterized by . See Eq 2.3

$$\zeta = \rho\, C_{10}\, U_{10}^{2} \quad (\mathrm{Nm}^{-2}) \qquad \text{Eq 2.3}$$

By using wind drag coefficient C_{10}, the wind speed U_{10} (measured at a standard 10-m height above the surface) is affected not only by the existence and condition of surface waves. The wave field, in fact, is critical for the amount of momentum carried into the water as well as its vertical distribution inside the SBL.

2.2 **Lake Transport Mechanisms**

Advection and diffusion are the fundamental processes associated with material movement inside a fluid mass. It's the water in this study. Advection causes the material to travel in the direction of its mean velocity. If an oil mass spills into a river, advection will move the oil particles to the river's bottom. Diffusion, on the other hand, is a distinct mode of transport from advection. Diffusion creates random oscillatory motions, which reduces abrupt discontinuities in the solute/ tracer substance (Lorrai, Umlauf & Becherer et al., 2011). In a nutshell, advection currents cause the highest concentration point (center) of the tracer material to migrate along the flow direction. Diffusion causing the tracer material to spread all over the space losing its intensity.

The diffusion process is rather intricate and must be addressed in detail. The moving fluid mass contains a variety of random oscillatory movements. In general, diffusion from random spatial molecule motion is referred to as molecular diffusion. However, this sort of diffusion differs from eddy diffusion / turbulent diffusion (Imboden, Lemmin & Joller et al., 1983).

Turbulent diffusion is a mixing phenomenon caused by the movement of mass inside a fluid caused by turbulent flow motion. This turbulent aspect, however, is caused by random movement in a fluid motion, not by the solute. Turbulent diffusion is a considerably quicker process than molecular diffusion, and it exists when the only flow velocity is present and it is above critical limits (Cloutman & Eoll, 1976). The Eddy diffusion coefficient is another name for the turbulent diffusion coefficient. The degree of turbulence is always depending on the substance with which it has come into touch. Assume that a rough surface has more turbulent flow than a smooth surface. Increasing the turbulent motion always increases in rapid mixing (Csanady, 1963).

Diffusion of solute mass within the fluid medium can be explain using Fick's law shown in Eq 2.4

$$F = D \frac{dc}{dx} \qquad \text{Eq 2.4} \quad .$$

F - mass flux of solute per unit area per unit time

D - diffusion coefficient (area/time)

C - solute concentration (mass /volume)

$\frac{dc}{dx}$ - concentration gradient (mass /volume /distance)

For systems where the concentrations may be changing with time Fick's second law of motion may be applicable (Fetter, 2001)

Dispersion

Tracer material advecting at the same rate as the median linear velocity of water. As fluid moves, it will combine with clean water. As a result, the contaminant will be diluted through a process called as dispersion. The blending. Longitudinal dispersion refers to the mixing that happens along the streamline of fluid flow. Lateral or transverse dispersion is fluid flow dispersion that generates a longitudinal route. Mechanical dispersion due to the preceding factors is equal to the product of the average linear velocity and dynamic dispersivity (Fetter, 2001).

The processes of molecular diffusion and mechanical dispersivity cannot be separated in moving water. Instead, a quantity known as the coefficient of hydrodynamic dispersion is generally incorporating both the concerns. It considers mechanical mixing and diffusion. Diffusion ahead of the advecting water may have led some of the non-reactive tracer to reach the outflow before the water that was advecting it. The amount of distilled nonreactive tracer available for dilution gradually reduced until it had received all of the potential tracer ingredients. The concentration then gradually decreases to a minimum, depending on the amount of tracer injected; in this study it is 1000kg.

The tracer moves at the same speed as the average linear ground velocity. Moreover, it is assumed that hydrodynamic dispersion causes the tracer to spread out both ahead of and behind the center of mass in a pattern that follows a statistically normal distribution, which is known as the bell shaped curve Example(see Figure 7-8, 7-9). The normal distribution is also known as the Gaussian distribution. The solute front is travelling at a faster pace than average linear surface velocity would indicate. Mechanical dispersion can be changed over the course of current turbulence. For example, the surface layer with higher velocity profiles and gradients has high coverage conductivity. The longer the distance measured for dispersivity, the bigger the value observed. This is known as the scalar effect.

2.3 **Mixing Mechanisms in Lakes**

The energy necessary for turbulent mixing in the surface layer is caused by the shear-induced by the wind, buoyancy, and inflow in the river (Peeters, Wüest & Piepke et al., 1996). The mixing in the top layer is primarily caused by wind-induced stress. The density layers discussed in section 2.4 are a result of buoyancy flux caused by water cooling at the top layer, which eventually leads to convection. Turbulence in the lake inlet is a separate phenomenon that is not covered in this section. Furthermore, the turbulent lake inflow is inapplicable because the model used in the study omitted river inflows and outflows to be confined to investigate wind impacts. Therefore in this section some background information related to wind induced turbulence and convective turbulence are elaborated (Wüest et al.1994) .

$$\tau_0 = \rho_{air}\,\overline{U'_{air}\,W'_{air}} \quad [\mathrm{Nm^{-2}}] \qquad \text{Eq 2.5}$$

The horizontal and vertical airflow vectors are represented by $[\![U']_{air}$ $[\![W']_{air}$, respectively. These are the variables influencing the water column. The stress acting from the air layer to the liquid layer is denoted by τ_0. According to the abovementioned formulation, the constant wind velocity and water depth down the wind are the major

parameters causing wind-generated stress. The well-known logarithmic profile relationship in the air-water interphase may be obtained using this equation Eq 2.6.

$$U_{(h)} = \frac{U_*}{K} \ln \frac{Z}{Z_o} \qquad \text{Eq 2.6}$$

k - 0.41 (von Karman constant)

U - horizontal velocity u on depth

Z - h (positive downward, h =-z)

Therefore this leads to friction velocity defines as $U_{*\,\text{shown}}$ in Eq 2.7

$$U * = \left[\frac{\tau_0}{\rho air}\right]^2 \qquad \text{Eq 2.7}$$

The second law of Fick's is appropriate here, and the rate of kinetic energy production J_r r owing to turbulence is proportional to the verticle gradient of energy flux. As a result, inside the constant stress layer, the Kinetic Energy per unit mass may be expressed as Eq 2.8

$$J_r = \overline{U'_{air}\, W'_{air}} \quad \frac{du}{dh} \qquad \text{Eq 2.8}$$

Many studies in the discipline of oceanic sciences have been conducted on this topic. Dillon et al. (1981), Imberger (1985), discovered that turbulence may be properly estimated in the setting of well mixed layers.

Convective mixing occurs in addition to wind-induced turbulence. This process included the heating and cooling phenomena of water molecules evaporating into the atmosphere (Xing, Davies and Jones, 2012). The sinking of heavier liquid particles from the top surface of the take is thought to be the initiator of this process. When these liquid particles reach an unstable form, they act in the opposite direction and generate rising plumes. Finally, the surface layer is subjected to a continual stirring action. In this configuration, energy dissipation to the environment is scaled by the buoyancy flux

mentioned in the previous section. A relatively lesser number of researches have been made on these aspects of convection mixing. However, Soloviev (1990) discovered that these rising and sinking plumes had a more structured composition. More than the mixing kinds listed, several other types of mixing processes have been uncovered, such as Dypinacal Diffusion and Langmuir circulation. However, because they are beyond the scope of this research, they are not examined in detail here.

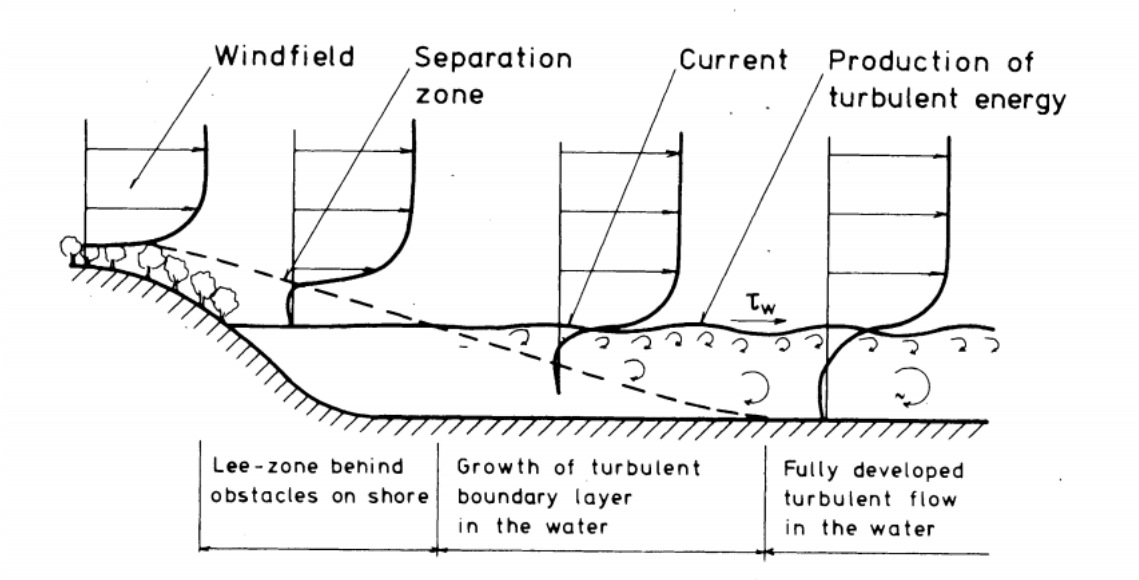

Figure 2:2 Turbulent flow generated due to Wind shear acting on surface of the lake (Source: Hansen 1978)

Turbulence is the primary cause of mixing in lakes. Figure 2.2 can be used to understand the relevance of turbulence. However, this is not a simple phenomenon. There are essentially two methods by which this turbulence might be created. The first is caused by direct wind force, whereas the second is caused by shear induced by currents. The controlling external force causing turbulent energy at the surface level is wind. The created kinetic energy is lost into the surrounding environment, with some being transferred to the lake bottom. Brengtsson (1973) demonstrates that such dissipated energy to the bottom is weak in nature.

The lakes with lesser area show the turbulence effects which are diversely distributed over the lake surface. This is mostly due to the Shelter effects created by the Lake's coastline. Furthermore, as explained in basic fluid mechanics, a portion of the flow will be a boundary layer, reducing entirely formed turbulent flow. In Hydromechanics, fully developed turbulent flow is quite similar to regular channel principles. According to Bye (1965), the lake's surface layer corresponds to the channel bottom in this situation.

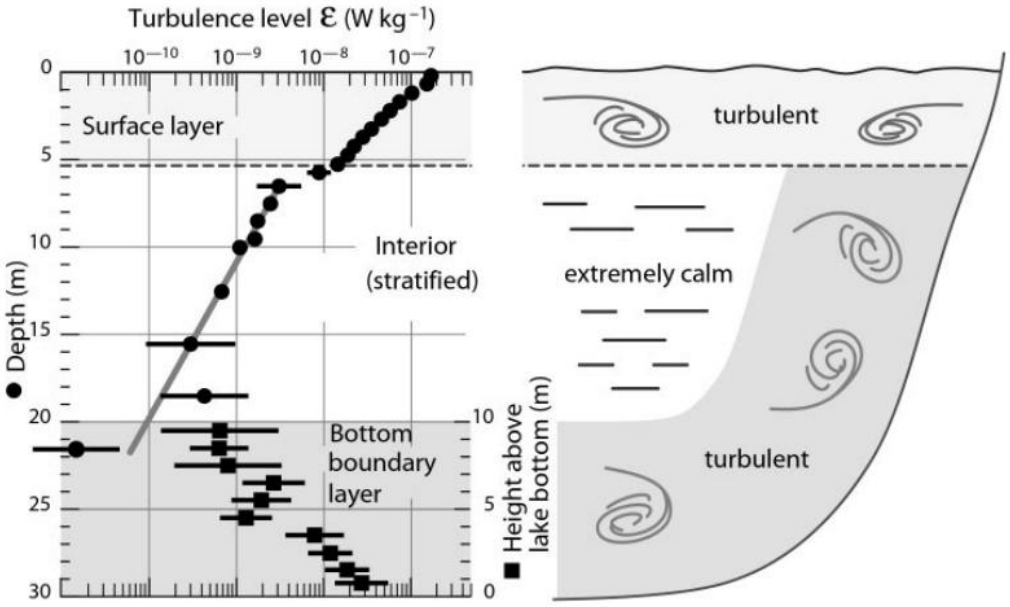

Figure 2:3 Mesuremnts for Turbulance levels along crosss section in a Medium size Lake (Source Wiest et al. (2000b))

Figure 2.3 shows approximate turbulence ranges for the surface layer, middle layer, and bottom boundary layer for a medium-sized lake. Turbulence levels at boundary layers on top of Figure 2.3 are significantly higher in the profile, with the surface boundary layer being the most turbulent (SBL). Then there's the bottom boundary zone, which is generally less turbulent than the SBL. Finally, we've arrived at the middle zone. The zone may experience a strongly stratified and laminar in flow nature.

2.3.1 Boundary mixing

Boundary mixing is critical because it occurs during the interphase of sediment and water (Hansen, 1978). Along the border region, there exist chemical components and diverse chemicals. The fluxes of these components govern the border mixing phenomena. Internal and surface waves, input rivers, turbidity currents, and other energy sources regulate mixing at the border. The fundamental distinction between the water atmosphere inter-phase and the boundary is that in this zone, currents have no velocity, and fluid and sediment particles are in touch with each other. As a result, the shear between boundary layers is generated by the current at the sediment surface. The boundary layer is regarded to be the zone where currents can impact the sediment layer.

The velocity structure of the bottom boundary is referred to as the viscous layer, and it has a considerable influence on the viscosity of the water molecules (Caldwell and Chriss 1979). In the viscous layer, turbulent eddies are minimal. They are most likely to act in a laminar fashion. However, turbulent eddies are common above the viscous layer. It is worth noting that the force causing the mixing in the bottom boundary is friction. This has been discovered that a significant amount of energy is transferred to the water molecules inside the area of viscous flow. These energy dissipations, however, are molecule level and these dissipations are discovered via viscous stress.

The Molecular-level interaction occurs in the context of the boundary layer in the heat and solute flow. This is mostly due to viscosity being greater than molecular diffusion. The region where pure molecular transport occurs is referred to as the diffusive sublayer. This layer is much thinner than the viscous sublayer. The dissipation of heat at the molecular level, resulting in a thermal diffusive sublayer. This layer is lying in between the viscous and diffusive sublayers.

Recent evidence showed that bottom boundary mixing has an impact on the entire lake. The radioactive isotope of Rn -222 with a half-life of 3.8 was used in the observations

and studies on this boundary mixing. Chung and Kim(1980) Imboiden and Joller (1984) discovered that mixing near the lake's edge is much higher than in the center of the water body. This discovery was later supported by several studies utilizing microstructure measures (Wüest et al.1994).

2.3.2 Time Scales of Mixing

From a holistic standpoint, mixing can happen in a matter of seconds or it might take hundreds of years. This is a phenomenon involving a wide range of external factors. It might be wind gust effects, or it can be mixing caused by seasonal changes (see the section 2.4), thus it is necessary to compare the force involved in the mixing phenomenon simultaneously. For example, Surface waves, turbulent currents, oscillation in stratified water, and Langmuir circulations can endure from seconds to a minute, according to Leibovich (1983).

However, in the case of internal waves, diurnal mixed layers, and turbidity currents, mixing can take hours Lombardo and Gregg (1989), Horsch and Stefan (1988), but mixing owing to storms and topographical waves can take more than 24 hours Imboden et al (1988). Wüest et al. (1988) observe that lake basin-wide interaction owing to horizontal density fluctuations producing seasonal stratification cycles can take months to reveal mixing effects.

Furthermore, certain portions of the lakes remain permanently stratified due to inadequate convective mixing to heat loss, and thermal stratification is significantly higher, such that wind shear cannot break the thermocline. Meromixis is the term used to describe this scenario. The lakes which showing this behavior are taking years for the mixing process.

2.4 Seasonal lake cycles

Lakes have been known to contain multiple strata with varying temperatures. The density of lake water is also affected by its temperature. In general, when the temperature rises, the density of water decreases. It is more difficult to blend two liquids with differing densities. Similarly, when it comes to lakes and climate, spring to summer stratification begins as a result of temperature differences in lake water layers. Lakes can have strata with varying temperatures as a result of solar radiation. When heat absorbs and ice melts, the surface layer of lakes absorbs heat energy considerably faster than previously. However, solar radiation has a low capacity to penetrates deep into the lake's bottom (Wetzel, 1976). As a result, it only penetrated a few meters. As previously said, when water is heated, its density decreases significantly and it prefers to float on top of the lake water mass. As a consequence, this less dense water mass is floating on top of a greater density, colder water mass underneath it. See the Figure 2.4

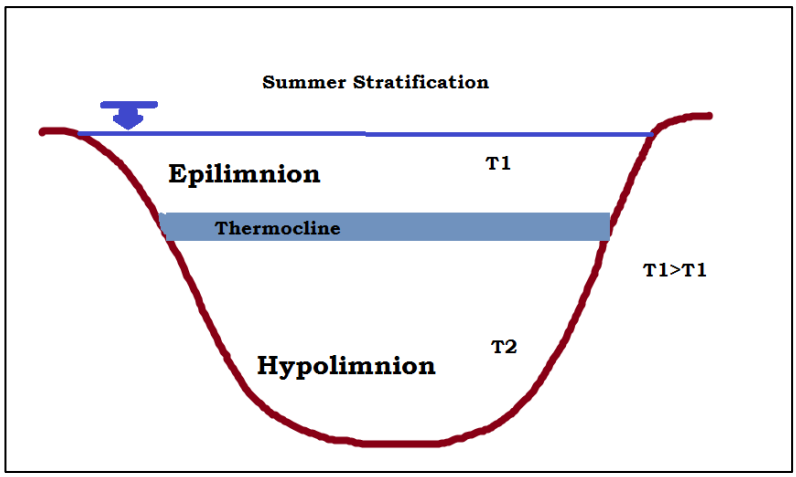

Figure 2:4 Summer Stratification in a Lake

As a result, this lake stratification has a substantial impact since it is one of the processes that regulate the oxygen concentration in the deeper water. Lake stratification often results in three layers, the topmost of which is a warmer water layer known as the epilimnion. The direct interaction of solar radiation and wind forces is known as epilimnion. Because direct aeration is possible in this layer due to wind forces, it generally has the maximum oxygen content. This supports aquatic life in its survival. The hypolimnion is found in deeper zones with lower temperatures and denser water. Generally, this layer contains $4^{o}C$ water throughout the year, hence the hypolimnion does not get much solar radiation (Livingstone, 1977). This area has lower oxygen

concentrations and can sometimes reach zero oxygen values. The midway zone between the Epilimnion and the Hypolimnion is known as the Metalimnion, and it is made up of the. The water in the Metamilion has a transitory temperature until it mixes with the water layer above it, the epilimnion. The greater temperature gap that can lead to separated water layers owing to density is referred to as a thermocline, and it occurs within Metalimnion.

During the summer, the breezes cause the water in the epilimnion to blend with the water underneath it. As a result, hypolimnion water will progressively flow up via the Metalimnion (Wetzel, 1983). The capacity to mix water through wind turbulence is dependent on the temperature stratification's stability. The greater the distance between the Epilimnion and the Hypolimnion, the more stable the stratification.

Eventually, the top surface layer reaches a temperature where the density difference between the hypolimnion and epilimnion is substantially larger, resulting in wind and bigger waves being unable to provide sufficient energy to mix the water. Likewise, when summer transitions into fall, the top water layer cools and sinks. As a result, the epilimnion and hypolimnion achieve similar temperatures, thinning the thermocline. Once this epilimnion and hypolimnion reach similar temperatures, the wind may create water mixing between the layers again. Finally, the entire lake reaches a single temperature known as “**isothermal**.” The occurrence of the entire lake turning to one temperature and mixing completely owing to wind is known as "**turnover**." (Agrawal, 1999).This is not a one way process, This is a having cyclic pattern dependent with the Climate , More comprehensive Figure is shown in the below diagram.

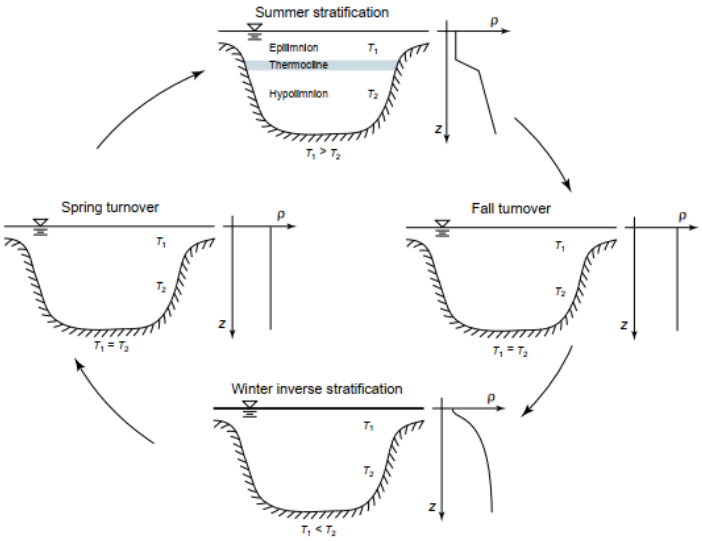

Figure 2:5 Variations in Density in a Dimictic Lake Due to Seasonal Changes (Source: Socolofsky & Jirka, 2004)

A thermally stratified lake has separate layers of water on a density gradient. These layers differ in their characteristics: normally, oxygen is higher in surface waters, nutrients are greater in bottom waters, and plankton is trapped in their respective layer. Chemical stratification is outside the scope of this study and is not discussed here. Project assume temperature stratification in one wind configuration and do the simulation for specific wind direction, not chemical stratification. Density gradients caused by changes in water chemistry (e.g. salinity) can be a key factor influencing stratification in some lakes, but this study focuses on thermal density gradients as a stratification.

Quantitative indicator in mixing in Stratified Lake Condition

Several attempts have been made to discover and measure mixing capacities in a stratified lake setting (Robertson & Imberger, 1994). Schmidt stability criteria and Birgean stability criteria (Schmidt 1915, 1928; Hutchinson 1957) were the first established indices to define these degrees (Birge1916). These indicators attempt to measure and assess the degree of stratification. The Schmidt stability (S_t) given in Eq 2.9 specifies the amount of energy necessary to mix the entire specified region of the lake to uniform density without the use of any heat exchange.

$$S_t = \frac{1}{A_m}\int_0^{Zm} (Z - Z_g) x\, A_z x (1 - Q_Z) x d_z \qquad Eq - 2.9$$

Where: S_t = Schmidt Stability [g cm cm^{-2}]

Z = Height above the bottom [cm]

A_m = Surface area of the lake [cm^2]

Z_g = Maximum depth of the lake [cm]

Z = Center of volume in [cm] above the bottom

A_Z = Area of the lake at height z [cm^2]

Q_Z = Density of the water at depth z [g cm^{-3}]

Lake Number and Mixing

Imberger and Patterson (1990) later added the parameter to quantify deep level mixing and dynamic stability in a lake (Dalem. Roberts, 1994.). According to Roberts, this index offers a realistic evaluation of the dynamic stability of the water column with no dimensions. The lake number is described as the ratio of destabilizing factors such as inflow, outflow, wind, and cooling to the momentum created by the stabilizing force. Density stratification is the stabilizing factor in play here. For further information, see the lake number equation Eq- 2.10.

$$L_n = \frac{g \;\; X \;\; S_t \;\; X \;\; (1 - \frac{Z_t}{Z_m})}{\rho_m \;\; X \;\; U_*^2 X \;\; {A_m}^{1.5} \;\; X \;\; (1 - \frac{Z_t}{Z_m})} \qquad Eq - 2.10$$

G = Acceleration due to gravity (980 cms^{-2})

Z_t = Thermocline height (cm above the bottom),

ρ_m = Density of water at the surface [g cm^{-3}],

u* =Tthe water friction velocity [cms^{-1}]

When the thermocline is moved to the lake's top surface by strong winds, Ln = 1. This is happening in upwind setup. Ln is more than one when stratification is significantly stronger and wind forces are under the domination of stratification (Robertson & Imberger, 1994). Ln value higher than one indicates that mixing under the thermocline has no impact. This configuration isopycnals, horizontal layers will predominate. In this configuration, seiching effects and turbulent mixing in the hypolimnion are possible. When the Ln is less than one stratification, the wind force created is substantially weaker. Strong searching might be predicted in the hypolimnion under these conditions.

3 STUDY AREA AND DATA AVAILABILITY

3.1 General overview of study area

Lake Bolmen is located in south-western Sweden latitude: 56.8373° N; longitude: 13.6738° E (Based on World Geodetic System (WGS) 1984 geographic coordinate system) in three counties: Kronoberg, Jönköping, and Halland (Figure 3-1), and it is Sweden's tenth largest lake, covering an area of 184 km^2 (Romare & Cronberg, 2004). The Bolmen basin covers 1640 km^2 and is the main sub-basin of the River Lagan drainage, which covers 6454 km^2 (Persson, 2011).

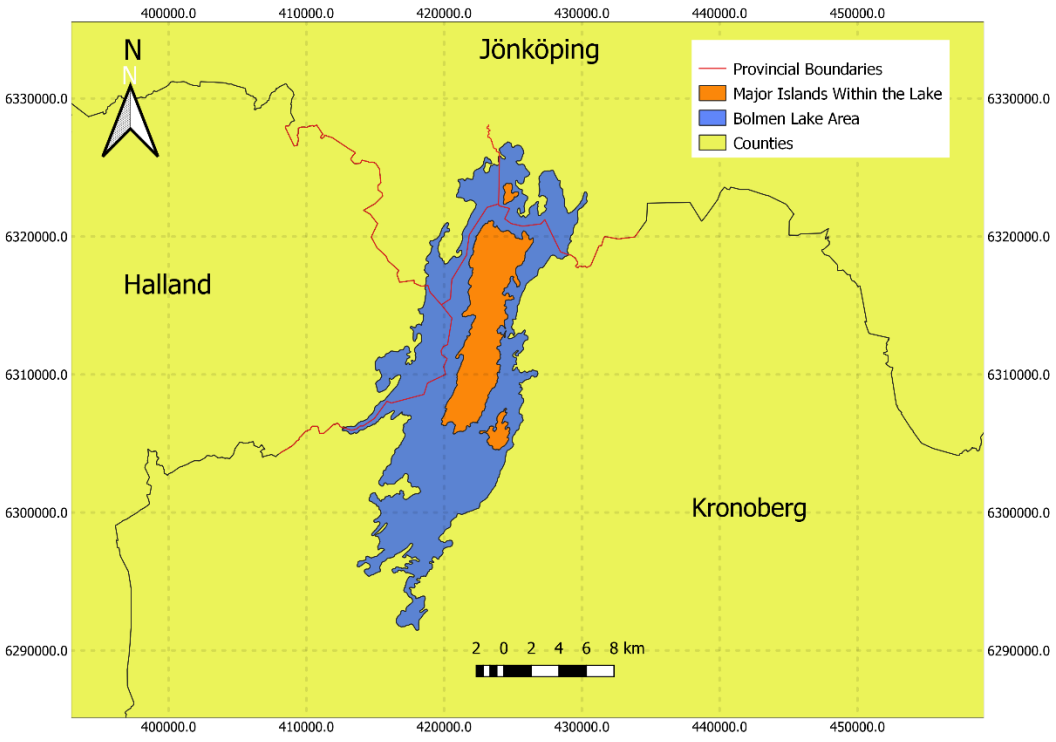

Figure 3-1 Bolmen Lake Territory with Provincial Boundaries

As per Tumdedo (2010), about 48 percent of the Bolmen Lake basin area is covered woodlands, 22 percent is swamp, 20 percent is lake, and 9 percent is crop lands. The lake's three main tributaries are the Storån River, the Lillån River, and Unnen Lake. There are also a number of smaller streams such as: dannäsn, mjösjöbäcken,

harasjöbäcke, and Murån. The humic substances abundance or water color is only determined at the lake's entrance from the streams Storån, Lillån, Murån, and Unnen. The existence of a massive island in the center of the lake separates the lake into sub-lake basins in the north, south, east, and west. The southern region of the lake is the deepest, with a maximum depth of 37 meters and an average depth of 8 meters. The northern region has a median depth of 13 meters and an average depth of 5-6 meters. The northern portion of the lake receives about half of the overall inflow from the Storån and Lillån rivers. Borgström (2020) reported that during the summer, the southern portion normally stratifies, with a thermocline between 10 and 20 meters deep referring Romare (2004), Persson (2011). The lake's retention period is about 2.8 years (Tumdedo, 2020).

3.2 **Bathymetric data**

Bathymetry, or underwater topography, is an important aspect of lake or reservoir modeling. The bottom topography of the lake basin region was provided by Clemens Klante. According to Clemens this information is based on old bathymetric data and fishing maps. In the most southern part (the Kafiofjord) measurements using an echosounder was available. There were sufficient number of locations were inspected. The information is based on average sea-level elevation. Bathymetric data processing is covered in detail in the relevant chapters. Topographic maps depict the three-dimensional characteristics (or relief) of overland terrain, whereas bathymetric maps depict the land that lies beneath the water level. Variations in lake bottom can be represented by color and contour lines known as depth contours or isobaths, which are discussed in further detail in following chapters. The data was delivered in the form of a vector GIS file with coordinates based on EPSG:4326 - WGS 84 – Geographic.

3.3 **Wind data**

Using the SMHI, The Swedish Meteorological and Hydrological Institute (https://www.smhi.se/data/meteorologi) website the long-term wind speed and direction data for Lake Bolmen from 1995 to 2021 was collected. I'd like to thank the Swedish Institute for making quality control data available to the public audience. Quality controlled data is available, with the exception of the previous three months. Aside from that, the exact data may be downloaded at any point after the year 1995. These data can be downloaded during this period, last 24 hours, or last hour timelines. The wind data were gathered at the Ljungby Station, SMHI number 63510, as indicated in Figure 3-2. The image based on World Geodetic System (WGS) 1984 geographic coordinate system (datum). Latitude: 56.8525, Longitude: 13.8794, Elevation: 148.485m Wind speed and direction are monitored at measurement stations. This site's mean value over 10 minutes every three hours was thought to reflect the lake's wind characteristics.

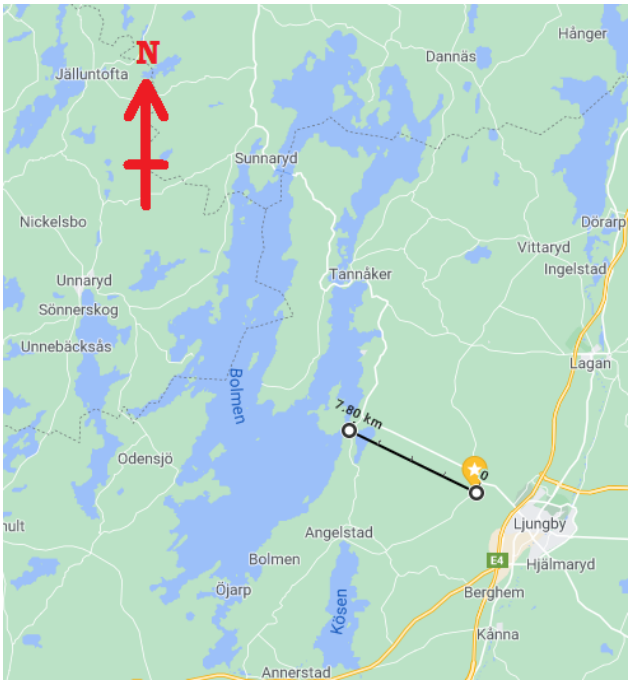

Figure 3-2 Location of Ljungby Wind Measurement Station Highlighted in Star symbol .The approximate closest distance between the station and the lake is shown here. (Extracted Google Imagery https://www.google.com/maps)

The Wind rose diagram shown in Figure 3.3 was created using the measured data obtained from 1995 to 2021. Each color represents a range of speed in ms^{-1}. The circumference scale is $0\text{-}360^0$ degrees and represents the divisions of cardinal directions.

This wind rose diagram has constructed using the Microsoft Excel computer tool. Examine the Figure 3.3 and arranging the statistical data using Excel software it can be said that the wind speed of 2.5 -3.5 ms^{-1} is the mostly occurrence frequency dominating in this region. Furthermore, the wind blowing from the southwest direction is comparatively more occurring than in the other direction.

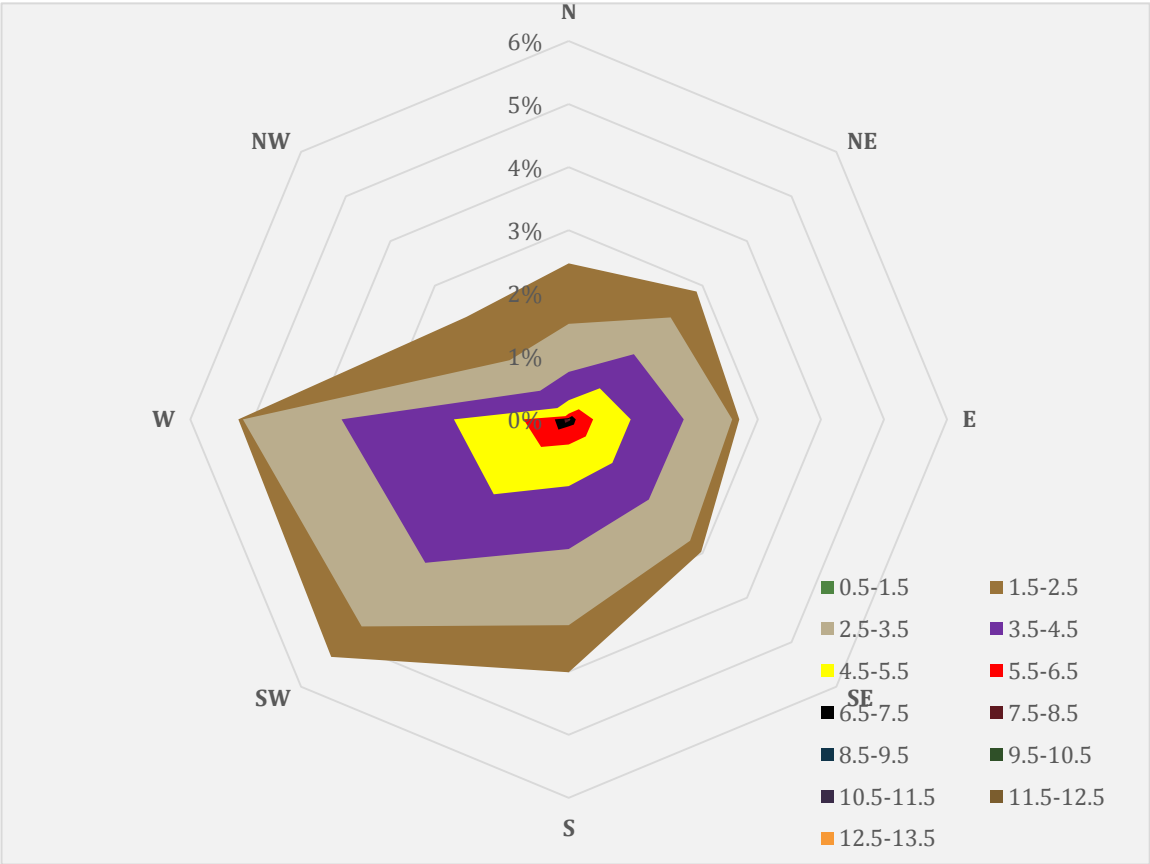

Figure 3-3 Wind Rose diagram for the wind data from year 1995 to 2001 at Ljunby Station

Wind direction variations are tabulated for each month during the previous two years. During 9 months of the year, the wind blows from the southwest on average. When compared to the other months, April, October, and November show a modest deviation in the other direction. The wind observations were from SMHI, and the raw data was supplied as a true bearing to the north. However, for the sake of analysis, this study considers numerous separate wind directions. Therefore sound notation for identifying

directions is required. In order to create the general notation for entire study see the Figure shown below,

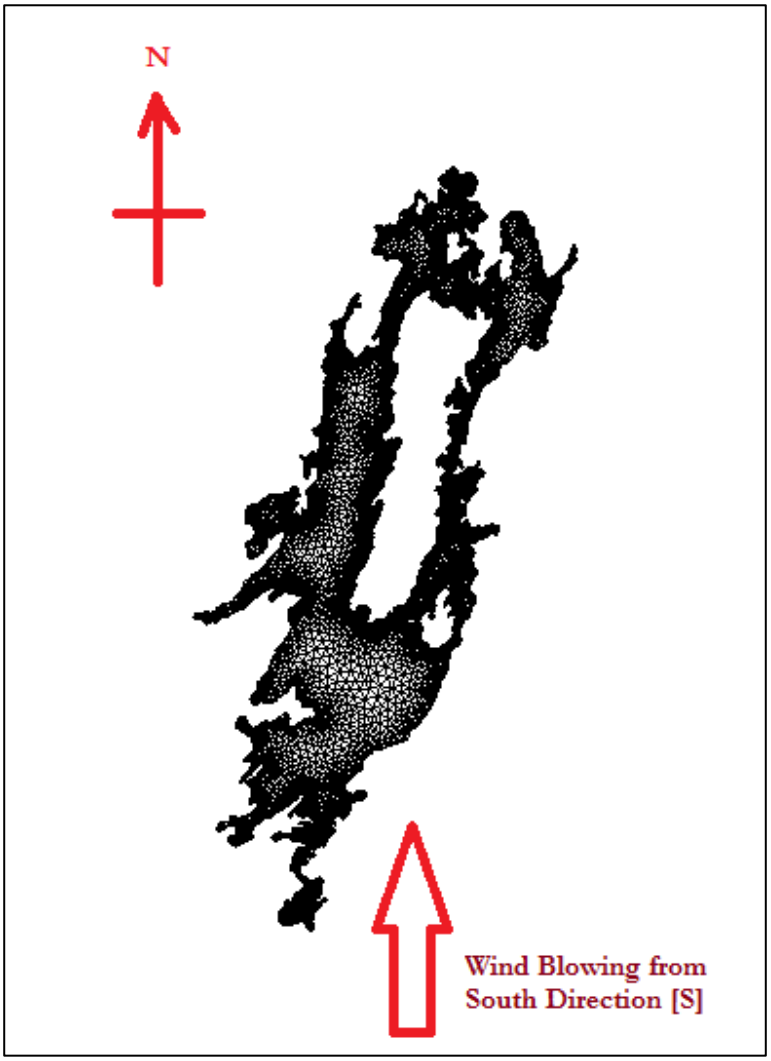

Figure 3-4 Wind Direction Notations

Figure 3.5 above shows the wind blowing towards the lake Bolmen from the south direction relative to the Lake. Which flow from the South to the North direction along the Bolmen Lake when referring to the cardinal directions. This has the true bearing of 180^0N respective to the Bolmen lake. This case is identified as [S] in this study. Every time wind blowing direction is considered with respect to lake .For example, the steady-state wind of $10ms^{-1}$ blowing from the south direction towards the lake is symbolized with $10ms^{-1}$[S]. For the readers, clarity see the Table 3-1 for other directional notations.

Table 3-1Wind directions notation adopted in the study

True Bearing of Wind with respect to the Bolmen Lake (degrees)	Simplified Notation
0^0	[N]
45^0	[NE]
90^0	[E]
135^0	[SE]
180^0	[S]
225^0	[SW]
270^0	[W]
315^0	[NW]

4 TELEMAC MASACARET SYSTEM

4.1 Introduction to TELEMAC

The *National Environmental and Hydraulic Laboratory of French Electricity Boards research and Development Directorate* was pioneering in developing the TLEMAC - MASCARET modeling system (Ladwig, Heinrich, Singer and Hupfer, 2017). Anyone can use the TELEMAC without purchasing the software or subscription. It is entirely free and open-source software. The advantage of TELEMAC is it can be modified or upgraded to user requirements by programming with FORTRAN 90. Furthermore constantly revised an upgraded versions are released for its users. TELLEMAC can solve the Depth average two-dimensional Saint Venent equations or three-dimensional Navier stokes equations in TELEMAC 3D. The solving 3d equations TELEMAC uses the hydrostatic Pressure principle and Boussiness approximation for solving the momentum equations. There are six major turbulent models available in TELEMAC 2D version 8. Constant viscosity model and k-ϵ turbulence model were utilized in TELEMAC 2D for numerical simulations. This is the latest version of TELEMAC 2D available presently. The model domain is spatially discretized using an unstructured grid of triangular components and, in 3D, prisms via the sigma transformation. TELEMAC-2D concurrently solves the shallow water equations (continuity, momentum, and transport) for the two-dimensional setup (Hervouet and Ata, 2017b), This is now explicitly supported for the two dimensions model in x and y. According to TELEMAC user manual version v8p2 which was released in December 1, 2020.

$$\frac{\partial h}{\partial t} + u.\vec{\nabla}(h) + hdiv(\vec{u}) = S_h \qquad \text{Eq 4.1}$$

$$\frac{\partial u}{\partial t} + \vec{u}.\vec{\nabla}(\mathrm{u}) = -\mathrm{g}\frac{\partial Z}{\partial x} + S_x + \frac{1\,\mathrm{div}\,(\mathrm{h}V_t\vec{\nabla}\mathrm{u})}{h} \qquad \text{Eq 4.2}$$

$$\frac{\partial v}{\partial t} + \vec{u}.\vec{\nabla}(v) = -g\frac{\partial Z}{\partial y} + S_y + \frac{1\,\mathrm{div}\,(h V_t \vec{\nabla} v)}{h} \qquad \text{Eq 4.3}$$

$$\frac{\partial T}{\partial t} + \vec{u}.\vec{\nabla}(T) = S_T + \frac{1\,\mathrm{div}\,(h V_t \vec{\nabla} T)}{h} \qquad \text{Eq 4.4}$$

The symbols and variables shown above represent the following parameters

h (m) : depth of water

u,v (m/s) : velocity components

T (g/l or °C) : passive (non-buoyant) tracer

g (m/s^2) : gravity acceleration

ν_t, ν_T (m^2/s) : momentum and tracer diffusion coefficients

Z (m) : free surface elevation

t (s) : time

x,y (m) : horizontal space coordinates

Sh (m/s) : source or sink of fluid

S_x,S_y (m/s^2) : source or sink terms in dynamic equations

ST (g/l/s) : source or sink of tracer

h, u, v and T are the unknowns.

The above-mentioned equations are based on Cartesian coordinates. However, TELEAMC supports the Spherical coordinate system too. When working with the geometry and steering files the specific adjustments need to be done to simulate in the Spherical coordinate system. According to the TELEMAC manual the Wind forces, Coriolis effects, bottom friction are governed by the source words defined as S_x and S_y (m/s^2) in Eq 4.3 and Eq 4.2. Furthermore, these terms are responsible to act domain is a source or sink of momentum. The respective properties given from these terms are processing in one or more steps in TELEMAC. Such as

- Advection depth , scalar velocities and Tracer measurements ,
- The dynamic equations' transmission, dispersion, and source terms,
- The tracer transport equation's diffusion and source terms.

Many of these processes can be omitted, resulting in the solution of numerous equations. In addition, each of the variables depth of water, velocity along x, velocity along Y, and tracer concentration can be presented separately In this way it makes it easier to solve the tracer diffusion and advection equations. Adopting a fixed advective velocity field is an example. Turbulent viscosities can be determined by the consumer or calculated using a model that simulates the transfer of the turbulent variables k (turbulent kinetic energy) and Epsilon (turbulent dissipation), These differential equations are shown below.

$$\frac{\partial k}{\partial t} + \vec{u}.\vec{\nabla}(k) = \frac{1}{h} div\left(\frac{h V_t \vec{\nabla} k}{\sigma_k}\right) + P - \varepsilon + P_{kv} \qquad \text{Eq 4.5}$$

$$\frac{\partial \varepsilon}{\partial t} + \vec{u}.\vec{\nabla}(\varepsilon) = \frac{1}{h} div\left(\frac{h V_t \vec{\nabla} \varepsilon}{\sigma_\epsilon}\right) + \frac{\varepsilon}{k}(C_{1\epsilon} P - C_{2\epsilon}\varepsilon) + P_{\epsilon v} \qquad \text{Eq 4.6}$$

According to TELEMAC Manual, the formation and dissolution of the turbulent quantities are governed by right-hand side terms. When non-hydrostatic effects are involved, Saint Venant calculations need to be modified by using extra terms. Number of studies (Serre, Boussinesq, Korteweg and De Vries) were carried out regarding this matter. To employ Boussinesq hypotheses, the terms are applied to the right-hand side of Saint Venant equations and implemented, this is referred to as Boussinesq equations and shown below.

$$\frac{H^2{}_0}{6} \overrightarrow{grad}\left[div\left(\frac{\partial u}{\partial t}\right)\right] + \frac{H^2{}_0}{2} \overrightarrow{grad}\left[div H_0 \left(\frac{\partial \vec{u}}{\partial t}\right)\right] \qquad \text{Eq 4.7}$$

4.2 TELEMAC 2D Model Configurations and Simulation Parameters

In this chapter the general description about input data for TELEMAC 2D modeling and its importance is further is described. All the terms and descriptions are based on TELEMAC user manual version v8p2 which was released in December 1, 2020. Aside from the TELEMAC user manual, the specific reference materials used in this section are mentioned separately. It should be noted that only few of the model parameters are presented in this part (4.2), and the reader is advised to check the TLEMAC handbook

for the default model parameters which are not mentioned in this section. Also, unless otherwise specified, it is assumed that the TELEMAC default model parameters are reasonably accurate for this investigation.

Define the general TELEMAC simulation parameters

1. Frictional Coefficient

The friction coefficient defined in this section describes the friction between the interface of the lake bottom and the water flow. Many laws satisfactorily provide reliable values. Some of them are namely Chezy law, Manning law, Nikuradse law, Colebrooke-White law, etc. However, in this study Mannings, Law has been utilized since it is widely accepted by many researchers. It should be noted that TELEMAC can be supported with any of the above-mentioned boundary friction formulas. Before defining the Friction coefficient value the user needs to be defined as frictional low which is given by Keyword FRICTION LAW in TELEMAC 2D. Friction coefficient for lake bottom was based on guidelines given by Arcement et al., (1989) called Guide for selecting Manning's roughness coefficients for natural channels and flood plains. The suggested Mannings friction coefficient range is 0.026-0.035 During the entire simulation process, the manning roughness coefficient is assumed to be 0.035 between the lake bottom and the water. However, this should be noted that in reality, the entire lake bottom will not have a fixed frictional coefficient. Due to various sediment characteristics and morphological formations manning coefficient is varying within the lake bottom. During this study period, such frictional values could not be accessed or there were no previous researches data acquired regarding this. However, it should be noted that the TELEMAC is capable of working with spatially varied fractional step values and time-varying frictional coefficients.

2. Modeling Of Turbulence

This investigation is based on two-dimensional model that can be solved for various TELEMAC models namely constant viscosity model, K-ϵ model, ELDER model, SMAGORINSKI model, Mixing length model, Spalart-Allmaras model. However, the 2D numerical model is simulated using a constant viscosity model at the start of the simulations, yielding less accurate findings comparative to K-ϵ model. It should be noted that As per the study carried by Chorda et al., (2010) the constant eddy viscosity model doesn’t provide accurate results for mean flow patterns. The computation of the

solution for the convention model is done by the fractional phase approach mentioned in the TELEMAC user manual. The model equations are solved simultaneously with the Hydrodynamic variables. During the computation process, the Diffusion and dissipation turbulence is solved in a single step. Most of the time the K -ϵ model required finer mesh comparative to constant viscosity model. It should be noted that although the K -ϵ model gives more reliable answers, the computational time is high compared to the constant viscosity model. Therefore, to get the desired results within the time constraints, the constant viscosity model was used for all simulations. After completing all simulations with the constant viscosity model, some simulations can be performed again with the k- ϵ model and the results can be checked for greater accuracy if time permits.

3. Velocity Diffusivity

Using the key word VELOCITY DIFFUSIVITY assignment for molecular and turbulent viscosity can be made. Entire study the value of 10^{-6} m^2/s was used which also considered as default value in TELEMAC for viscosity in water. The default value of 10^{-6} m^2/s incorporate both molecular viscosity and eddy viscosity in the constant viscosity model. In addition it is widely accepted that slow traveling, deep, and stratified water in lakes has eddy coefficients in the range of $10^{-4} – 10^{-6}$ m^2/s (Marion, 2008). Moreover it should be noted that the magnitude of this parameter have significant impact on the results. For instance, the shape of recirculation and degree of recirculation is depended on quantity of the viscosity value provided. Using relatively low values for viscosity creates eddies with smaller in size (eddies mean circular currents of water). Similarly assigning larger values for viscosity resulting larger eddies. As a result, depending on the circumstances, the user should exercise discretion while selecting this value 10^{-6} (in particular as a function of the size of the recirculation user wishes to dissipate and the mean angular velocity of the recirculation). It must be ensured that eddy dissipation values bigger than two meshes have practically little effect on the calculations.

4. Atmospheric Pressure

The atmospheric pressure is the force created on unit area of surface water layer due to the weight of air column lies above it. It is reasonable to assume that the value of Atmospheric pressure is constant across the entire domain of Bolmen Lake. As per the

average data from SMHI this value adopted as 1.022000 Bar / 1.022 x 10^5Pa (Nm^{-2}). However there were no adequate information found regarding atmospheric pressure have significant impact on wind induced currents on lakes. Key word adopted for assigning the given value is ATMOSPHERIC PRESSURE.

5. Wind Influence

Wind stress prediction surely influences anticipated storm intensities, ocean waves, and so forth. Oceanic scientific conventions demonstrate that momentum transmission from the wind to the ocean drives energy exchange between the atmosphere and sea. When the fluid flow is parallel to the wind direction, drag is caused by shear stress, and when the flow is perpendicular to the wind, drag is caused by tensile stress. That being said, the vertical tension is caused by pressure drags and surface drags caused by shear stress. It should be mentioned that the drag coefficient is directly proportional to wind velocity. The wind velocity is indicated here according to the Coastal Engineering Manual, (2006)

$$U_Z = \frac{U_*}{K} \ln \frac{Z}{Z_o} \qquad \text{Eq 4.8}$$

U_Z = Velocity of wind observed at height z
U_* = Frictional velocity at sea level
Z_0= Surface roughness coefficient
K = Vonkarman Constant (0.4)

As per the Coastal Engineering Manual which was published in 2006 in Great Britain generated wind stress or The momentum transfer rate from wind to the water surface is computed as follows:

$$\tau = \rho_a \, C_d \, {U_{10}}^2 \qquad \text{Eq 4.9}$$

U_{10} = Wind velocity at 10 m above the sea level
C_d= Drag coefficient

As per the Coastal Engineering Manual, (2006) The drag coefficient can be defined as shown below after manipulations were made

$$C_d = \left[\frac{U_*}{U_z}\right]^2 \qquad \text{Eq 4.10}$$

When it comes to TELEMAC-2D, the software comply with Coastal Engineering Manual, (2006). To begin with wind applications use the keyword WIND. If this is the case to be continue, the coefficient is label COEFFICIENT OF WIND INFLUENCE is computed based on the feeder data to the TLEMAC as shown below. This keyword can have the following values assigned to it: Dynamic processes are included behind the wind impact coefficient a_{wind}. In actuality, the wind's influence is defined by the free surface's smoothness and fetch distance Fetch distance is the length where wind blows without any disturbances over a water surface for generating waves. The coefficient value can be calculated using a variety of approaches. TELEMAC uses the standards given be Institute of Oceanographic Sciences in Great Britain.

IF $\left[\vec{U}_{wind}\right]$ < 5 M/S $\quad a_{wind} = 0{,}565 \times 10^{-3}$

IF 5 < $\left[\vec{U}_{wind}\right]$< 19.22 M/S $\quad a_{wind} = (-0{,}12 + 0{,}137) \times 10^{-3}$

IF $\left[\vec{U}_{wind}\right]$> 19.22 M/S $\quad a_{wind} = 2{,}513 \times 10^{-3}$

To use the coefficient of wind influence in TLELMAC, Density of air is ρ_{wind} (1.2 kg/m^3) and Density of water is ρ_{water} (1000 kg/m^3) needs to be divided. Thus value use in TELEMAC is $\frac{\rho_{wind}}{\rho water}$. Its commonly recognized that unit of density of freshwater is 9807 kg/m^3 at 4^0C degrees Celsius. As a result, the default parameters used in TELEMAC software are expected to be valid and not deviate greatly from standard values. It should also note that the density of water and air does not vary over the lake's profile and assumed to be constant.

6. Coriolis Effect

The Coriolis effect is commonly accepted to play a role in wind-induced motion in larger, deeper lakes. Ekman suggests that wind propagation direction has roughly 45^0 degrees to surface current direction when considering the North Hemispherical Region.

The Coriolis force is caused by the rotation of the Earth. The Coriolis effects were incorporated to the model since Bolmen is located in the Northern Hemisphere and has a significant water mass. TLEMAC estimates the inertial effects caused by Coriolis. The keyword CORILIOLIS COEFFICIENT must be activated with a true assignment. The following formulae are used to calculate the initial impacts.

$$FCOR = 2\,\omega \sin(\lambda) \qquad \text{Eq 4.11}$$

$\omega = 7.27 \times 10^{-5}$ rad/s, Angular velocity of the earth

λ = Latitude (Depends on the 2D coordinate system assigned, value 56° 54' 59.99" N)

Typical values normally assign in the TELEMAC for FCOR = $1.236E^{-4}$ and Not varying in greater degree within the lake

The inertial forces on X and Y directions are respectively

$$FU = FCOR \times V \qquad \text{Eq 4.12}$$

$$FV = -FCOR \times U \qquad \text{Eq 4.13}$$

7. Managing Water Tracers and Water Sources

TELEMAC-2D enables the placement of external water sources (with or without tracer discharge) at any location within the domain. The user is required to assign the discharge at each source. This can be done by defining the quantity of flow (m^2-sec) and coordinates of the source. If the external flow is varying with the time, then the TELEMAC subroutine file needs to be attached. In this study, the Tracer is added with creating a subroutine file. The discharge is specified in m3/s using the keyword. However, outside water sources were utilized in this scenario only during smaller time approximately 200 Seconds and it assumed to be instantaneous comparative to simulation duration. This is adopted because the tracer material needs to be introduced to the system after the simulation has begun. Only one tracer material is examined in this investigation in a northern section of the Bolmen take. The tracer material of considerable mass is released to the lake instantaneously. The concentration of the tracer material and the position of tracer contacts should be specified in the TELEMAC steering file. TLEMAC can be programmed to accept numerous tracers from various spatial coordinates having transient characteristics.

8. Numerical Parameters

The steering file must define the form of the governing equations to be solved. The keyword EQUATIONS, which can have the following values, is used to make the selection: 'SAINT-VENANTFE' is an abbreviation for 'Saint-Venant-F (default value) The finite-element approach is used to solve the Saint-Venant equations in the first alternative. This is the "traditional" application of TELEMAC-2D.

9. Numerical Schemes

The primitive equations are used to solve finite element problems. It is feasible to substitute the original equations with a simplified wave equation obtained by removing the velocity from the continuity equation and replacing it with a value obtained from the momentum equation. This method improves computation speed but has the downside of smoothing the results. The keyword TREATMENT OF THE LINEAR SYSTEM needs to be introduced in the steering file. A default value of 1 is usually solving the general set of equations. When selecting option 2 automatically chooses a variety of other choices, including the use of mass lumping on depth and velocities and the use of explicit velocity diffusion. This computational practices can be adopted to decrease the computational time.

1: Initial equations, (Default)

2: Wave equation, (Optional)

In this 2D numerical model wave equation has been used for enhancing the solving of the set of equations because this model has locations with steep bottom topography gradients.

10. Law of Tracers Degradation

TELEMAC-2D tracers are treated as mass-conservative by default. In this model tracer is expected to be mass conservative inside the lake. This means the tracer has no effects on physical, chemical degradation. It is considered to be non-reactive as well as it has no impact on the hydrodynamic behavior in the Lake (non-buoyant tracers). If the user has specific requirements that need to fulfill such as reactive tracer, degrading, etc. If simulating oxygen concentration as stated in the latter cases, deterioration laws may be needed to be defined. Only the exponential degradation rule is available in version 7. However, if the user defining several tracers in the domain each tracer needs to be separately defined for reactive and degradation keywords. Users can Enable the tracer degradation using the TELEMAC keyword LAW OF TRACERS DEGRADATION. Tracer degradation processes are not included in this model.

5 DATA PROCESSING AND COMPUTATION TOOLS

5.1 QGIS

QGIS (previously known as Quantum GIS) is a cross-platform free and open-source desktop geographic information system (GIS) application that supports viewing, editing, and analysis of geospatial data. QGIS functions as geographic information system (GIS) software, allowing users to analyses and edit spatial information, in addition to composing and exporting graphical maps (Olamide, 2021). QGIS supports both raster and vector layers. Vector data is stored as either point, line, or polygon features. Multiple formats of raster images are supported, and the software can geo reference images. QGIS supports shape files, coverage, personal geo databases, dxf, MapInfo, Post GIS, and other formats. Web services, including Web Map Service and Web Feature Service, are also supported to allow use of data from external sources. QGIS integrates with other open-source GIS packages, including PostGIS, GRASS GIS, and Map Server. Plugins written in Python or C++ extend QGIS's capabilities (Asghar, 2017). Plugins can geocode using the Google Geocoding API, perform geo processing functions, which are similar to the standard tools found in ArcGIS, and interface with PostgreSQL/PostGIS, SpatiaLite and MySQL databases. QGIS can use to tackle common GIS problems, especially remote sensing analyses, Hydrological modelling using QSWAT, Different Interpolation methods, Python Programming for Spatial analyses, Creating Web based Maps and so on.

According to (Software Tools | DataONE, 2021) GIS (QGIS) is an open source Geographic Information System (GIS) that implements a large number of geospatial data access, visualization, processing, and analysis functions. It can access vector data stored in a wide variety of formats, including file-based (e.g. ESRI Shape Files, KML, GML), geodatabases (e.g. PostgreSQL/PostGIs, ODBC, ESRI Personal GeoDatabase, SQLlite), and network protocols (OPeNDAP, GeoJSON); raster data in one of over 40 formats supported by the underlying GDAL raster library (including NetCDF, HDF5, GeoTIFF, GRIB, and JPEG-2000); and Open Geospatial Consortium visualization and

data access services (Web Map and Web Feature Services [WMS and WFS, respectively]). Depending upon the host system configuration, QGIS can also act as an alternative Graphical User Interface for the large collection of GRASS GIS geospatial processing functions. QGIS includes a "plug-in" architecture in which extensions to the core functionality of the application may be developed and used, with current plug-ins including support for GPS integration, interaction with the Open Street Map data servers, and data transformation tools (QGIS Plugins, 2021).

5.2 **Blue Kenue**

According to (Ermilov, 2018) Blue Kenue has been under development for about20 years, and provides a framework for pre-processing, post processing and visualization of hydrodynamic model data. The National Research Council Canada makes this software freely available for use by the open TELEMAC-MASCARET user community and benefits significantly from the knowledge that the community shares

For hydrodynamic modeling, the Blue Kenue system provides highly developed data preparation interphase, analytical tools, visualization, and computation tools. The Blue Kenue serves as an interphase medium between the TELEMAC software and the User. BLUE KENUE integrates geographical data with modeling. Using the BLUE KENUE, immediate visualization of outcomes is possible for software such as TELEMAC, ADCIRC and HydroSim.

Blue Kenue's visualization features such as dynamic 1D, Polar, 2D, 3D, and Spherical views that may be captured as digital movies or saved as photos for use in reports or presentations. By describing a 3D flight via the model domain, it is simple to build 3D flights across the model domain. In default mode, all imagery and spatial data are geo-referenced. The BLUE KENUE can also be used to flip between projections (Blue Kenue™: software tool for hydraulic modellers, 2021). By just picking two points and pushing the "Play" Symbol, users may view two-dimensional time-series data during simulation duration. In the same way, time series in a single point may be analyzed for any chosen output parameter.

It should be noted that the Blue Kenue is capable of viewing and measuring the rotation of a two-dimensional plane relative to third axis perpendicular to the 2D plane. As a

result, Blue Kenue provides tools for rotating and translating the 2D working environment with respect to the 3D viewpoint. When looking at the Blue Kenue 2D plane, the compass leg with the Red arrow is always pointed to true north See the Figure 5:1. The rotation of the north axis counter clockwise relative to the 3rd Axis is displayed in degrees exactly down the red leg. These visual properties are useful while dealing with Maps. It should be noticed that the defined notation of compass characteristics is used in this report and is not mentioned in each Figure individually.

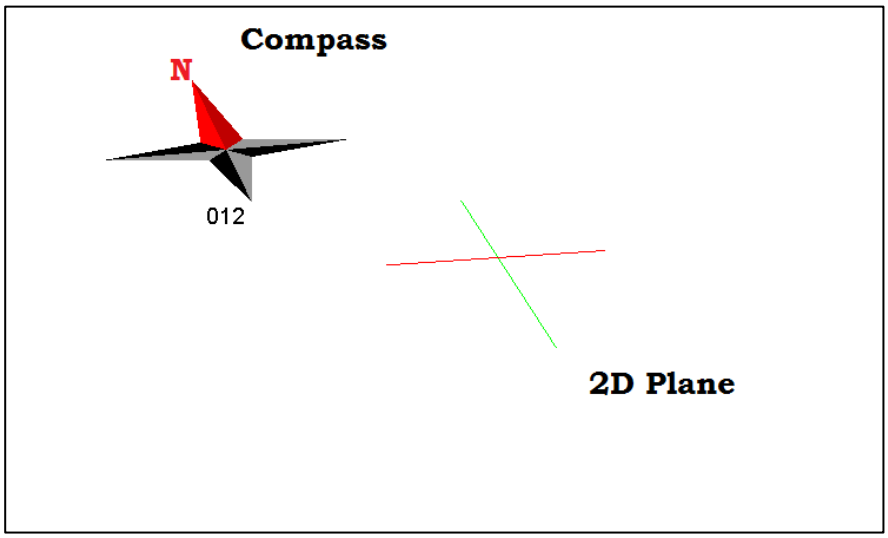

Figure 5-1 Blue Kenue Compass properties and configuration in 3D view

.

6 DATA PREPARATION AND MODEL IMPLEMENTATION

6.1 Bathymetric Data Processing

As per the received bathymetric data the elevation data has been processed before feeding to the Blue Kenue. Using QGIS 3.901 version the data received as a vector format has converted to raster format. For this task the raster creation tool plugin SAGA in QGIS was used.

Since the boundary elevation and island elevations are not specified in the vector data the suitable elevation for this has to be determined. Since the average lake water surface is 141.5 m from mean sea level the boundary and the Island elevation was fixed to 142 m for the convenience and to provide the TELEMAC model the optimum Wind effects.

As shown in the Appendix 1 Figure A1 the vector data was modified containing three boundary lines and the inside island boundaries within the lake. All the elevation at these points set to be 142.5 m. After fixing these elevations the vector layer transform to raster layer using afore mentioned SAGA raster creation tool. The specific interpolation technic B spline multilevel raster creation was utilized. In order to check for the deviation between in the raster layer and original vector layer the twelve points were selected and analyzed. Average deviation was limited to 0.012%. Hence multilevel spline used as interpolation. The raster layer generated using spline interpolation is shown below. The raster layer properties are displayed in the Figure 6-1.

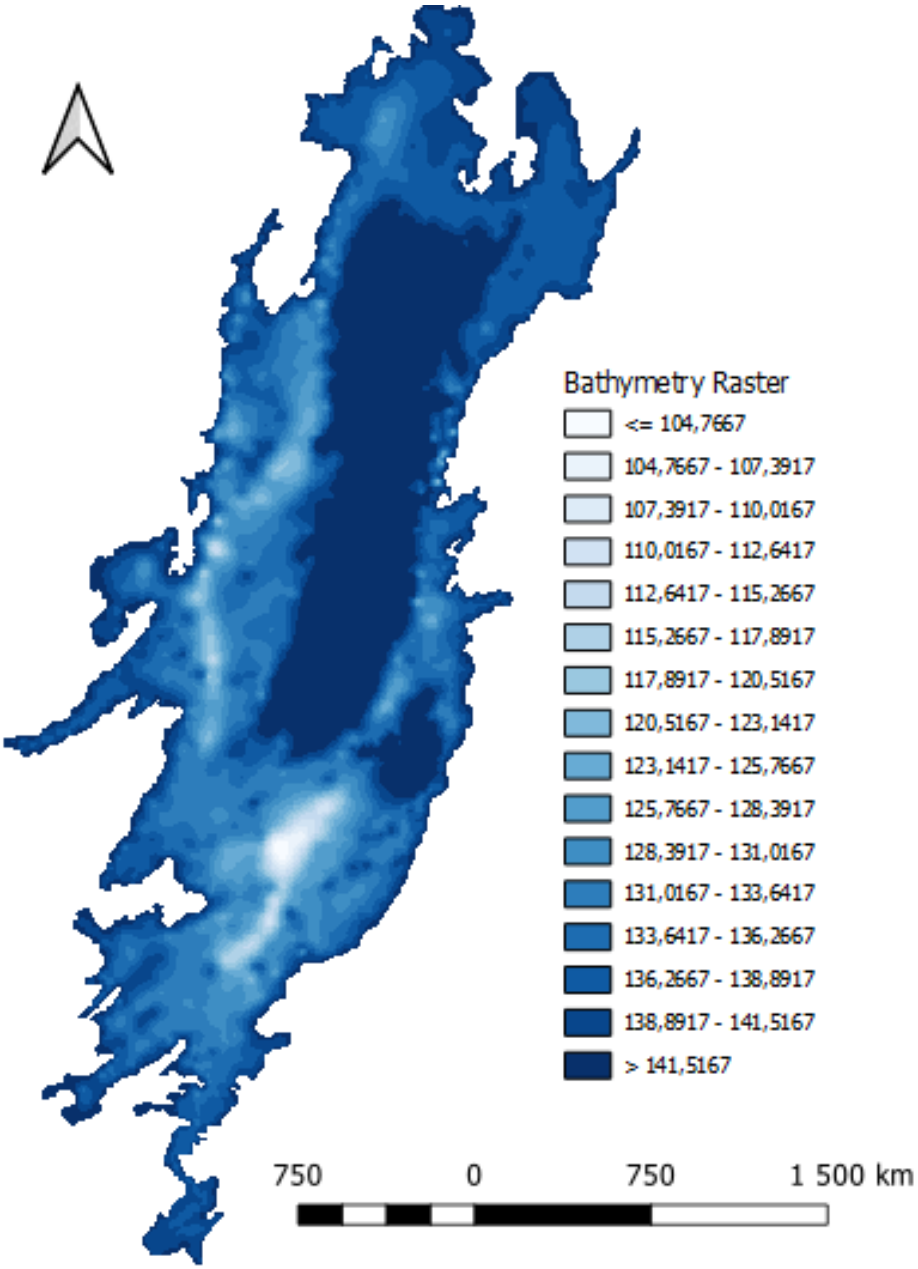

Figure 6-1 Bathymetry of Bolmen Lake , Raster created By QGIS

6.2 **Mesh Generation using Blue Kenue**

Blue Kenue functions with rectangular grids and triangular elements to create meshes. Points and lines can be used as input data for user-defined grids. It is worth noting that the TELEMAC has the capability of incorporating different rectangular or triangular grids that may be entered externally. The Hard Lines and Hard Points are kept during mesh creation during element subdividing. The point density of the user's feeding lines will establish the Node density in Hard borders or outline borders. Blue Kenue can be an excellent tool for creating hydrodynamic maps with roughness data. It should be emphasized that as the element resolution (elements per unit area) increases, so does the amount of information generated. More elements in a model, on the other hand, will undoubtedly take longer to simulate. Higher node density improves modelling calculation accuracy since it contains more information and prevents data smoothing.

Blue Kenue pre-processing was created by the Canadian Hydraulics Centre of the National Research Council and is used in this work to achieve the following objectives: 1. Create a Finite-Element mesh. 2. Create the boundary conditions that will influence the system. 3. Creating a visual representation of the TELEMAC-2D hydrodynamic data.

The mesh generating technique in Blue Kenue software might vary depending on the user's skill level. However, in this project, following steps were employed.

Step : 1 Creating the outside boundaries and internal hard boundaries, See the Figure 2 in Appendix 1

Step : 2 Define The triangulation edge growth ratio and default edge lengths See the Figure 3 in Appendix 1

Step : 3 Generating the 2D mesh See the Figure 6-2

Step : 4 Import the bathymetric file modified using QGIS to Blue Kenue See the Figure 6-3

Step : 5 Interpolating the Bathymetric data to the Generated mesh See the Figure 6-4

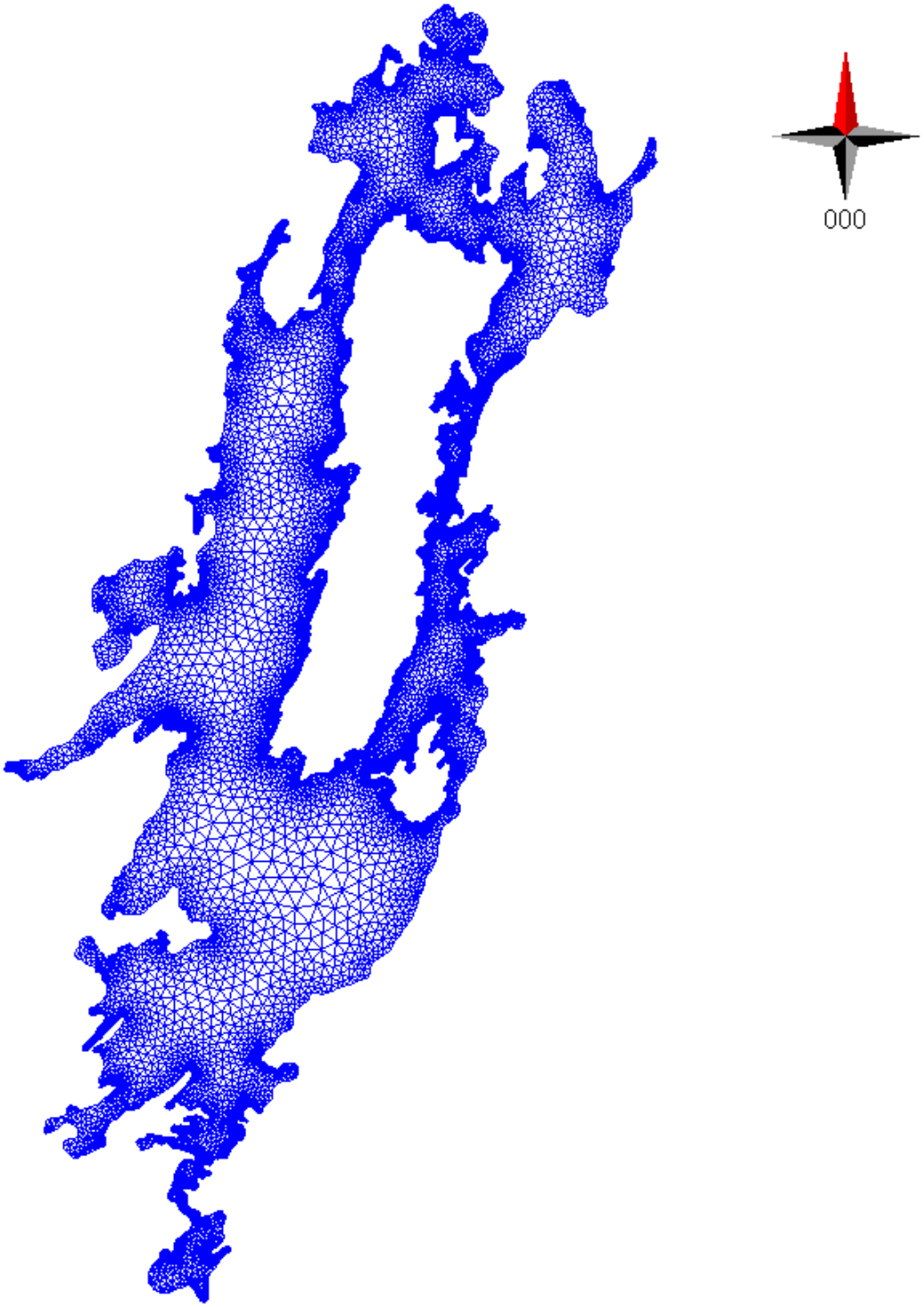

Figure 6-2 Triangular mesh grid generated using Blue Kenue

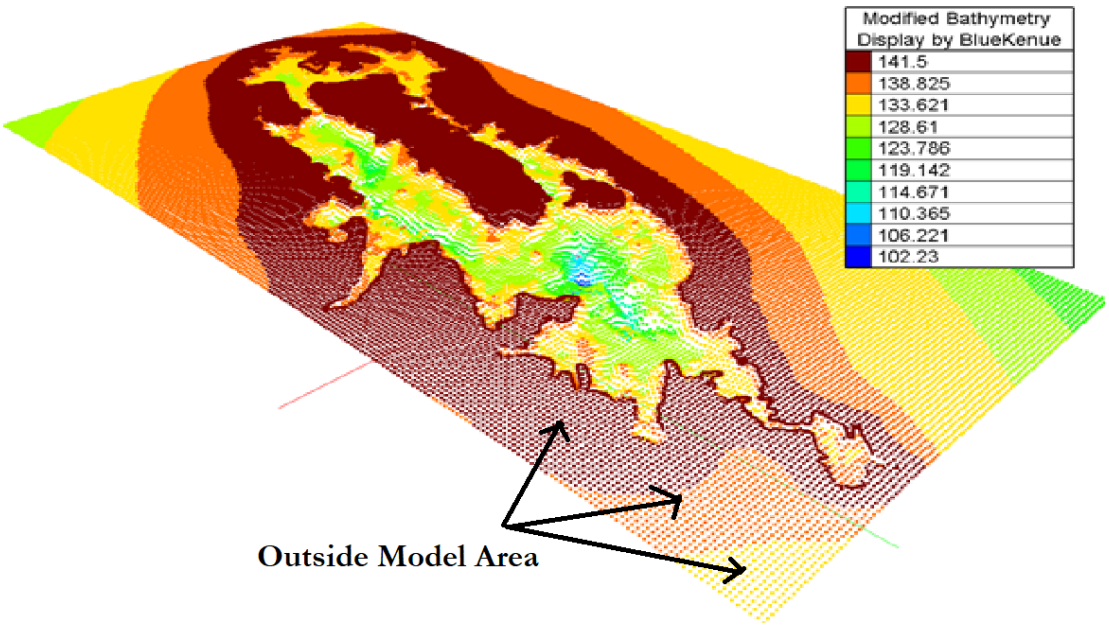

Figure 6-3 Bathymetry of Lake Bolmen imported to Blue Kenue The monotone colors named with the *outside model area* do not represent the actual altitudes and are outside the lake perimeter. The *outside model areas* are the result of the QGIS interpolation tool that was utilized in the process. Elevation data showing in outside the lake perimeter are not used in model computations.

After successfully creating the mesh, define the boundary conditions using the tool *Boundary Conditions(conlim)* in Blue Kenue. see the Figure A-4 in Appendix 1, in this case all the outside boundaries are no flow and impermeable boundaries. Therefor no specific boundary conditions needed to be define. Store this file as a boundary condition file in order to use in TELEMAC simulation in later time.

For the TELEMAC simulation, bottom elevation and bottom friction needed to be assign using the file imported to Blue Kenue from QGIS in Step 4 in section 6.2 . This is done by using Blue Kenue tool *Interpolation 2D* and *Map Objects*. After successfully assigning the bathymetry to the generated mesh the Grid can be view as Figure 6.2. To define the bottom friction to whole domain or part by part the *add variable option* should be selected in SELAFINE object tool in Blue Kenue . However the value assign here can be change if user wanted in later stage in TELEMAC CAS file .

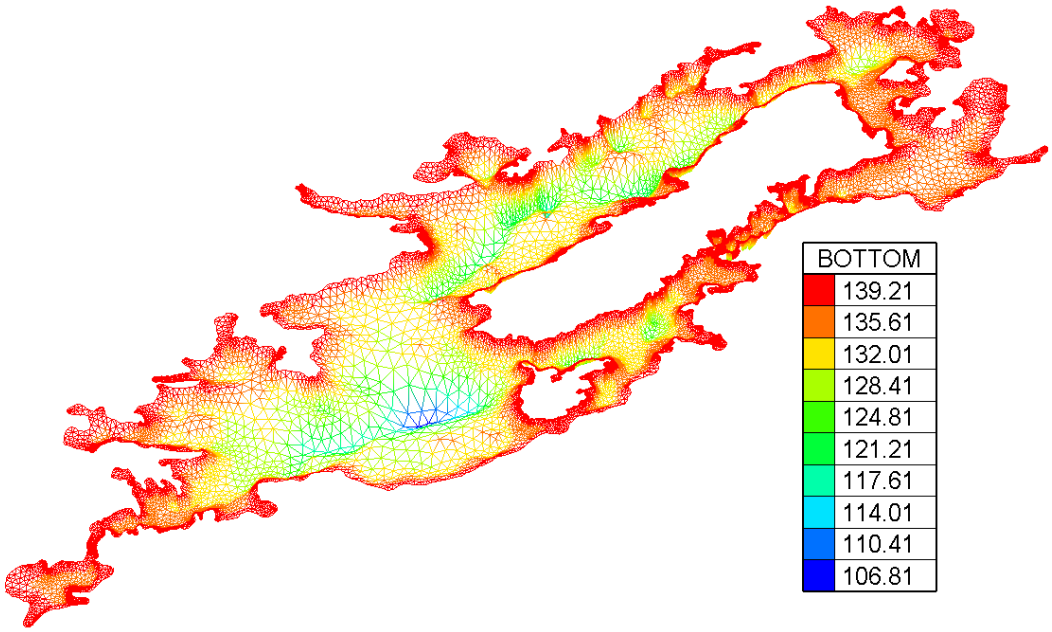

Figure 6-4 The Bathymetry data interpolated on Triangular mesh grid, Blue Kenue

6.3 Simulation using TELEMAC

Up to this section, all the preliminary steps that need to be completed in the TELEMAC model using the QGIS and Blue Kenue have complete. The remaining works need to be done in TELEMAC software. Three main files need to input into the TELEMAC software before initializing the computational tasks. They are.

1. Boundary Conditions in .CLI files
2. Geometry Conditions in .SELAFINE file
3. Governing Conditions in .CAS file

The 1 & 2 files are already obtained using the help of QGIS and Blue Kenue software. The remaining conditions have to be dealt with in the TLEMAC steering file called CAS. All the inputs such as tracers, water elevations, Simulations duration are defined in this file. Therefore all the changes defined in this following section under 6.3 are made under the steering file (CAS).

6.3.1 Spatially Constant Steady Uniform Wind Velocities

6.3.1.1 Directional Variations of Wind Velocity

This section attempted to model the variation in lake currents induced by changing wind direction. To accomplish this task, keep the wind speed ($10ms^{-1}$) constant and simulate the wind from other directions as shown in Table 6-1. All wind simulation parameters in the study are accompanied by a 1000 kg (1Ton) tracer discharge at the site illustrated in Figure 6-10 (at North) when the simulation elapsed duration reaches 100 seconds The lake has a volume of roughly $1x10^9m^3$. As a result, releasing a tracer material with a total mass of 1000 kg is estimated to provide enough concentration for detecting. In every situation in this part, the simulation time is set to 45 days. If the tracer detection time period is inadequate to achieve the peak value within the permitted 45 days, extend the current simulation for 90 days or longer, depending on the circumstances. In each case. The simulation results must be examined for scalar velocities (UV), tracer concentrations (non-reactive), and water depths at the relevant measurement locations and sections. The output results are based on the zones indicated in Figure 6-5, which were studied for the locations represented in Figure 6:7, as well as the sectional profiles displayed in Figure 6:6.

Table 6-1 Simulation configurations for Wind Direction

Simulation No	Direction of 10ms^{-1} Wind Velocity Relative to the Lake
1	[E]
2	[S]
3	[W]
4	[N]
5	[NE]
6	[SW]

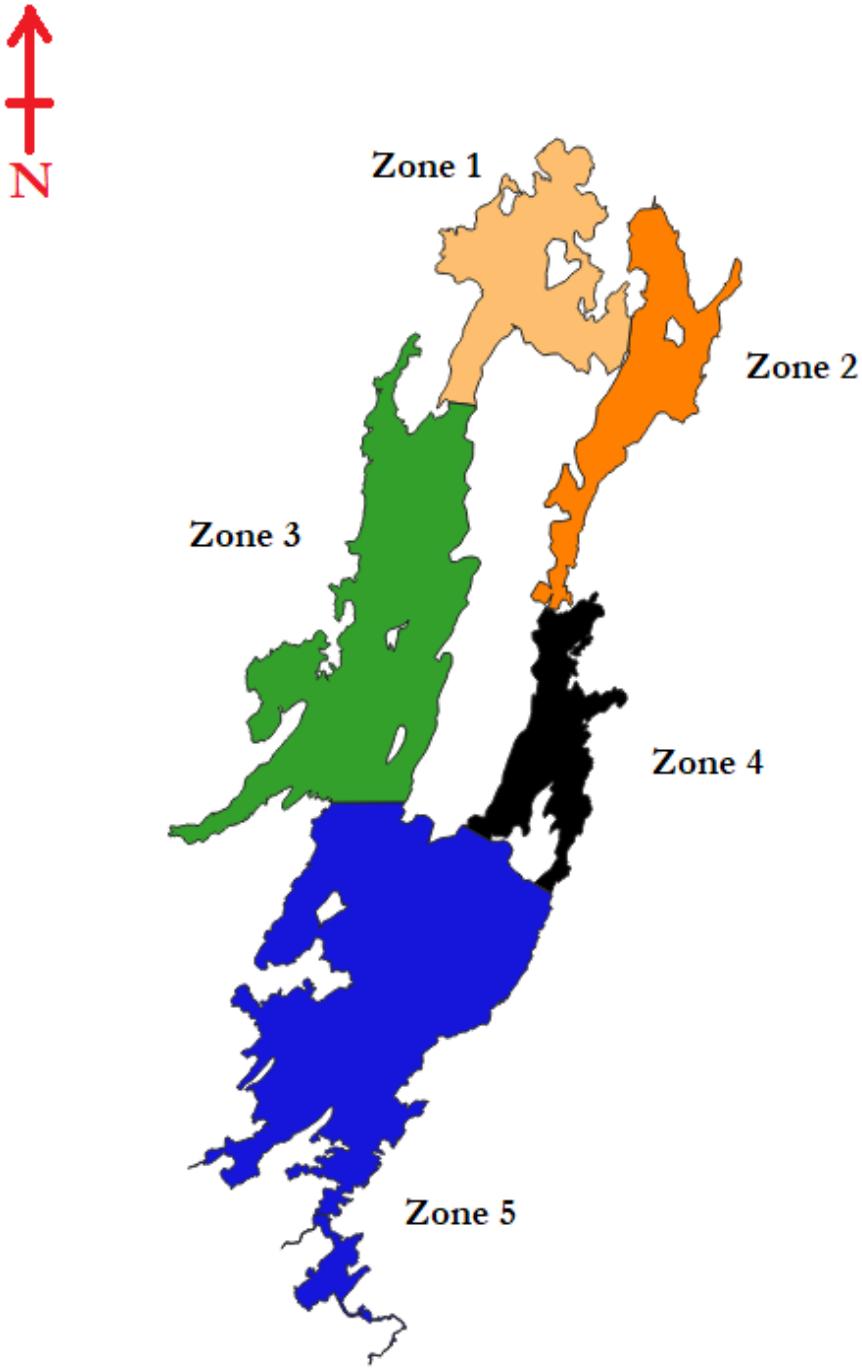

Figure 6:5 Zone Division of Lake Bolmen utilize in Results Analysis

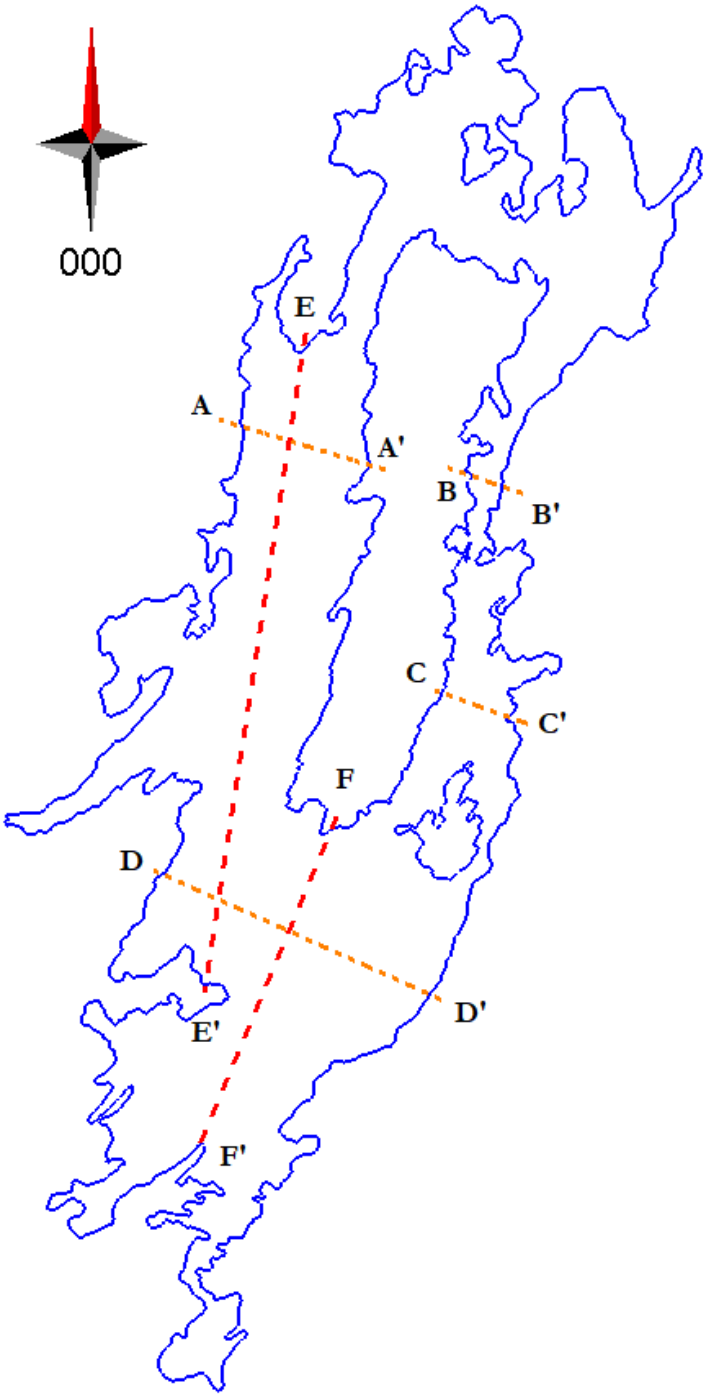

Figure 6:6 Cross sectional of Lake Bolmen utilize in Results Analysis

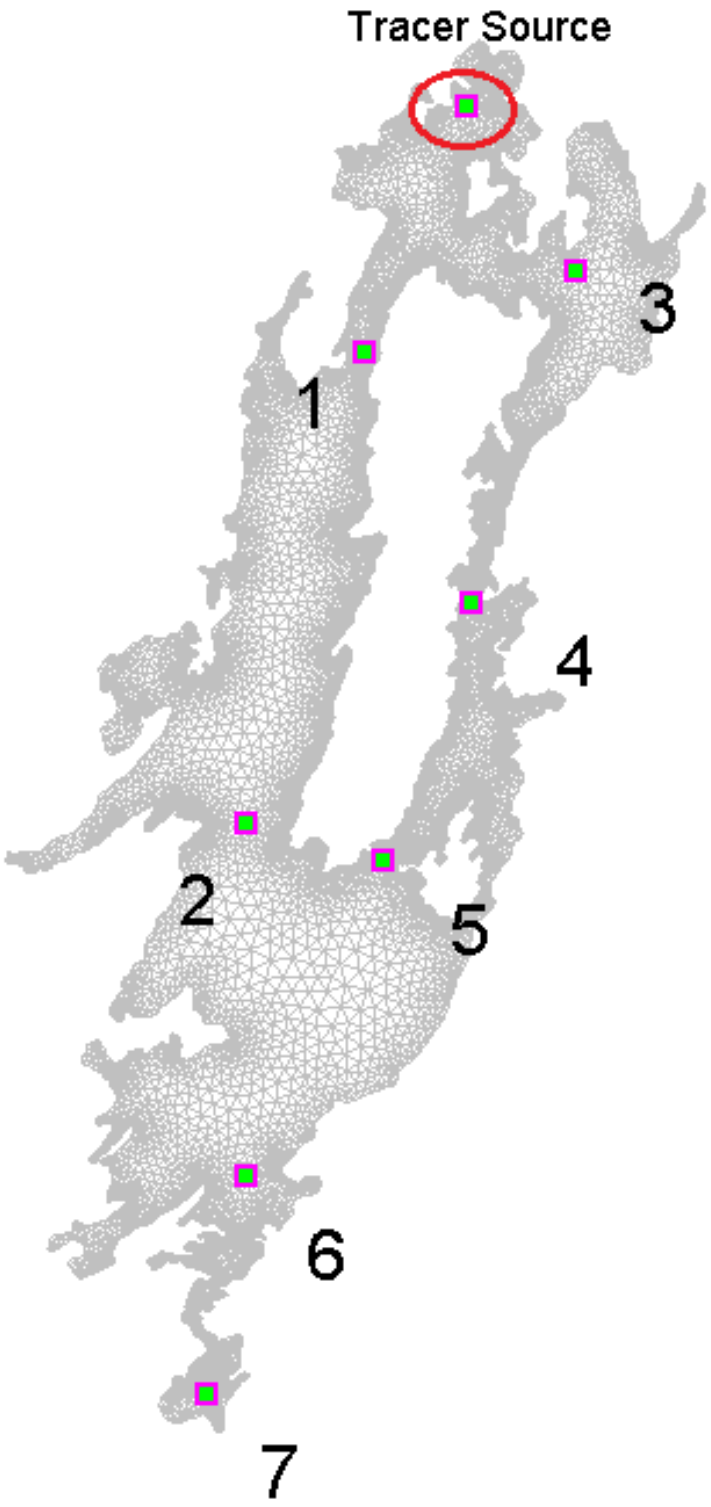

Figure 6:7 Model gauge points (Nodes) of Lake Bolmen utilize in Results Analysis

6.3.1.2 Wind Velocity Magnitude Variations

In contrast to the preceding section 6.3.1.1, this part The wind magnitude fixed at 2 ms^{-1},5 ms^{-1},10 ms^{-1},15 ms^{-1},20 ms^{-1} levels while the wind direction remains constant. This simulation was done using the most variable wind direction, which was south-west. The table below summarizes the simulated cases.

Table 6-2 Simulation configurations for Wind Magnitudes

Simulation No	Southwest Directional Wind Magnitude ms^{-1}
7	2
8	5
9	10
10	15
11	20

Similar to 6.3.1.1 the water surface velocity changes needed to be measures for water depth, scalar velocities, and tracer. Simulation can be stopped when the steady-state reached the given condition. Plot the velocities in specific nodes for variation in magnitude of wind to investigate if there are reasonable patterns between wind magnitude and surface water particle velocities. Time taken for receiving the peak concentration of tracer can be plotted and analyzed. Locations represented in Figure 6:10's schematic, as well as the sectional profiles displayed in Figure 6-9.

6.3.2 Stratified water Condition

This section is introduced to investigate the consequences of stratification. Vertical stratifications in density and temperature in lakes are feasible for a variety of reasons, as discussed in the theoretical section. However, because the simulations are confined to TELEMAC 2D, the stratification model cannot be built. As a result, the vertical layers with specified widths cannot be defined. As a consequence, the 10 m water layer was allocated, and a 130 m deep non-permeable barrier was built (see Figure 6-7). As a result, water less than 10m below the surface was not considered in this example. As a result, the uppermost layer may be simulated in this model configuration. Bottom boundary layer impacts, on the other hand, may not offer the exact boundary configurations. Compare the results to the non-stratified example with a wind velocity of 10ms-1 applied to the -southwest event.

Table 6-3 Simulation parameters for Stratified Configuration

Simulation No	**Wind Velocity**
12	10 ms^{-1} from Southwest

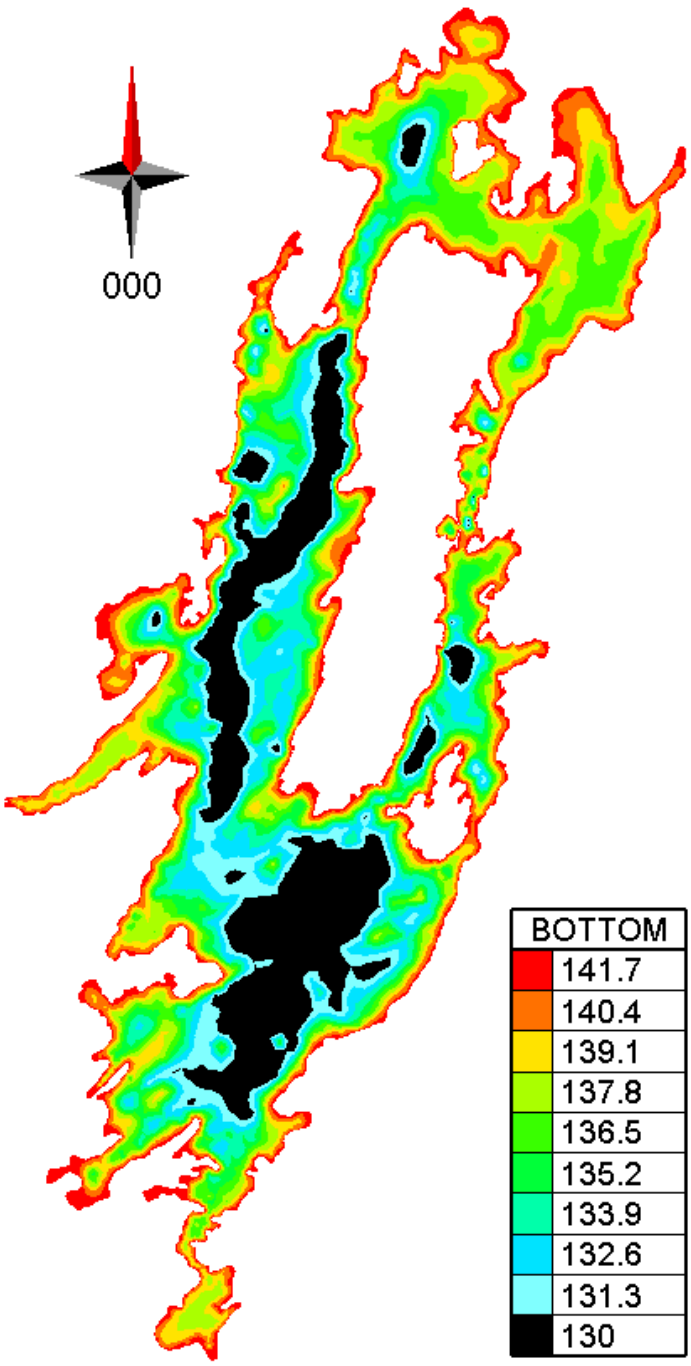

Figure 6:8 Stratified configuration Bathymetry using Blue Kenue

6.3.3 Transient Wind Velocities Actual Data Simulation

This section contains the simulation which was using actual data collected during a certain time period. The simulation was run employing transient wind data to examine how the velocities responded to the real observed wind during a special event. Storm wind conditions are defined as wind velocities more than 17.5 ms-1 (www.zurich.com, 2020). The wind speeds that dominate during days/weeks with high magnitude have been filtered using SMHI data. The Microsoft Excel program was used to extract high wind magnitude data from an existing SMHI data collection spanning the years 1995 to 2001. To simulate the transient wind, the data TELEMAC steering file must be modified to accommodate the transient wind data. The test was performed with the same output parameters such as water depth variation, scalar velocities (UV), and tracer concentration (non-reactive). Compare the results for stratified and non-stratified situations.

Table 6-4 Real Wind Data Simulation

Simulation No	Duration of Actual Wind data
13	2013 Oct-24- 2013 Oct 30 (6 Days)

7 RESULTS

7.1 Spatially Constant Steady Uniform wind 10ms^{-1}[SW]

As previously stated, the most common wind direction detected in SMHI data is from the southwest with respect to Bolmen Lake. Considering the dominant wind direction on Bolmen Lake, the first simulation was carried out using a 10ms^{-1} spatially consistent (operating across the lake) steady uniform wind. It should be mentioned that, even though 10 ms^{-1} is a rather high wind magnitude when compared to historical data, this value was utilized as the initial simulation in this investigation. The 10ms^{-1} magnitude was chosen to detect wind-induced current patterns easily and distinguish minor occurrences of hydrodynamic characteristics in an amplified manner. The observations might be more visible at 10ms-1than than at the 3ms^{-1} average wind speed.

Figure 7.1 depicts the steady-state velocity distribution of current patterns. This vector plot shows the direction of movement in the triangular elements in the mesh constructed. These elements are the representation of a water column having two triangular sides on top and bottom. The other three quadrilateral shaped surfaces at sides. The vector arrowhead pointing to the particles consisting of the elements mean flow direction, And the arrow stem length is proportional to the mean velocity of the particles. After around two days of applying the uniform winds in model simulation, the lake reaches a steady-state setup. The lake's zone number five has two major vortex patterns in the middle. One vortex depicts vector distribution in a clockwise motion, while the other depicts vector distribution in a counter clockwise manner. However, while closely observing, certain vortex patterns may be seen in zones 3 and 4. It can be seen that These vortex emerging areas are located above the deeper lake bottoms. Apart from that, the majority of the vectors are oriented from southwest to northeast. It should be noted that if the user increases the mesh resolution to a higher value, a greater number of vortex patterns may appear in the model results. More elements per unit area

are created as resolution increases. As a result, the model generating additional information throughout the simulation. If the user continues in this manner, further Gyre motions in the vector plots may be noticed that are not evident in Figure 7.1.

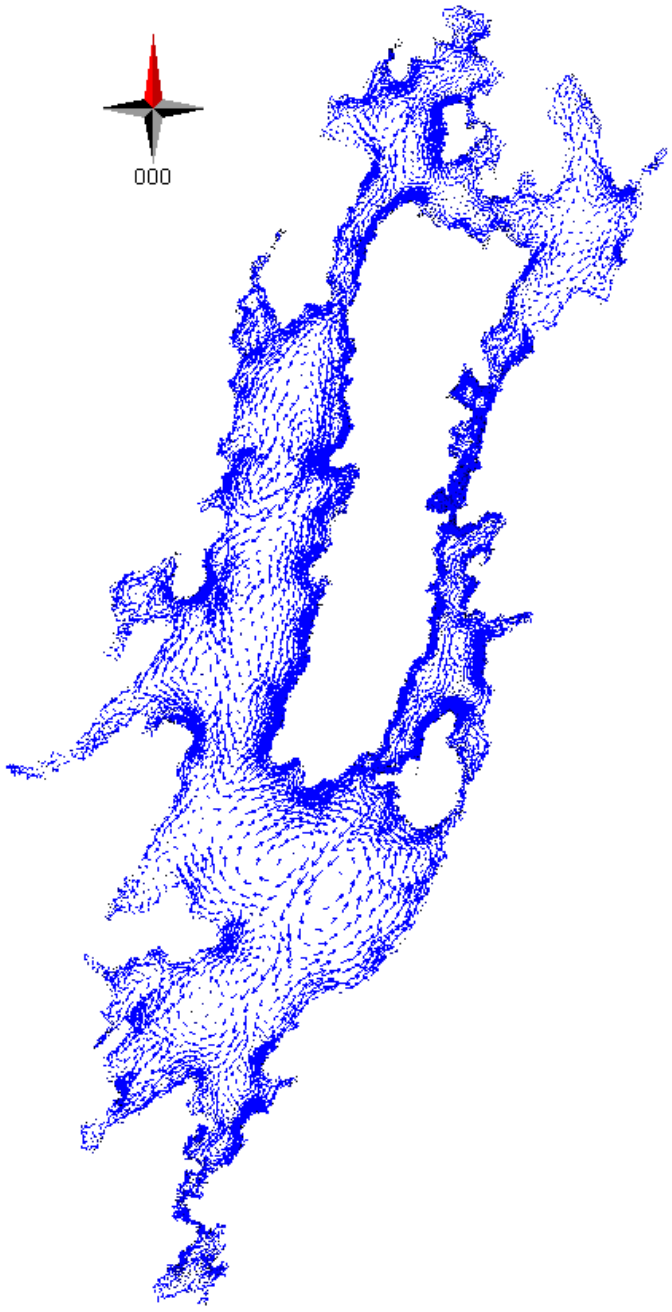

Figure 7-1 Lake current patterns observed for simulating 10ms^{-1} wind from Southwest. Captured 10 days after reaching Steady State Configurations

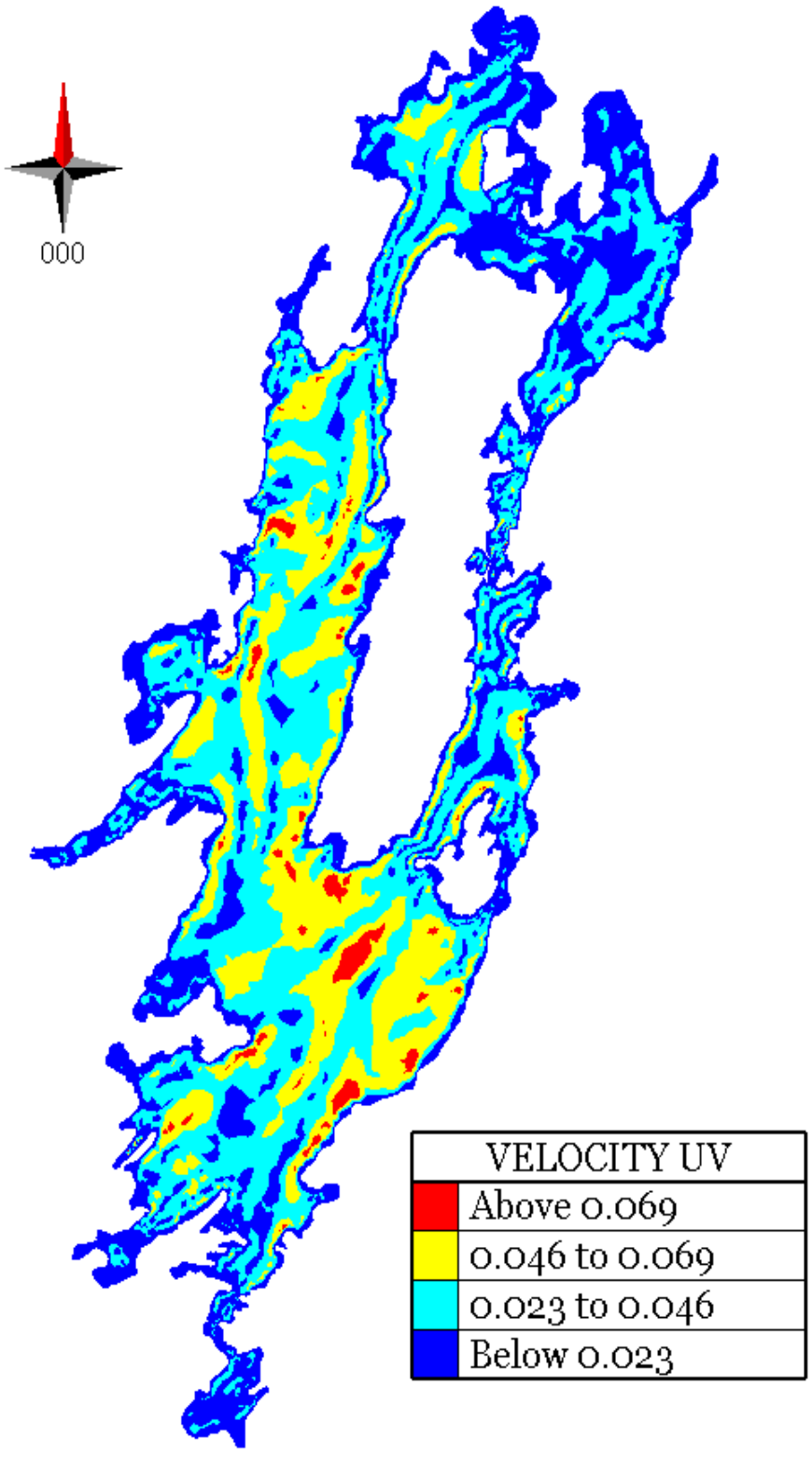

Figure 7-2 Velocity distribution of the surface layer for 10ms-1 (SW).

Figure 7.2 depicts the scalar velocity distribution for the event 10ms^{-1}[SW]. The lake's shoreline has the lowest magnitude of scalar velocities. Moving to the lake's interior reveals progressive scalar velocities, revealing a dependence on water depth. However, this is a not a useful finding because velocity sections with magnitudes smaller than 0.023 ms^{-1} are also seen in deeper areas. However, deeper places have relatively high scalar velocities based on Figure 7.2. Zone 5 has the most extreme scalar velocity distribution. In descending order, the average scalar velocity distribution is Zone 5, Zone 3, Zone 1, Zone 4, and Zone 2. When comparing Figures 7.2 and 7.1, the vortex patterns and the Yellow Red (highest scalar velocity range) appear to be overlap.

Figure 7.3 exhibits the velocity distribution of section F-F' in a steady state. Figure 7.4 depicts the depth profile of the same section taken at the same point in time. Figures 7-5, 7-7, and 7-8, as well as the corresponding Figures in Appendix 2 Figures A-15, A-16, A-17, A-18, show the extraction of velocity and depth profiles from various sections. When all five sections are considered, it is apparent that larger velocity profiles occur at rather deep depths. Because the lake terrain has steep slopes near the shore regions (see Figures 7.4 and 7.6), the velocity distribution profile reveals that the shorelines begin with null velocity magnitude but rapidly grow to a higher magnitude. When the depth profiles and velocity profiles of each part are compared, it is clear that this relationship is prevalent in all of the sections.

Figure 7-3Scalar Velocity along F-F’

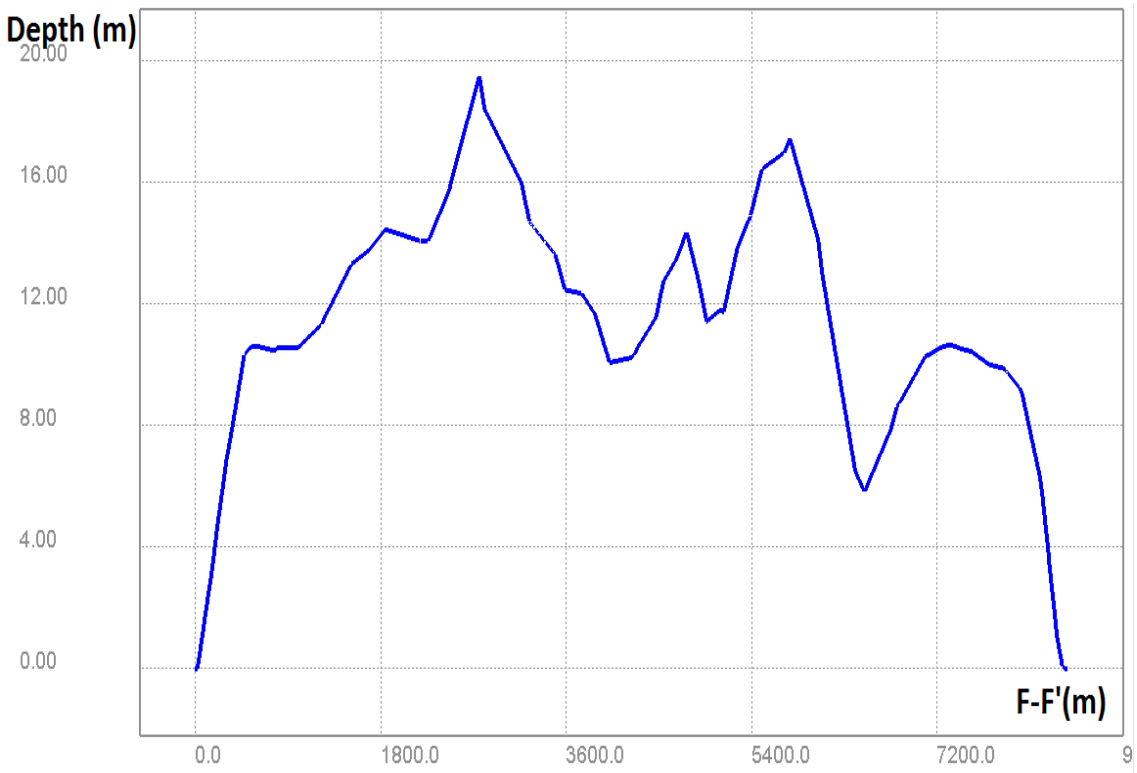

Figure 7-4 Water Depth at Section profile F-F'

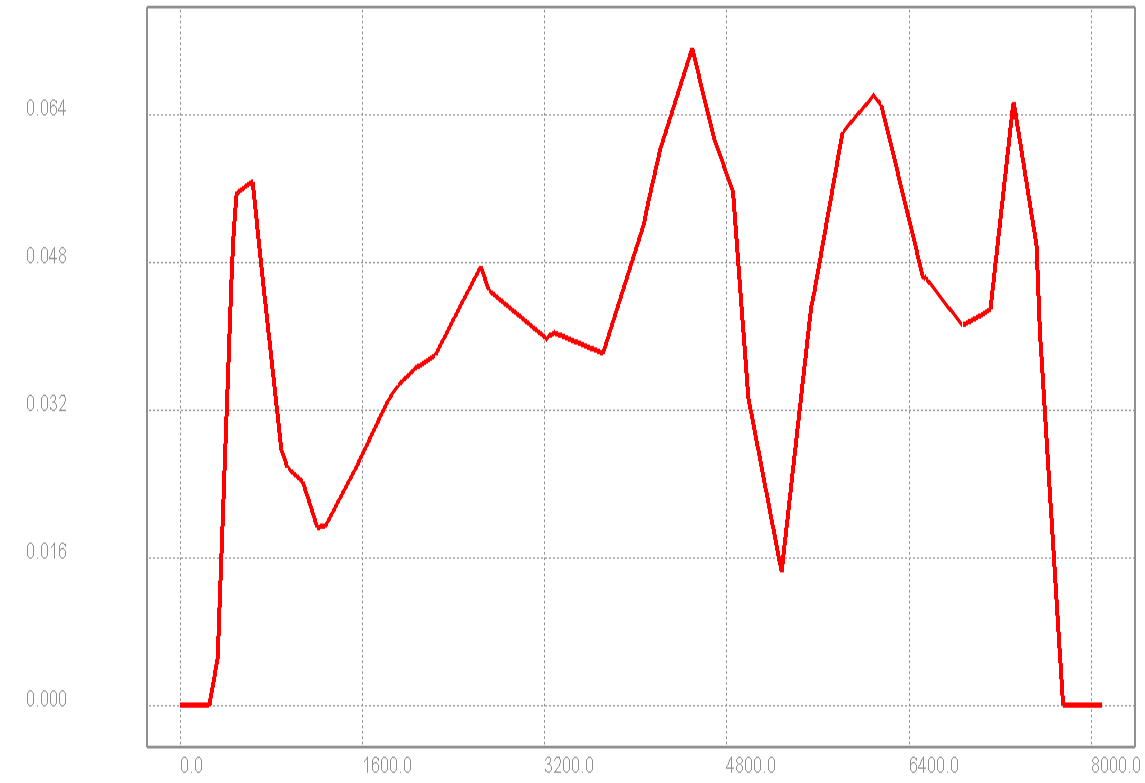

Figure 7-5 Scalar Velocity along section profile D-D'

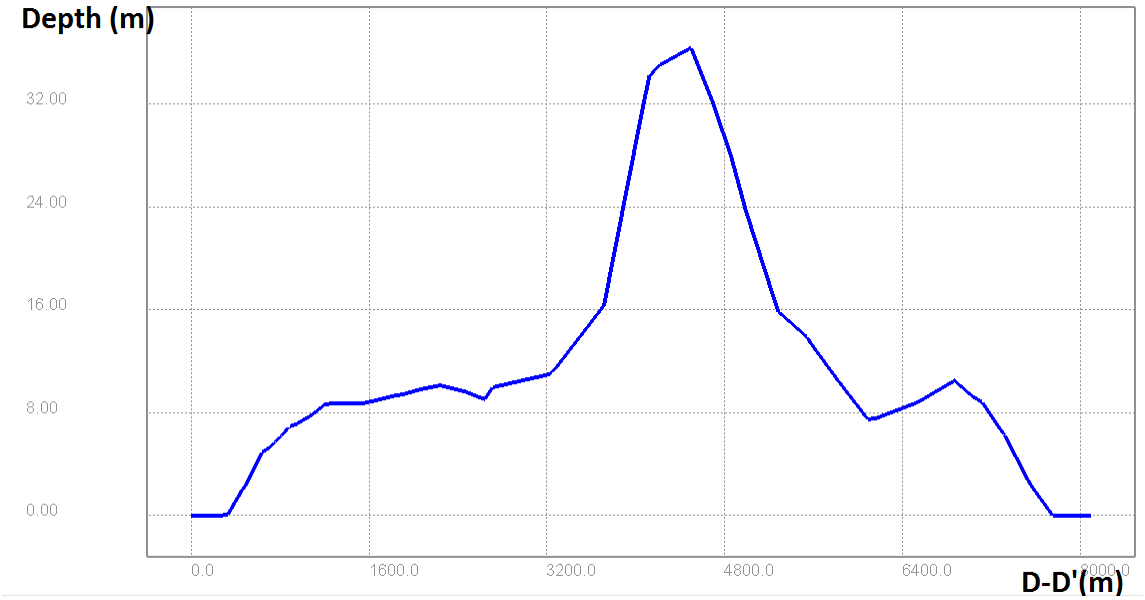

Figure 7-6 Water Depth section Profile D-D

According to Figure 6-10 in the methodology section (6.3.3), the tracer source was released from zone 1 at the Storån river outlet to the lake. It is presumed that the tracer substance is non-reactive to the environment. By modeling the 10ms-1 [SW], one may gain a basic grasp of how the plume coming with the inflow evolves over time. For 7 model gauge locations, the time series analysis for the tracer substance is presented. Figures 7.7 and 7.8 show the tracer material time series for nodes 1 and 2 for the convenience of the readers. The Y axis represents the concentration, while the X axis represents the time period commencing on April 1, 2021. Appendix Figures A19,A20,A21,A22,A23 provide the tracer time series analysis for various model gauge points. All seven measurement locations provide a smooth bell-shaped curve with distinct peak concentrations and periods to achieve the peaks. It is obvious that as the tracer measurement site moves away from the tracer source, the peak concentration decreases. In addition, the number of days required to reach the peak is greater. However, there is a little alteration in this behavior when it comes to Zone 4. It should be noted that measurement point 5 at Zone 4 yields slightly deviating results than the other measurement points.

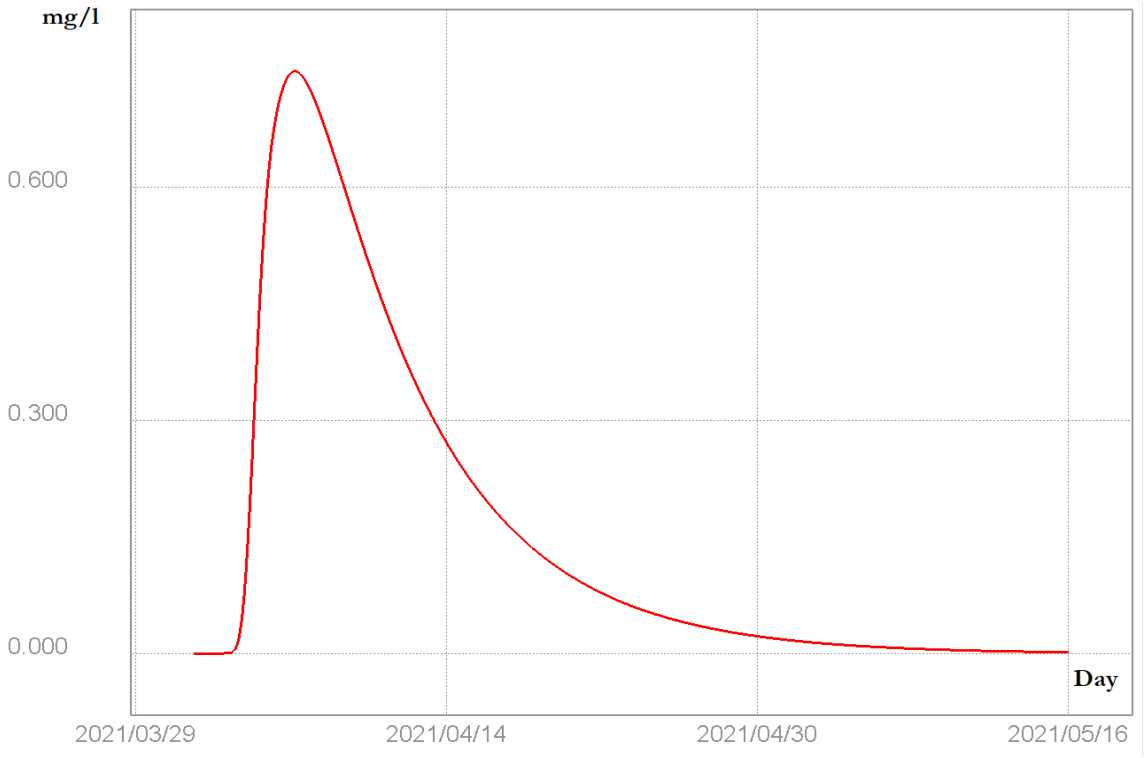

Figure 7-7 Trace concentration at Measurement point 1

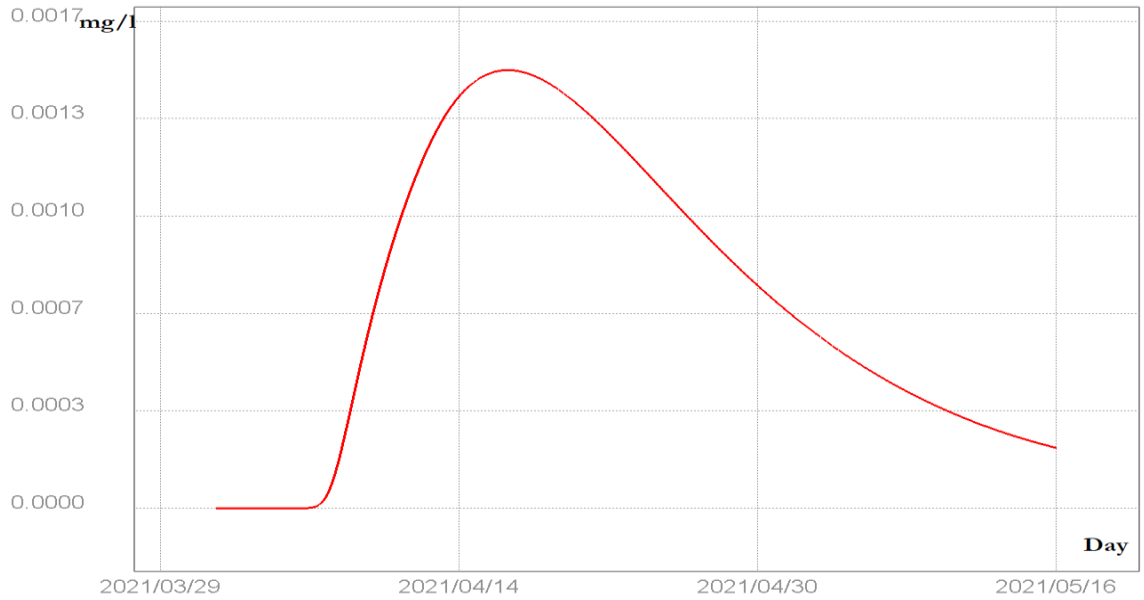

Figure 7-8 Tracer Concentration at Measurement point 2

Table number 7.1 was calculated by taking the tracer concentration duration to reach the peak concentrations into account. This table, however, only provides preliminary estimates and is only applicable for the $10ms^{-1}$[SW] case. However, some interesting results can be obtained by using this Table. In distinct zones, the effective speed is calculated along a given direction (downwards). Zones 1-3 have the greatest solute flux moving speed along the downward direction. Zone 5 with greater depth appears to have a lower mean solute flux moving speed in the particular downward direction.

Table 7-1 Approximate advection rate at different zones for (wind speed $10ms^{-1}$ South-west Direction)

Zone (Measurement Points)	Measurement Distance(m)	Time Elapsed (approx.)	Approximate solute flux moving speed
1 (S-1)	6570	6 day	1095 m/day
2 (3-4)	8827	15 days	567 m/day
3 (1-2)	12447	10 days	1244 m/day
5 (2-6)	8976	16 days	561 m/day

7.2 Steady Uniform Winds: Directional Analysis

The previous section (7.1) presented the findings obtained for the 10ms^{-1} [SW] setup. The simulated results for various wind direction configurations with constant wind speed magnitude 10ms-1 are provided in this section. The alteration in directions are [N], [S], [W], [E], [SE], [SW]. Figure 7-9 illustrates the evolution of tracer concentration in node 2 during a 45-day simulation period. Each color symbolizes a different direction. Winds coming from the south and southwest have a stronger influence. It should be observed that both the concentration and the duration to reach the tracer peak concentration seems to be high in these two directions[S] & [SW]. Everything other directions have relatively lower concentration, as well as higher time, is taken to reach peak concentration.

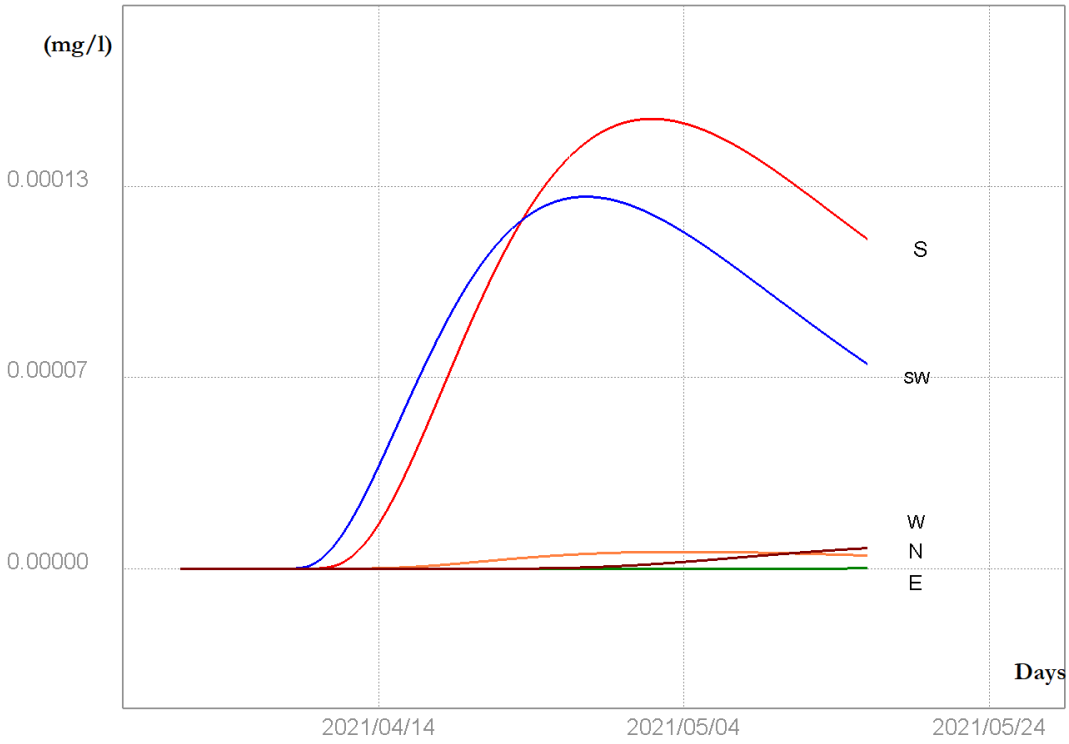

Figure 7-9 Wind Directional variation vs tracer detection time for Node 2

For each measurement point, a thorough examination of the tracer was performed. Table 7.2 contains a summary of the findings. When looking at the first row of the table, one can see that measurement point 1 is located in Zone number one and is 6814 m away from the tracer source. The cell value of 7 indicates that the highest tracer concentration was reached after 7 days in [N] wind setup. Similarly, Another cell value of 9.5 is [E] configuration. Likewise, other row cell values for the remaining direction are tabulated. Similarly, the values of all measurement points are listed in this table.

Table 7-2 Results : Tracer detection time for Directional wind variations

Zone	Node Number	Distance from tracer source (m)	Time Taken to Detect Plume Center (Days)					
			N	E	S	SW	W	NW
1	1	6814	7	9.5	4	6	10	13
2	3	6757	11	10	13	12	13	8
3	2	19261	20	31	13	16	37	35
5	6	28233	33	44	27	31	53	53
5	7	34433	50	51	47	45	60	57
4	5	22799	37	43	19	20	42	35
4	4	15576	45	58	28	27	47	45

Figure 7.10 is a graphic representation of how each wind direction affects tracer peak concentration timings. The horizontal axis represents the various wind directions, while the vertical axis depicts the time measurements in days. Examining the first column in the graph, which depicts the case 10ms-1[N] setup. Each color band reflects the time taken to the measurement point to reach the highest concentration of tracer material. As a result, the black band on the first column denotes the time required to achieve the maximal concentration at node number 3 while the wind is blowing from the north.

Similarly, the additional color bands correspond to the nodes listed in the legend. With a careful examination of Figure 7.10, it is possible to conclude that all nodes have a substantially shorter number of days to report the greatest peak concentrations when the wind is blowing from the south. Similarly, the opposite extreme event occurs in the west direction.

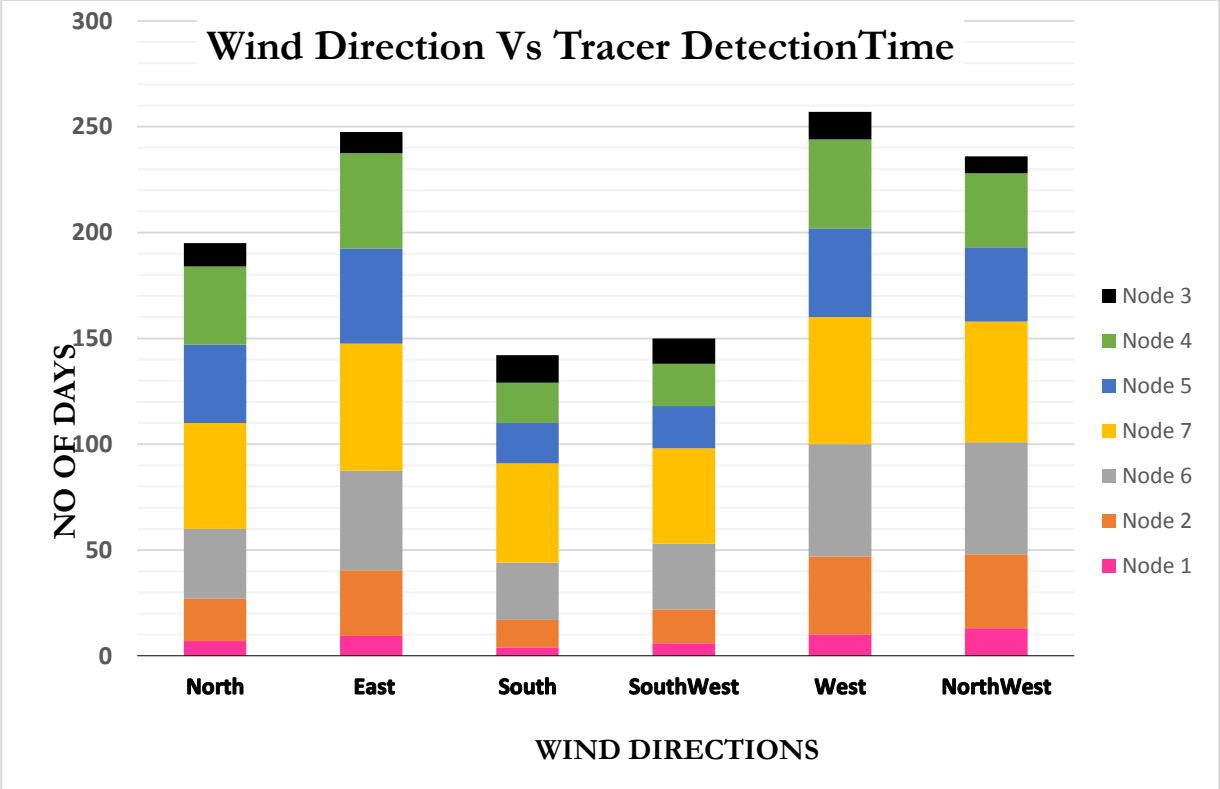

Figure 7-10 Graphical representation for Wind Direction vs Tracer Detection Time

Figures 7-10(A), 7-10(B), and 7-10(C) show the tracer distribution for wind from the north and south at random time intervals during the simulation period of 45 days. To enable for comparison comprehension, the figures are positioned with the left and right sides parallel to each other.

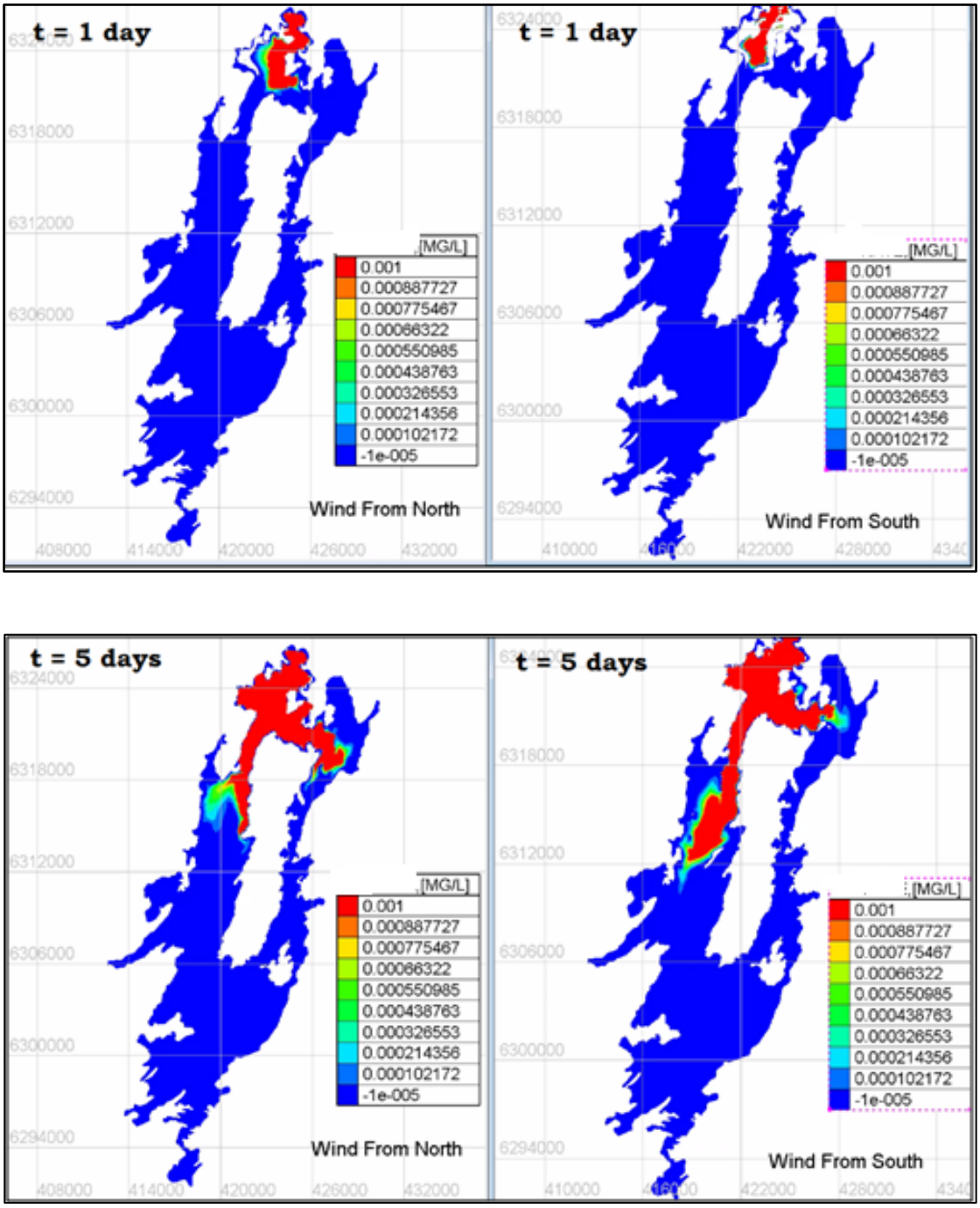

Figure 7 10 (A) Graphical representation for tracer concentration after time of 1 & 5 days

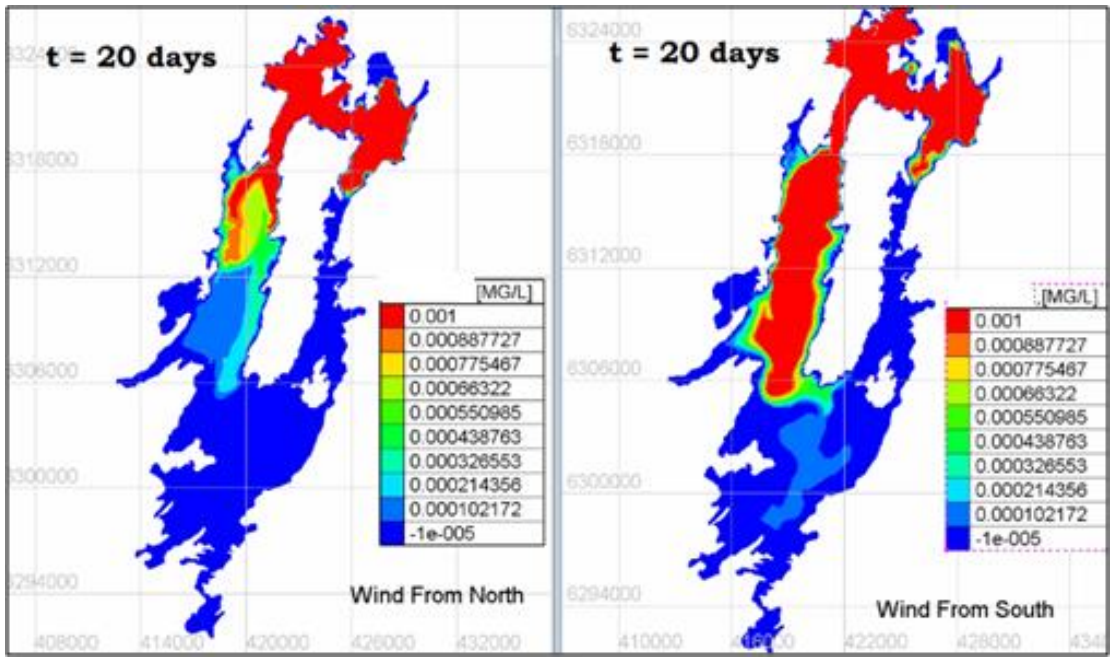

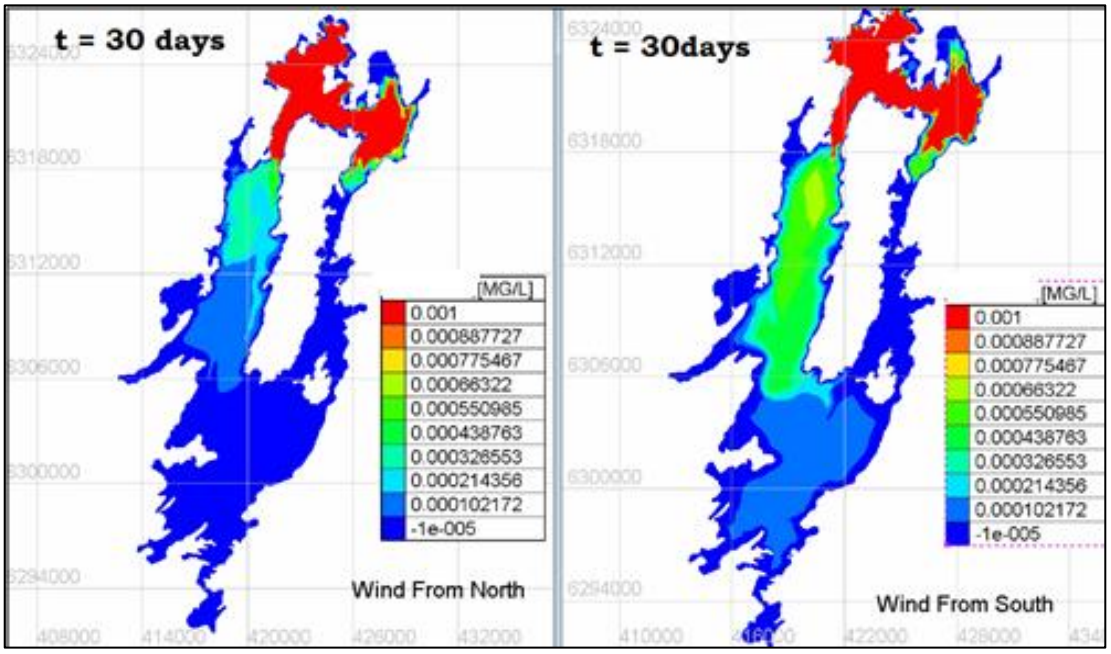

Figure 7 10 (B) Graphical representation for tracer concentration after time of 20 & 30 days

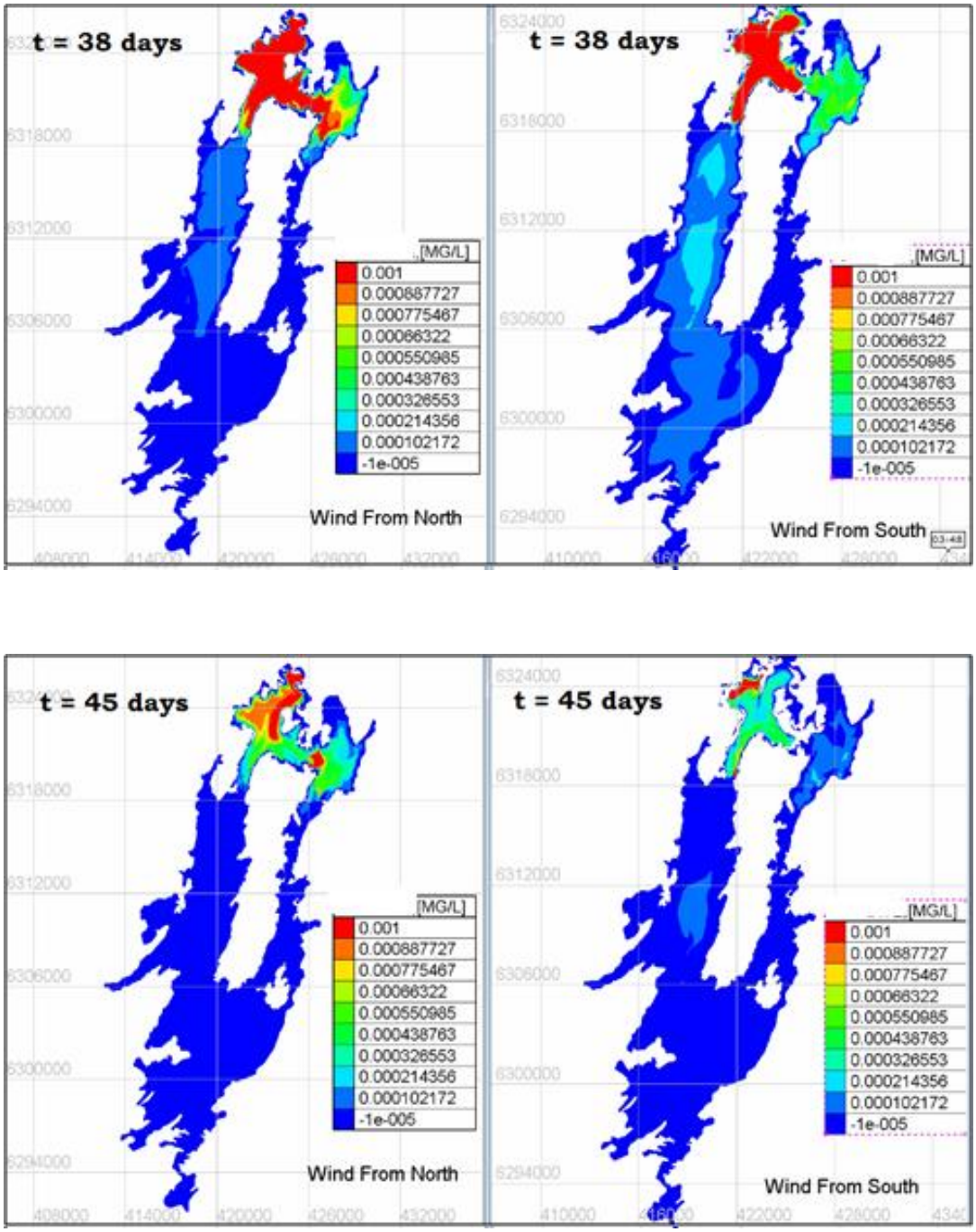

Figure 7 10 (C) Graphical representation for tracer concentration after time of 38 & 45 days

7.3 Steady Winds : Magnitude Analysis

The magnitude of the wind was changed over multiple simulation settings according to the methodology section guidelines. The wind magnitude of 2 ms^{-1},5 ms^{-1},10 ms^{-1},15 ms^{-1},20 ms^{-1} was simulated in 5 independent simulations with the wind direction fixed at southwest[SW]. TELEMAC time series analysis can be used to acquire the scalar velocity variation in a location in a specific simulation. See the Figure 7:11. The time series analysis for all measurement points may be obtained using the same approach. The line graphs in Figure 7:12 were created using the time series analysis for five distinct wind settings stated above.

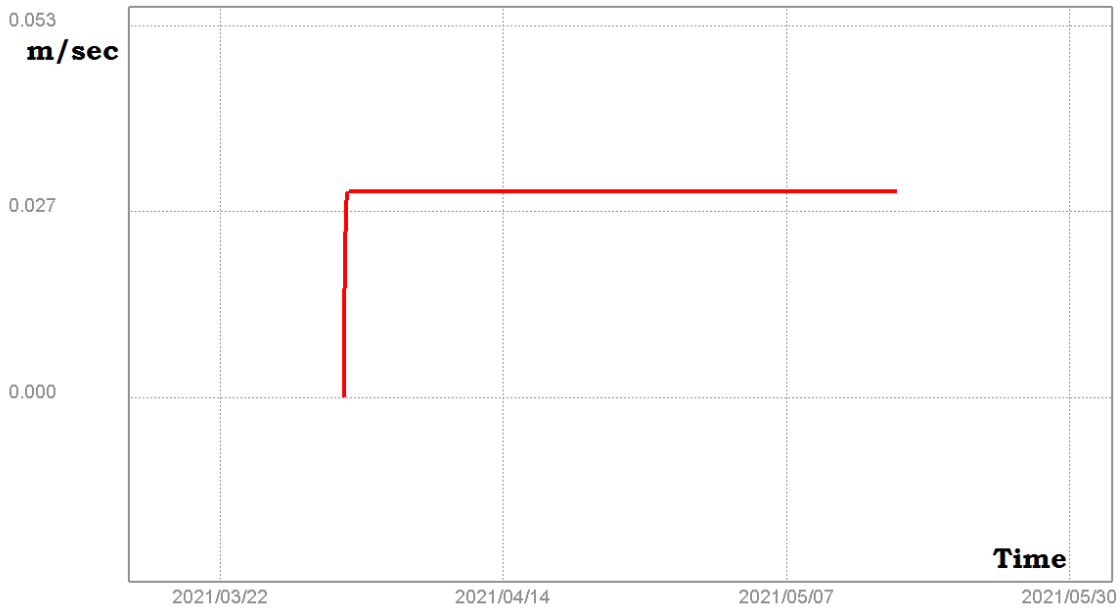

Figure 7-11 Velocity Time series analysis for 10ms^{-1}[SW] in measurement point 2

According to the legend, each line in the graph shown in Figure 7.12 represents a certain node. If one examines Node 1 in dark red, one can see that the steady-state velocity reached for the 5ms-1 [SW] arrangement is around 0.01ms-1. Similarly, the corresponding steady wind velocities for different magnitudes may be calculated. All measurement locations exhibit the same behavior, which is exponential in nature. The same information that may be obtained from 7,12 can be represented in a bar graph for

the convenience of the viewer, as illustrated in Figure 7.13. It is obvious that both Figures depicting the exponential increases in surface velocities as wind speeds increase.

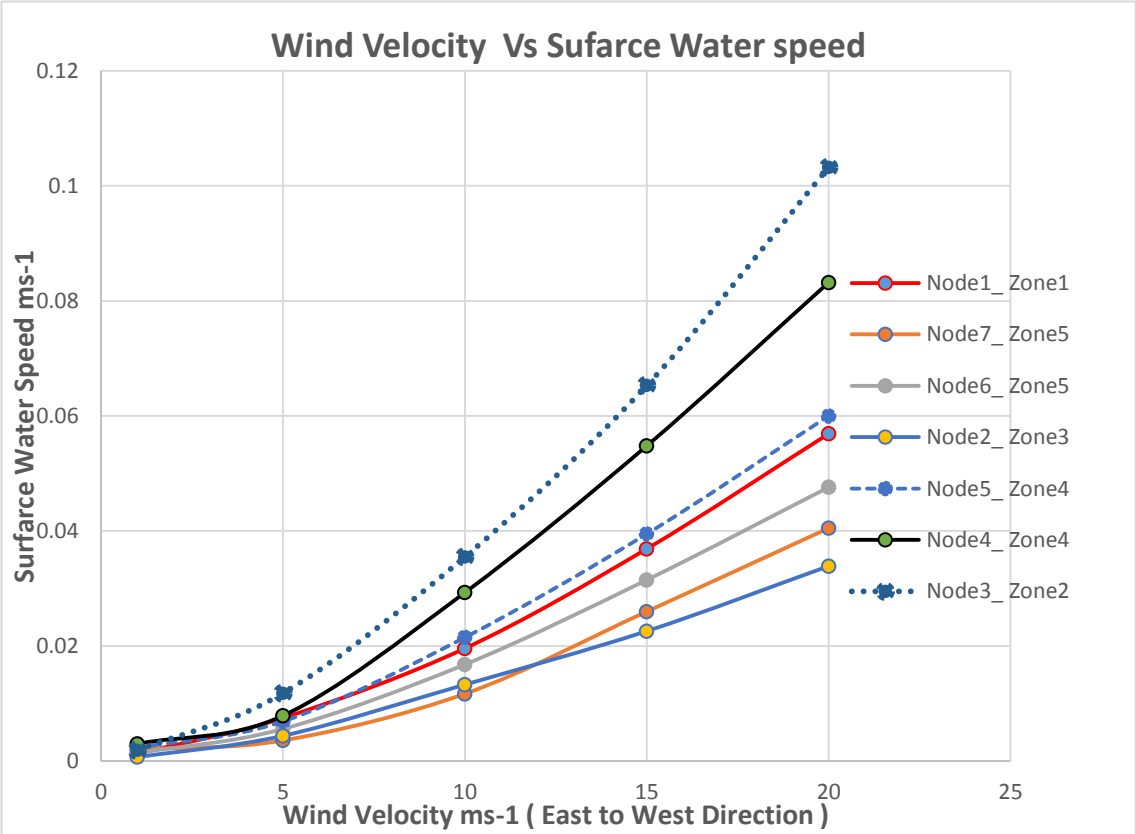

Figure 7-12 Wind Velocity Vs Surface Scalar Velocities at Measurement Points

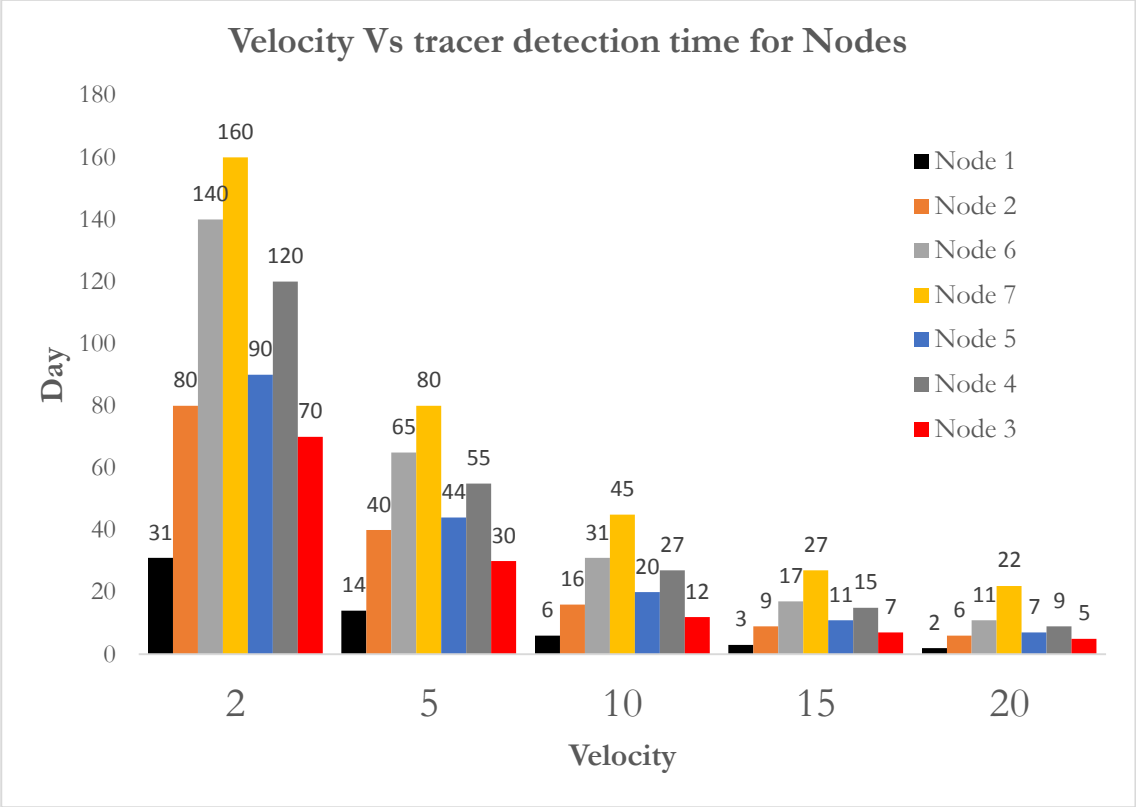

Figure 7-13 Graphical representation for tracer detection time for measurement points vs wind magnitude variations

7.4 Simulation for stratified lake conditions

The main wind direction 10ms-1[SW] was used to approximate the stratified state in the lake. However, there are certain shortcomings in this simulation that can have a considerable influence on the real conditions that predominate in stratification. The comparative evidence is available in both stratified and non-stratified modes. Section 7.1 describes the non-stratified scenario with a prescribed 10 ms^{-1}[SW]. As a result, the reader requests to referring section7,1 for non-stratified simulation.

Considering the vector diagrams in Figures 7.1 and 7,14, which represent stratified and non-stratified lake settings, the vector arrowhead distribution is identical in both cases. However, it is noticeable that the stratified lake simulation has the same size (length) of vector stems in zone 5, which is not the same in the unstratified scenario. Examining Figure 7.15 validates this observation. The scalar velocity distribution in stratified and unstratified cases is depicted in Figure 7.15. The scalar velocity distribution in Zone five is between 0.023 and 0.046 ms^{-1}, with no noticeable red color spots as in the unstratified example. As a result of these findings, it is obvious that the stratified case velocity does not fluctuate in the study area in a wider spread.

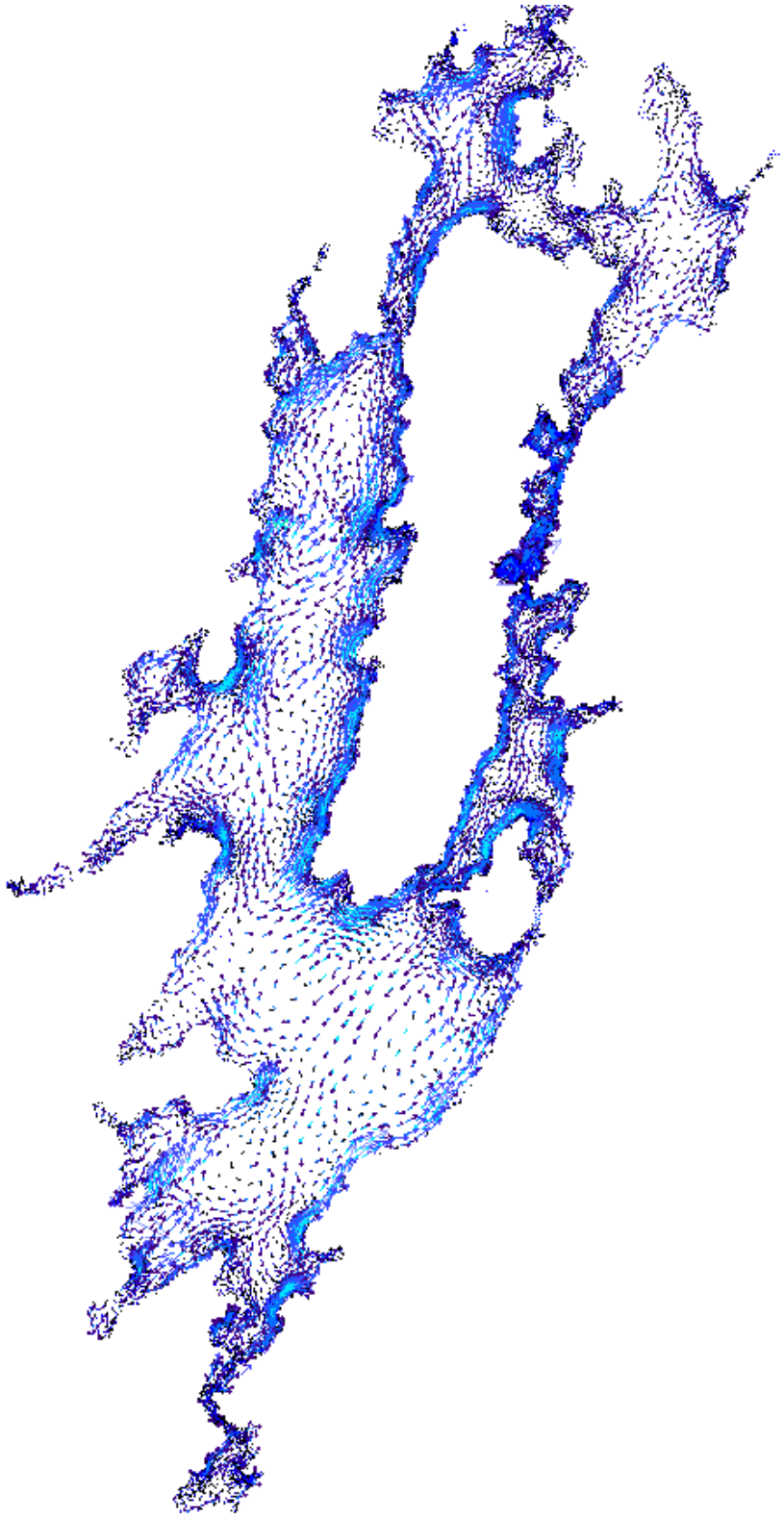

Figure 7-14 Vector plot generated for steady South-west wind of 10ms^{-1}

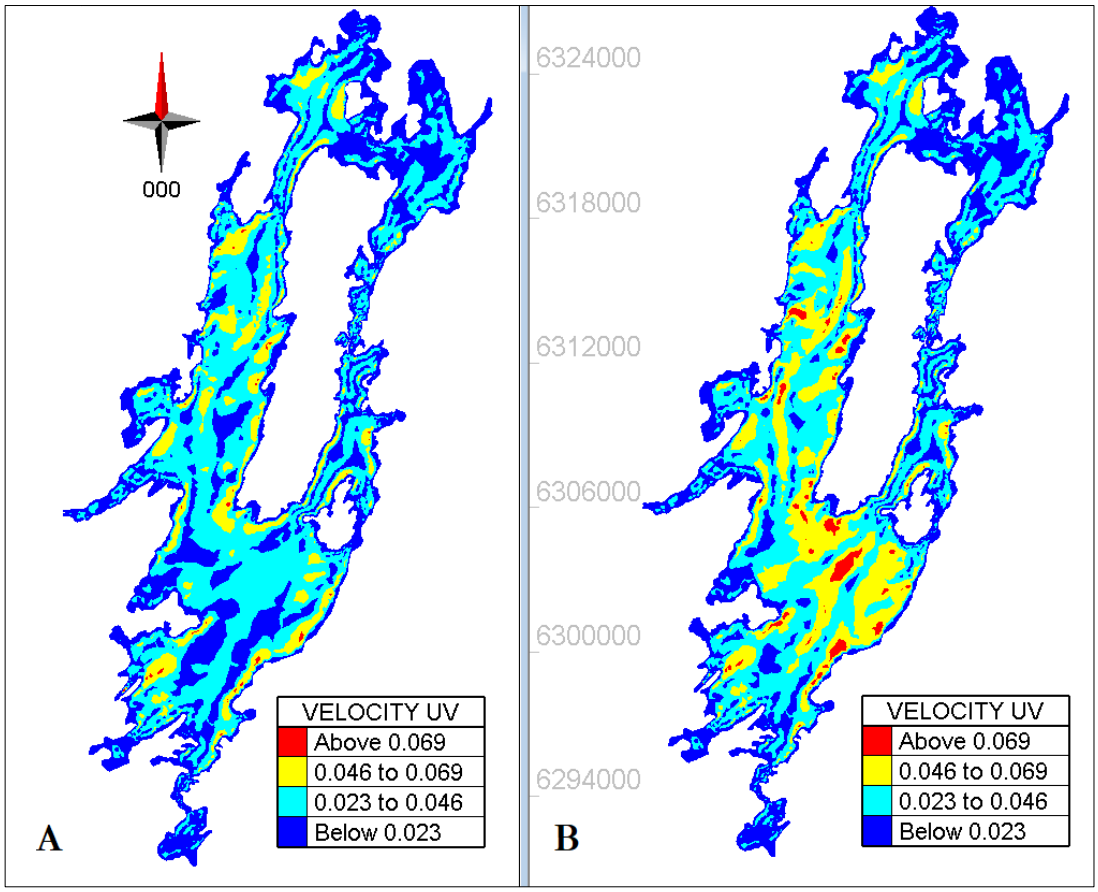

Figure 7-15 Scalar Velocity distribution (uv), A – Velocity contour stratified condition , B - Velocity contour non-stratified condition

Lake sections E-E' and D-D' are depicted in Figures 7.16 and 7.17, respectively. One frequent feature is that the non-stratified portion has higher velocities than the stratified simulation. These Figures depicted the velocity distributions over the length of the cross-sections. It should be mentioned that the stratified and non-stratified plots were built at the same time. For example, after 100000 seconds passed in the simulation and also reached steady-state configuration.

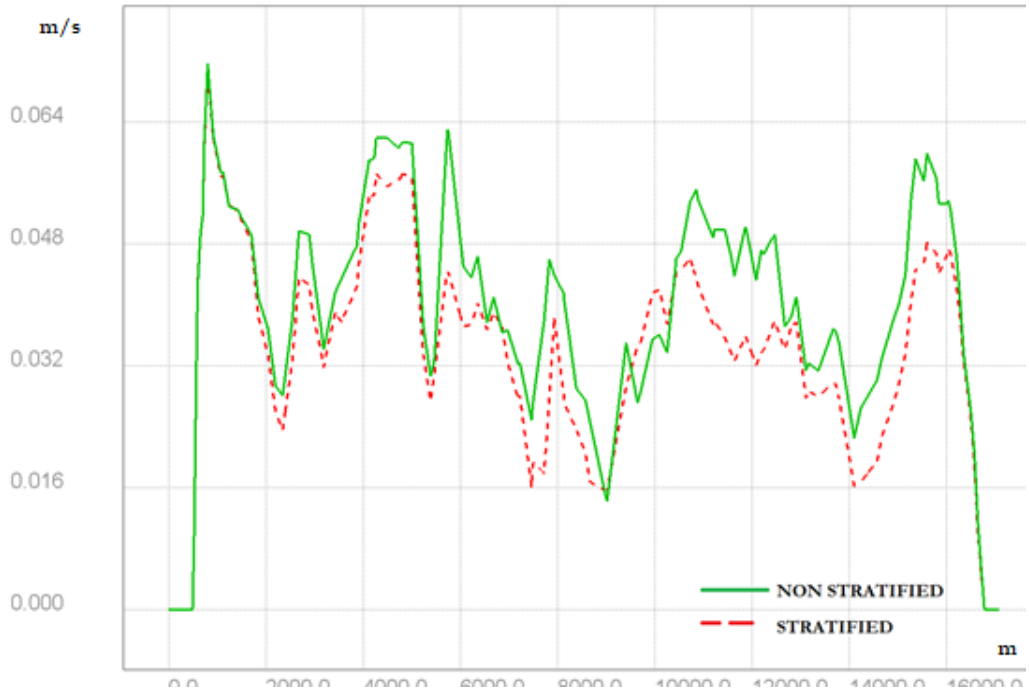

Figure 7-16 Steady State scalar velocity distribution in cross section E for stratified and non-stratified condition

Figure 7-17 Steady State scalar velocity distribution in cross section D for stratified and non-stratified condition

Table 7-3 displays the extracted tracer detection time for seven measurement sites in stratified and unstratified instances. When looking at the detection timings, it is difficult to draw distinct observations and patterns. However, for the Stratified instance, the majority of the measurement stations anticipation of higher durations to detect the tracer peak concentrations.

Table 7-3 Results : Tracer time detection for Stratified and Non stratified simulations

Node Number	Zone	Distance (m)	Time Taken To Reach Tracer Plume Center	
			Stratified $10ms^{-1}$[SW]	Non Stratified $10ms^{-1}$[SW]
1	1	6814	6	6
2	3	19261	17	16
6	5	28233	30	31
7	5	34433	37	36
5	4	22799	21	20
4	4	15576	28	27
3	2	6757	12	12

7.5 Transient wind: Simulation for storm event

As described in the methodology Simulation of wind for 24/05/2013 to 1/06/2013 for the period including the storm even “Jude” following results were generated. It should be noted that the most frequent wind during this period is from Southwest. Since the simulation is based on the actual time-varying wind data only the time-varying parameters can be presented. Such as nodal depth variations, velocity variation. Time series analysis for measurement points 1, 6, and 5 are shown below. In contrast to the steady-state situation, the temporal transient wind simulation exhibits varying scalar velocities at each measurement point. The storm event is easily distinguished from the rest of the graph by its rapid peak appearance. During the storm, the greatest wind speed was 13 ms-1. When the graphs are compared, it is clear that the wind influence is stronger in Zone 1, which is located in the northern half of the lake. However, it should be noted that the depth variation in the nodal points are insignificant and do not discussed in this chapter.

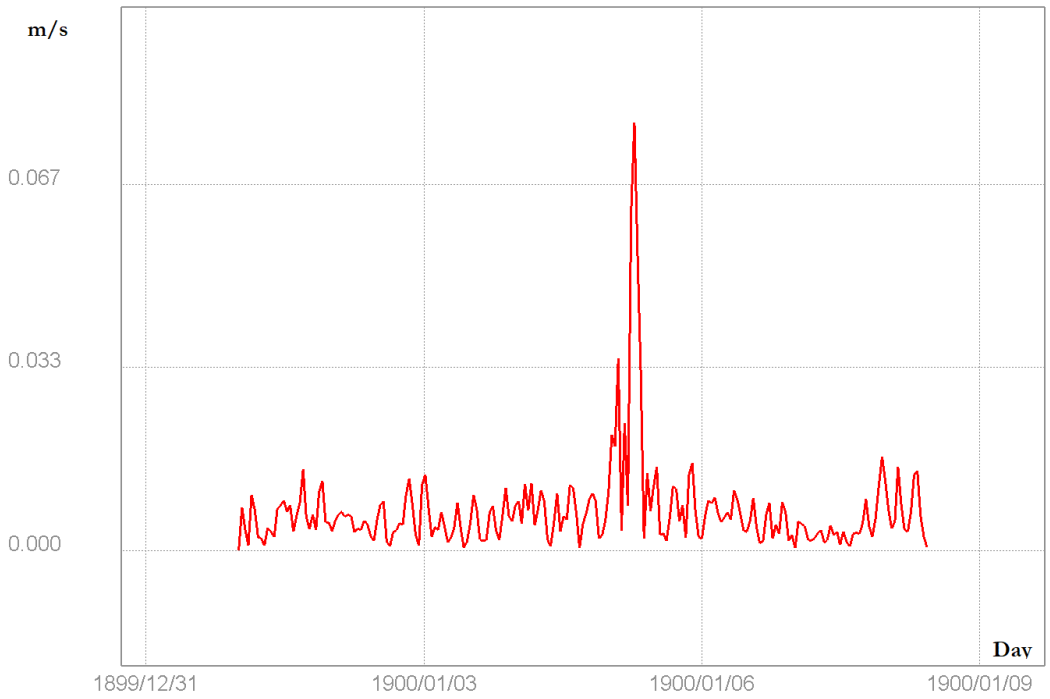

Figure 7-18 Velocity time series analysis for storm event at measurement point 1

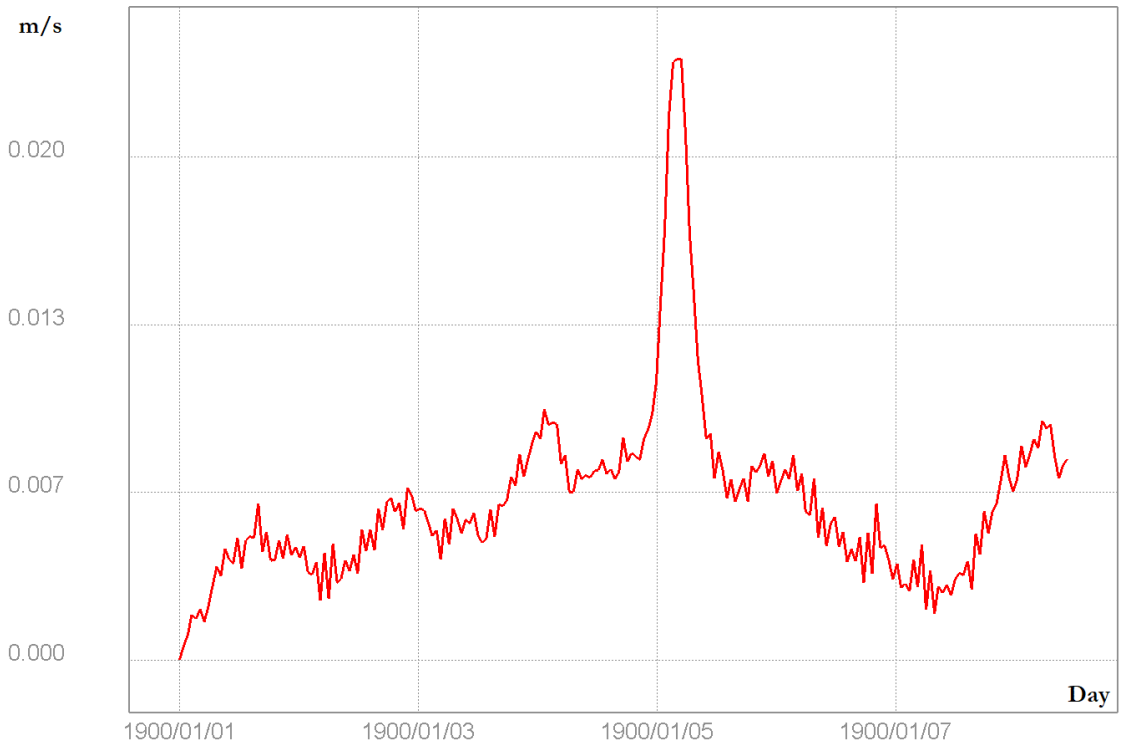

Figure 7-19 Velocity time series analysis for storm event at measurement point 6

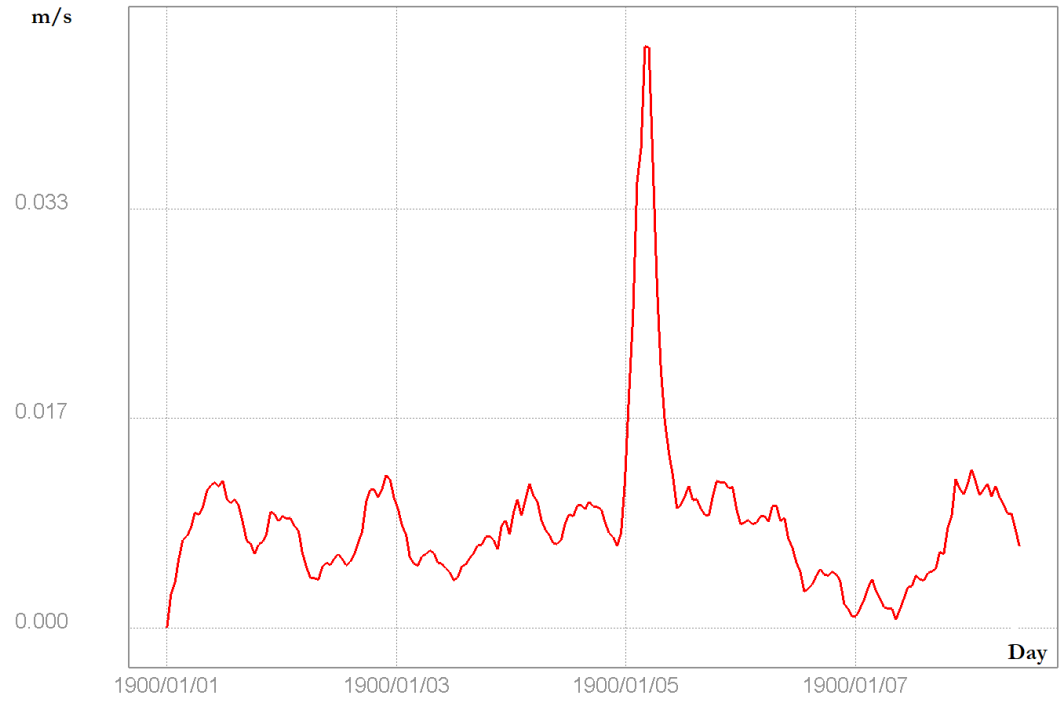

Figure 7-20 Velocity time series analysis for storm event at measurement point 5

8 DISCUSSION

8.1 Spatially Constant Steady wind 10ms^{-1}[SW]

Swirling motion/eddies can be found in deeper places, such as zone number 5. This might be caused due to the magnitude of wind-induced shear stress. According to Eq number 2.1, the wind-induced shear force increases as the wind shear acting surface area increases. A closer look at Figure 7.1 reveals that zone 5 has a larger undisturbed surface area than the other zones. In this area, there are no islands or obstructions. As a result, the drag force on the water is greater in zone 5. Then wind-induced drag force is proportional to the velocity of the turbulent water flow created. As a result of the greater drag force, there is more turbulence. Due to this high turbulent nature, the mixing effect in these areas could be relatively higher. In closer relation to this, zone number 3 has the second-largest undisturbed area, and this zone also has relatively higher scalar velocities. Because of the strong turbulence in these regions, the lake bottom sediments may be influenced by these eddies. These eddy currents may mix sediments with the water mass over them. Because of the swirling effects, sediments immediately under these swirling motions may have a chance to reach the top.

The tracer analysis results are more important when evaluating the material transport phenomena in the lake. According to table 7.1, the mean advective flow is higher in zone number 3. It is three times greater than zone number five. As explained in section 2.2, advection is the mean flow of solute/tracer material along the direction of the flow movement. As a result, for this [SW] wind configuration, zone number 3 has a greater solute flux moving speed. Therefore, advection is expected to be high in this zone. The presence of swirling motion in zone 5 indicates that the advective flow has been disturbed and the turbulent flow has begun. As a result, it is losing its flow direction. This might be one of the reasons why zone 3 has a higher advective velocity than zone 5. However, if the lake's inflow and outflow were taken into account, the findings would be more realistic. As a result, turbulence at the inlet and outflow is also taken into account.

The tracer time series analysis of the measurement stations is depicted in Figures 7.7 and 7.8. Each graph has a bell-shaped curve, as anticipated due to the diffusion transport process. Diffusion is important, as stated in section 2.2. It is reasonable to consider that the setup is in a dynamic state, with both molecular diffusion and turbulent diffusion present within the lake. Because of diffusion, some tracer-solute molecules will arrive at the measurement site before the advective movement at the plume's core. However, looking at the tracer time series analysis of all the measurement locations, it is evident that the tracer detection to the peak takes longer when it moves down the side of the lake (southern). This might be attributed to a variety of factors. The turbulent and diffusive fluid behavior is anticipated to be more prevalent in zone 5 than in zone 1 due to apparent swirl motion. As a result, the material transport mechanism inside zone 5 is higher than zone 1 due to turbulent diffusion.

The majority of the elements in Figure 7.1 vector plot diagram are oriented south-west or northeast. This might be caused by the instant drag force on the water layer. During the steady-state configuration, continuous wind direction and an intense uniform wind field might create the drag, resulting in vectors heading SW. As shown in theory section 2.2, drag forces cause water flow movement.

8.2 **Steady Wind: Directional Analysis**

According to the wind directional variation results, the [S],[N] orientations had much shorter tracer detection times. This demonstrates a strong correlation between wind direction and continuous water surface along that path. When we evaluate the wind from the south, the most unbroken uniform wind drag exists in zones 5 and 3. Because of the major islands (Bolmsö, Rääöns) in the lake's center, the wind shear may be disrupted, thus induced shear velocity from [W][E] directions may be blocked.

As a result, these directions have low scalar velocities and higher tracer detection times. Skeletal effects, such as [W],[E], may have an influence. This argument is more likely to be adequate since the tracer detection periods from West and East are almost the same and longer than those from South and South West. When considering the wind from the [N], this appears to be a similar surface area to [s] directional drag.

8.3 Steady Winds: Magnitude Analysis

According to the results of scalar velocity distributions obtained from Figures 7.2, A 24, A25, A26, and A27, wind velocity has a direct influence on water flow in the lake. According to equation 2.2, wind induce share is proportional to the square of wind speed ($\boldsymbol{\tau} = \rho\, C_{10}\, U_{10}^2$ (Nm^{-2})).This provides a solid rationale to support the behavior of the diagrams above. The stronger the steady wind, the more turbulence the velocity generates on the surface layer. This also implies that the high velocity may intensify the mixing effects in the Lake.

Figure 7-14 depicts the tracer time necessary to reach each measurement station. As a result, low wind magnitude necessitates a longer detection time. Strong wind magnitudes, on the other hand, need fewer days to show the tracer material. This demonstrates that higher wind magnitudes produce stronger advective currents than lower velocity winds. This also lends credence to the notion that higher velocity magnitudes result in more mixing in the lake. This might be the cause for displaying exponential nature in the Graph for Velocity increments.

8.4 Simulation for stratified lake conditions

Section 7.4 provides the simulation results, which illustrate the less developed scalar velocities in a stratified condition compared to a non-stratified one. It is assigned that the depth of the water layer in the stratified version is restricted to 10 m. Zone 5 regions with resulting constant speeds ranging from 0.023 to 0.046 in stratified configuration. Non-stratified flow conditions exhibit greater velocities for the same wind in corresponding locations in zone 5. Possible justification is not evident based on the theoretical background provided. Model input data can be used to offer plausible reasoning. The friction coefficient in the layer was set at 0.035, the same as in the non-stratified situation. This, however, may cause the resistance to produce a more dynamic flow. This stratification model may be further investigated by varying the frictional coefficients and seeing the output. However, based on the available data, the stratified configuration is less turbulent, resulting in lower mixing capacities.

In the perspective of lake transport, the non-stratified condition has a greater advective mean flow current. However, considering the scale of the simulation timeframe, the variations are minor. As a result, this implies that lake stratification has very little impact on the formation of convective currents. However, as previously stated, the simulation settings are not near to reality. friction coefficient might have a significant influence on these results. Therefore results might not accurate. .

The model was simulated under the lake setting with a Lake number higher than one, as indicated in the theoretical portion. This suggests that the thermocline in the center of the layer is stronger than the wind-generated currents to deflect. However, this simulation only shows the changes that are significant due to the summer winds. Temperature variations eventually cause stratification in lake Bolmen layers owing to changes in water density. Previous research has shown that density variations can be observed. Stratified water conditions have been seen in prior research during the summer and winter. Figures 28-29 in Appendix A provide evidence for stratification in Bolmen Lake. However, the 2D model cannot accommodate for density changes in the vertical depth profile (layer by layer approach).

To have a better understanding, the user may create a 3D model and apply different density profiles to the horizontal layers. Actual wind data gathered over the course of a year may be used to simulate this model. As a result, the user may recreate all seasonal fluctuations. This enhanced model will provide more detailed information than the existing model. In this way, the frictional coefficient problem that arose in the current model will be eliminated. However, 3D modeling was not within the scope of this study, and it was not produced due to time and budget restrictions.

8.5 **Transient wind: Simulation for storm event**

Comparing Figures 18, 19, 20 showing the time series analysis, it is apparent that storm events have created abrupt velocity changes in water. During the entire simulation, the steady current directions were not observed due to varying wind directions. Rather Observed continuously fluctuating vector plot distribution over time. Since momentum is changing in the surface layer due to wind-induced shear, it is anticipated that flow is more turbulent during this simulation duration.

8.6 **Model Validation**

According to multiple researches based on Swedish lakes, Bengtsson(1978) revealed that the ratio between wind and surface current speeds is in the 1-2 percent range. By comparing the results obtained in this study for surface water speeds for uniform steady spatially constant winds section 7.4, it can be observed that the Bengtsson statement is greater conformity and valid. As a result, in terms of water current speeds, the model behaves more realistically. In the second conclusion, Bengstonn claims that the ratio is dropping as the wind increases. This is in direct opposition to the results obtained from Section 7.3 Because it is apparent that the surface layer's scalar speed increases with increasing wind speed, even if the magnitude is tiny. The second conclusion, on the other hand, is not particular with wind speed magnitude to compare meaningfully.

As per Lick(1976) research work on numerical modeling of lake currents in three dimensions, the results are very congruent with this study. The most accountable aspect of his work is that He used the constant viscosity model, which is also used in this analysis of Bolmen Lake. Lick demonstrates detailed analysis of the model and physical measurements in Lake Detroit, Niagara. Lick's test of 10 ms^{-1} wind from 50 degrees to the south from the west is more comparable to the 10 ms-1 [SW] condition in this study. In the overall profile of Lake Detroit, the surface water speed at 0.4 m from surface water level gives scalar velocities ranging from 0.005 to 0.5 ms^{-1}. This Bolmen investigation yields 0.003-0.1 ms^{-1}, which is quite close to the range of the Lick's trials. However, lake dimensions are not directly analogous because Detroit dimensions are substantially larger and deeper than Lake Bolmen. The Lick's research shows that the average depth in Detroit Lake is 60m, but the average depth in lake Bolmen is substantially lower, that is approximately 16 m. As a result, high magnitude surface water velocity can be expected in Detroit Lake surface water. This criterion confirms Licks' investigations, which demonstrate 0.5 ms^{-1} in the maximum speed of surface water. The Lick experiment results show that the findings of this investigation are more reasonable.

Mofidi and Hesari (2018) presented a comprehensive analysis of the link between water depth and eddy movements in the Caspian Sea for wind-induced currents. In this work, the finite difference approach was used to do numerical analysis to determine wind-induced currents. And the Mean Absolute Percentage Error (MAPE) was used to calibrate this specific investigation. According to this study, the monthly mean velocity over the Caspian Sea is 3-6 ms^{-1}on this period of time. The model simulation shows to have maximum values of roughly 5 cms^{-1} in shallow water locations. This data also indicated a close relationship between Bolmen lake surface scalar velocities. The gyre movements are concentrated towards the sea's deeper regions due to average winds. This is remarkably similar to the results observed in Zones 5 and 3 of this investigation. Furthermore, depending on the wind direction, this study reveals more evidence in the directions of the gyre motion (cyclonic or anticyclonic). The Mofidi and Hesari's study shows that winds coming from the north and northeast cause cyclonic gyres in deeper locations. Figure A 7 shows how the vector plot patterns in the Bolmen Model behave similarly in clockwise motion in deeper areas owing to north winds. However in Bolmen simulation cannot extract definite direction inclined to cyclonic or anticyclonic motion very clearly.

Lake Taihu in china was modeled using the shallow water three-dimensional model in Delft 3D(Liu, Ye, Wu and Stive, 2018). The non-buoyant conservative tracer was used to simulate and demonstrate the temporal and geographical scale of the hydrodynamic circulation produced by the wind across Taihu Lake. That is similar to the modeling and tracer analysis performed in Bolmen Lake. In the Bolmen Study setup, the $10ms^{-1}$ [NW] wind in Taihu Lake northwest wind exhibits very similar proximity twin gyres patterns. It should be highlighted that the water current vector distribution in the Southeast wind and Northwest wind configurations in Taihu Lake and the North and South wind configurations in Bolmen Lake are quite comparable. The commonality in both experiments is the production of completely opposing current patterns in opposite wind directions. It should be emphasized that in both studies, the clockwise and counterclockwise movements are just interchanged in contrast to the above-mentioned configurations. As previously stated, the gyre patterns in both studies are seen in deeper regions rather than shallower ones.

Cheng and Rochfort (2011) conducted similar tests on Kamaniskeg Lake, which is located in the Madawaska Valley in northern Ontario. The depths of this lake are comparable to those of Bolmen Lake, which are less than 40 meters. The lake's direction also exhibits more complicated bathymetry, similar to that of Bolmen Lake. The Danish Hydraulic Institute's 3D hydrodynamic model "MIKE 3" was used in this work. A 30-day simulation period was used in this investigation. The observed flow patterns for the top surface are quite close to the Bolmen findings. That is, the relative velocity at the surface is 2-3% of the wind speed, and the observed gyre patterns are closer to the deeper areas. Furthermore, another comparable research (Baduna and Önder, 2004) reveals similar surface velocity distributions and gyre patterns.

9 MODEL LIMITATIONS AND MEASURES TO DEVELOP

Shear forces operating on the water's surface as well as Coriolis effects were taken in to study for TELEMAC 2D modeling in Bolmen Lake. The constant temperature, density, and viscosity conditions were assumed to exist across all simulation configurations. In actuality, however, this situation would have been very different from the mathematical modeling in TELEMAC 2D. A uniform homogeneous water profile with constant temperature, density, and viscosity will not exist in reality. However, by effectively utilizing TELEMAC subroutine programming, these non-homogeneous time-varying environment characteristics can be integrated. However, these minute computing parameters will consume more time and power to processing.

The layer stratification was considered as a no-flow static boundary, which requires a liquid layer surface at the bottom, the simulation of stratified lake conditions may have a lesser depiction of actual findings. However, there is no way to add vertical density or temperature fluctuations in a 2D model. As a consequence, if the simulation can be done using a 3D model while taking into account layer stratification based on temperature and density distribution, the findings will undoubtedly be more accurate.

In addition, vertical currents in lakes are completely ignored in this research, which solely considers horizontal currents caused by horizontal tractive force. However, this is a deviation from realistic behavior. Water mass is subjected to create Langmuir circulations in a vertical direction. These vertical currents causing sediment transport and mixing in the lake. So future studies can consider this aspect for more realistic modeling.

Wind-induced transport and mixing is a combination of diverse forces and energies. Considering all these influences of components like Chemical reactions, Evaporation, and precipitation (water budget), inflow and outflow, water level data, temperature stratifications, density stratifications is a challenging task. However, accurate results can

be obtained from such mathematical models. Precipitation and evaporation, inflow, outflow effects were not considered in this study. Hydrodynamic behavior has a significant dependency on turbulence movements due to inflow and outflow specifically.

10 CONCLUSIONS AND RECOMMENDATIONS

In this study, hydrodynamic circulation in lake Bolmen simulated with the TELEMAC 2D software. Wind-induced currents predominate the transport and mixing mechanisms. Wind influences can be steady or transient in nature, resulting in complicated hydrodynamic behaviors within the lake. The wind is the main force which determines the flow conditions in the lake studied and drives the flow-passing through. Simulation results have shown that wind stress applied at the surface of a basin of variable depth sets up a circulation pattern characterized by relatively identifiable lake currents in the direction of the wind. For uniform wind direction after approximately after two days water currents almost gave steady stable behavior, on average, with steady model of Bolmen Lake, driven by steady and wind, It should be noted that the inflow and out of the lake was not considered in the simulation. The Coriolis force on this forced flow pattern are relatively minor.

Directional variation of the wind simulation shown that the wind blowing from the south of the lake have higher effect in forming faster advective currents and speed mixing effects. Tracer analytics providing good evidence for this conclusion. Furthermore, the magnitude variation in the wind speed have direct correlation with the water speed at the surface level. It can be seen that exponential increment of surface speed of lake The Stratified lake condition in lake Bolmen assumed to be extend for 10 m in water depth and simulation was carried out. However the measured wind speed are relatively lesser than the lake without stratification. Tracer analytic shows higher capturing time for stratified condition than the non-stratified condition, therefor supports the experimental evidence.

The experimental results show that wind configurations influence the transport and mixing processes in Lake Bolmen. The behavior of induced currents is affected by both the magnitude and direction of the wind. In future investigations, the information gained in wind-induced currents can be linked to water quality aspects. brownification in the

Bolmen, in particular, may be related to sediment mixing and transport mechanisms. Not only that, but wind-induced currents may contribute to eutrophication and algae development in the lake. The results show how hydrodynamic behavior in certain events, such as storms, stratification may be anticipated. Wind barriers in certain direction will be affecting the lakes hydrodynamic behavior for some degree.

11 LIST OF REFERENCES

Agrawal, S. (1999) *Limnology*. New Delhi, A.P.H. Pub. Corp.

Alfred Wiiest, A.L., 2003. *Small-Scale Hydrodynamics In Lakes*.

Anis A, M.J.J.P., 1995. Surface wave-turbulence interactions—scaling nearthe sea-surface. *Oceanogr. 25:2025—45*.

Anon., 2000. http://www.epa.state.il.us/water/conservation/lake-notes/lake-stratification-and-mixing/lake-stratification.pdf. [Online] [Accessed 2021].

Anon., 2020. www.zurich.com. [Online] Available at: https://www.zurich.com/knowledge/topics/windstorms/hurricanes-typhoons-and-tropical-cyclones-whats-the-difference [Accessed May 2021].

Attar, S. and Li, S., 2012. Momentum, Energy And Drag Coefficients For Ice-Covered Rivers. River Research and Applications, 29(10), pp.1267-1276.

Azizian, Asghar. (2017). Application of QGIS in Water Sciences and Engineering (In Persian).

Baduna, M. and Önder, 2004. *Numerical Study of Wind-Induced Currents in Enclosed Homogeneous Water Bodies*. Turkish J. Eng. Env. Sci., pp.28 (2004) , 207 { 221.

Bengtsson, L., 1978. Wind Induced Circulation In Lankes. *Nordic Hydrology*, 9, pp.75-94.

Bengtsson, L., Hellström, T. and Rakoczi, L., 1990. *Redistribution of sediments in three Swedish lakes*. Hydrobiologia, 192(2-3), pp.167-181.

Blottiere, L., 2016. The effects of wind-induced mixing on the structure and. Lund: Université Paris-Sud.

Borgström, A., 2020. *Lake Bolmen Past , Present and Future*. Lund University.

C.W.Fetter, 2001. *Applied Hydrogeology*. 4th ed. PrenticeHall.

Commerce, U.S.D.o., 02/26/2021. *National Oceaninc and Atmospheric Administration, U.S Department of Commerce*. [Online] Available at: https://oceanservice.noaa.gov/welcome.html [Accessed 2021].

Cloutman, L. & Eoll, J. (1976) *Comments on the diffusion model of turbulent mixing*. The Astrophysical Journal. [Online] 206548. Available from: doi:10.1086/154411.

Csanady, G. (1963) *Turbulent diffusion in Lake Huron*. Journal of Fluid Mechanics. [Online] 17 (03), 360. Available from: doi:10.1017/s0022112063001403.

Chorda, J., Maubourguet, M., Roux, H., Larinier, M., Tarrade, L. and David, L., 2010. *Two-dimensional free surface flow numerical model for vertical slot fishways*. Journal of Hydraulic Research, 48(2), pp.141-151.

Dalem. Roberts, J.I., n.d. *Lake Number, a Quantitative Indicator of Mixing Used to Estimate Changes in Dissolved Oxygen*. Centre for Water Research, University of Western Australia, Nedl Docs.qgis.org. 2021. QGIS Plugins. [online] Available at: <https://docs.qgis.org/2.8/nl/docs/user_manual/plugins/plugins.html> [Accessed 11 June 2021].ands WA 6009.

Dieter M.Imboden , A. Wuest, 1995. *Mixing Mechanism in Lakes*. NewYork: Springer Verlag.

Ermilov, A.A., 2018. *Numerical simulation of sediment flushing in reservoirs*. Norwegian University of Science and Technology.

George J. Arcement, Jr., Verne R. Schneider, 1989. *Guide for Selecting Manning's Roughness Coefficients for Natural Channels and Flood Plains*. 2339th ed. U.S. Geological Survey, Information Services.

Hamrin, S. F. (1979), Bolmen - Bolmån - Lagan: Resultat från limnologiska undersökningar under 1976 - 1978 med en sammanfattning av resultaten från åren 1966 - 1975. Undersökningen utförd i smaband med AB Sydvattens projektering för Skånes framtida vattenförsörjning, Technical report, Institute of Limnology, Univeristy of Lund, Lund.

Hutchinson, G., 1941. Limnological Studies in Connecticut: IV. The Mechanisms of Intermediary Metabolism in Stratified Lakes. Ecological Monographs, 11(1), pp.21-60.

He, C. and Rochfort, Q., 2011. Numerical Modelling Approaches for Assessing Improvements to the Flow Circulation in a Small Lake. Modelling and Simulation in Engineering, 2011, pp.1-21.

How and Why Lakes Stratify and Turn Over: We explain the science behind the phenomena – IISD Experimental Lakes Area. (2021). Retrieved 30 May 2021, from https://www.iisd.org/ela/blog/commentary/lakes-stratify-turn-explain-science-behind-phenomena/

Jin, KR & Ji, ZG & Hamrick, JH. (2002). Modeling winter circulation in Lake Okeechobee, Florida. Journal of Waterway Port Coastal and Ocean Engineering. 128. 114-125. 10.1061/(ASCE)0733-950X(2002)128;3(114).

Kang-Ren Jin, M.A.D.S., 2007. Sediment Resuspension and Hydrodynamics in Lake Okeechobee during the Late Summer. Journal Of Engineering Mechanics © Asce.

Klante, C., 2018. Sediment transport and bathymetric change at Hornafjörður tidal inlet. Lund.

Krisztián Homoródi ,János Józsa , Tamás Krámer, 2012. On the 2D modelling aspects of wind-induced waves in shallow,fetch-limited lakes. *c Periodica Polytechnica 2012*, pp.127-40.

Ladwig R., Heinrich L., Singer G., Hupfer M, 2017. Assessment of the spatial and temporal composition of Lake Tegel's. *Environ Sci Pollut Res. 24: 25166- 25178*.

Liu, L., 2018. Application of Hydodyanmica nd water quality Model for Inland Surface Water Systems. http://dx.doi.org/10.5772/intechopen.7491.

Lorrai, C., Umlauf, L., Becherer, J. & Lorke, A. et al. (2011) Boundary mixing in lakes: 2. Combined effects of shear- and convectively induced turbulence on basin-scale mixing. Journal of Geophysical Research. [Online] 116 (C10). Available from: doi:10.1029/2011jc007121.

Livingstone, D. (1977) Golterman, H. L. 1975. Physiological limnology. Elsevier Sci. Publ. Co., Amsterdam, Oxford, and New York, xiii + 489 p. $51.95; Dfl 125. Limnology and Oceanography. [Online] 22 (5), 973-974. Available from: doi:10.4319/lo.1977.22.5.0973.

Lick, W., 1976. Numerical Modeling of Lake Currents. pp.49-74.

Marion, A., 2008. Physical Transport Processes in Ecology: Advection, Diffusion, and Dispersion. Encyclopedia of Ecology.

Mofidi, J. and Rashidi Ebrahim Hesari, A., 2018. Numerical Simulation of the Wind-Induced Current in the Caspian Sea. International Journal of coastal and offshore engineering, 2(1), pp.67-77.

Nrc.canada.ca. 2021. Blue Kenue ™: software tool for hydraulic modellers. [online] Available at: <https://nrc.canada.ca/en/research-development/products-services/software-applications/blue-kenuetm-software-tool-hydraulic-modellers> [Accessed 29 May 2021]

Ottesen Hansen, N. (1978) Mixing Processes in Lakes. Hydrology Research. [Online] 9 (2), 57-74. Available from: doi:10.2166/nh.1978.0006.

Nrc.canada.ca. 2021. Blue Kenue™: software tool for hydraulic modellers. [online] Available at: <https://nrc.canada.ca/en/research-development/products-services/software-applications/blue-kenuetm-software-tool-hydraulic-modellers> [Accessed 11 June 2021].

Olamide, O., 2021. GIS Programming : QGIS Software - Geoinfotech. [online] Geoinfotech. Available at: <https://geoinfotech.ng/gis-programming-qgis-software/> [Accessed 11 June 2021].

Parker, D., 2003. *Mesoscale Meteorology* | Overview. Encyclopedia Of Atmospheric Sciences, (ISBN 9780122270901).].

Peeters, F., Wüest, A., Piepke, G. & Imboden, D. (1996) Horizontal mixing in lakes. Journal of Geophysical Research: Oceans. [Online] 101 (C8), 18361-18375. Available from: doi:10.1029/96jc01145.

Paul Fafard, May 16, 2018. https://www.iisd.org/ela/blog/commentary/lakes-stratify-turn-explain-science-behind-phenomena/. [Online] [Accessed 07 May 2021].

Prandle, D. and Matthews, J., 1990. The dynamics of nearshore surface currents generated by tides, wind and horizontal density gradients. *Continental Shelf Research*, 10(7), pp.665-681.

Peeters, F., Wüest, A., Piepke, G. & Imboden, D. (1996) Horizontal mixing in lakes. Journal of Geophysical Research: Oceans. [Online] 101 (C8), 18361-18375. Available from: doi:10.1029/96jc01145.

R. Thomas, M.M.A.B., 1996. Water Quality Assessments - A Guide to Use of Biota, Sediments and Water in Environmental Monitoring - Second Edition. *UNESCO/WHO/UNEP*.

Reynolds, Deb & Reynolds, John. (2006). Reynolds, J.W. and D.W. Reynolds. 2006. Sobre algunas lombrices de tierra (Oligochaeta) de Honduras, C.A. Medadrilogica 10(11): 87-91. Appendices

Robertson, D. & Imberger, J. (1994) Lake Number, a Quantitative Indicator of Mixing Used to Estimate Changes in Dissolved Oxygen. Internationale Revue der gesamten Hydrobiologie und Hydrographie. [Online] 79 (2), 159-176. Available from: doi:10.1002/iroh.19940790202.

Scott A. Socolofsky , Gerhard H. Jirka, 2004. *https://ceprofs.civil.tamu.edu/kchang/ocen689/ocen689ch9.pdf*. [Online] [Accessed April 2021].

Søndergaard, Martin & Jensen, Jens & Jeppesen, Erik. (2003). *Role of Sediment and Internal Loading of Phosphorus in Shallow Lakes. Hydrobiologia*. 506-509. 135-145. 10.1023/B:HYDR.0000008611.12704.dd.

Starosolszky, Ö., 1974. Lake Hydraulics. *Hydrological Sciences Bulletin*, 19(1), pp.99-114.

Tumdedo, M.E., 2010. *Dynamics of Humic Substance in Bolmen Lund, Sweden*. Department of Building and Environmental Technology , Lund University.

Toggweiler, J.R. & Key, R.M., 2001. *Thermohaline Circulation*. Encyclopedia of Ocean Sciences, (ISBN 9780122274305)

Thomas, Daniel & Schallenberg, Marc. (2008). Benthic shear stress gradient defines three mutually exclusive modes of non-biological internal nutrient loading in shallow lakes. Hydrobiologia. 610. 1-11. 10.1007/s10750-008-9417-x.

Witten, A. and Thomas, J., 1976. Calculation of Steady Currents in Lake Ontario with Variable Eddy Viscosity. Journal of Great Lakes Research, 2(2), pp.357-363.

Xing, J., Davies, A. and Jones, J., 2012. Influence of sea surface wind wave turbulence upon wind-induced circulation, tide–surge interaction and bed stress. Ocean Dynamics, 62(7), pp.1017-1042.

Yunlin Zhang, Kun Shi, Xiaohan Liu, Yongqiang Zhou, Boqiang Qin, 2014. *Lake Topography and Wind Waves Determining Seasonal-Spatial Dynamics of Total Suspended Matter in*

Turbid Lake Taihu, China: Assessment Using Long-Term High-Resolution MERIS Data. Nanjing Institute of Geography and Limnology.

APPENDIX - A

BLUE KENUE SOFT WEAR APPLICATIONS

Figure A 1 Bathymetry point Data QGIS Vector representation (elevations at boundaries and within the lake basin)

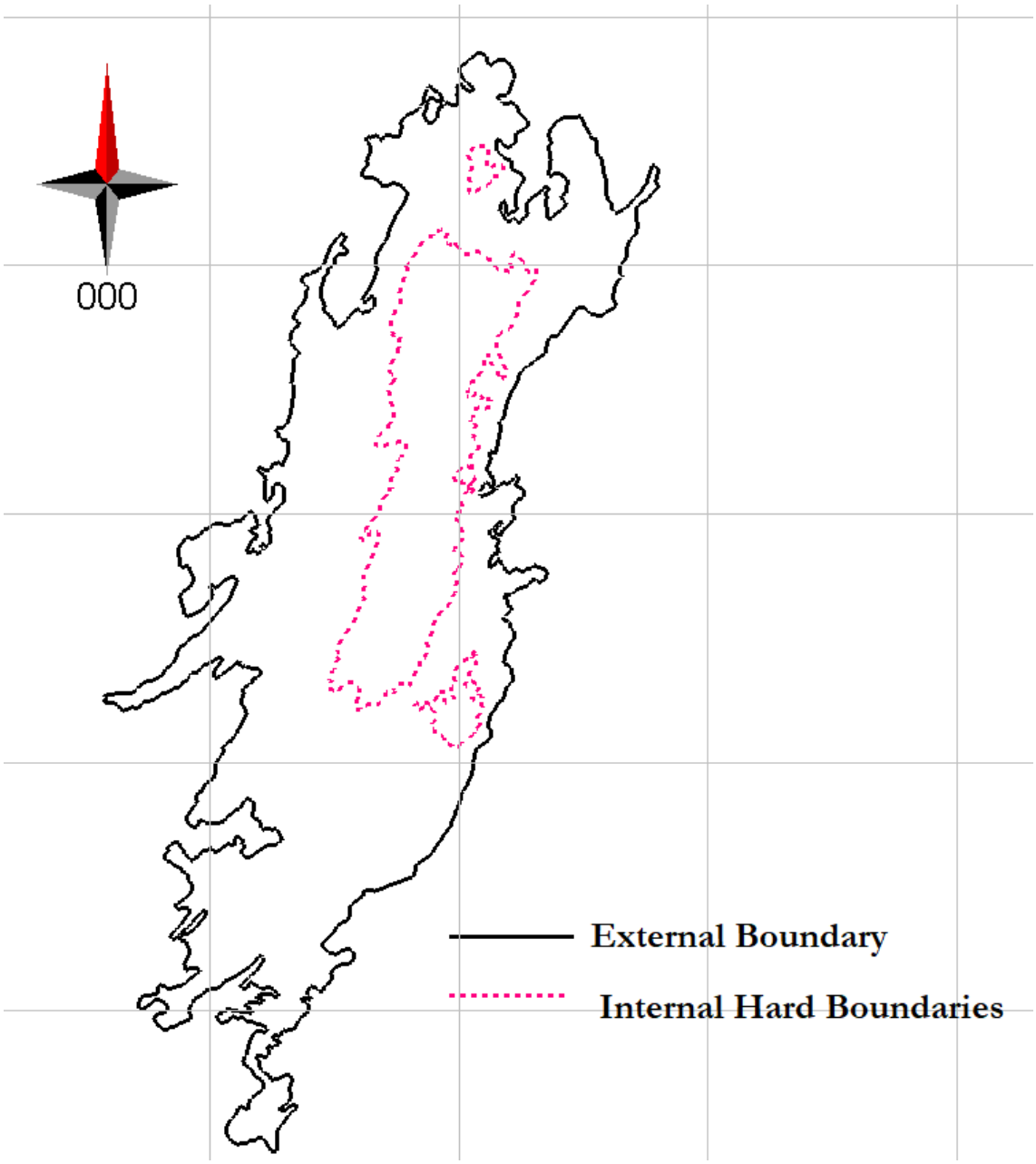

Figure A 2 Defining the Boundary of Bolmen Lake and creating Internal Hard boundaries using Blue Kenue

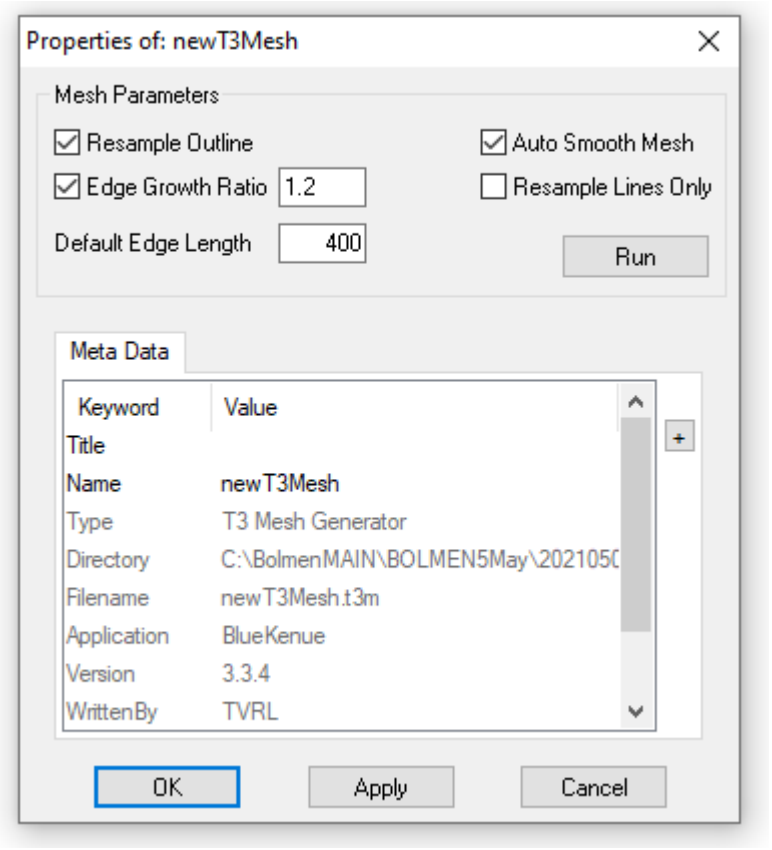

Figure A 3 Defining the Mesh parameters using Blue Kenue

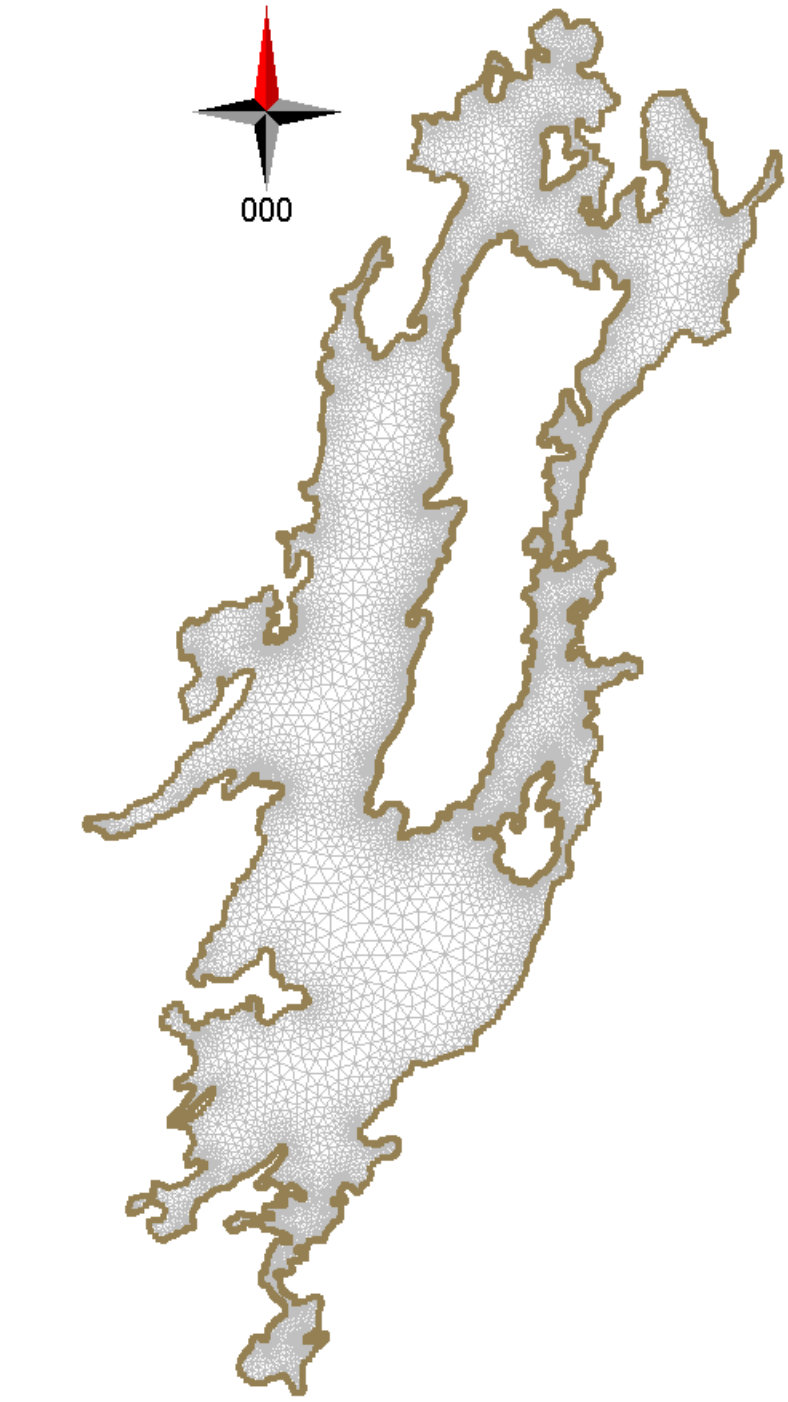

Figure A 4 Defining the no flow boundaries(non permeable) and liquid boundaries in the mesh , Blue Kenue

APPENDIX -B

SIMULATION RESULTS USING TELEMAC 2D FOR DIRECTIONAL VARIATIONS OF WIND

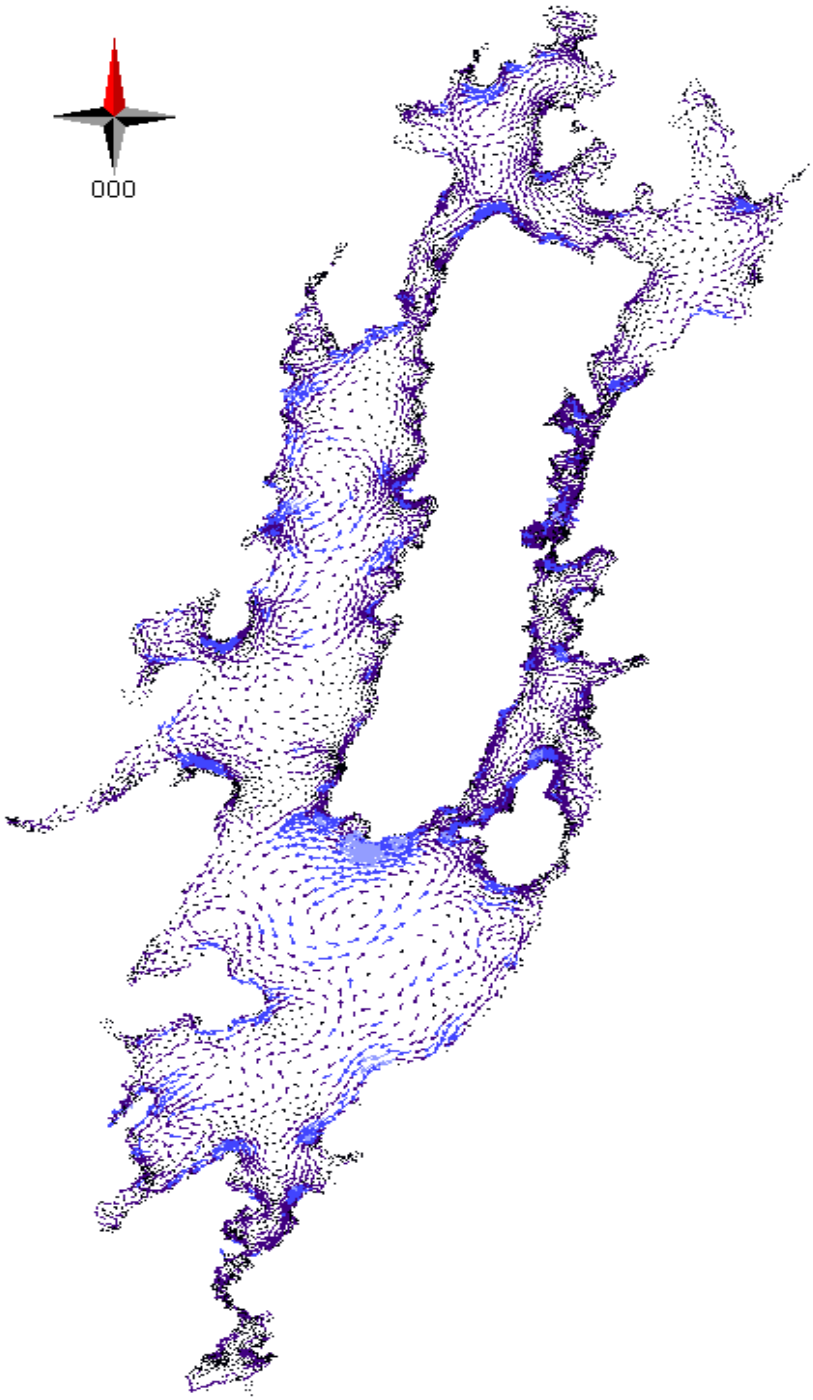

Figure A 5 Lake current patterns observed for simulating 10ms^{-1} wind from East

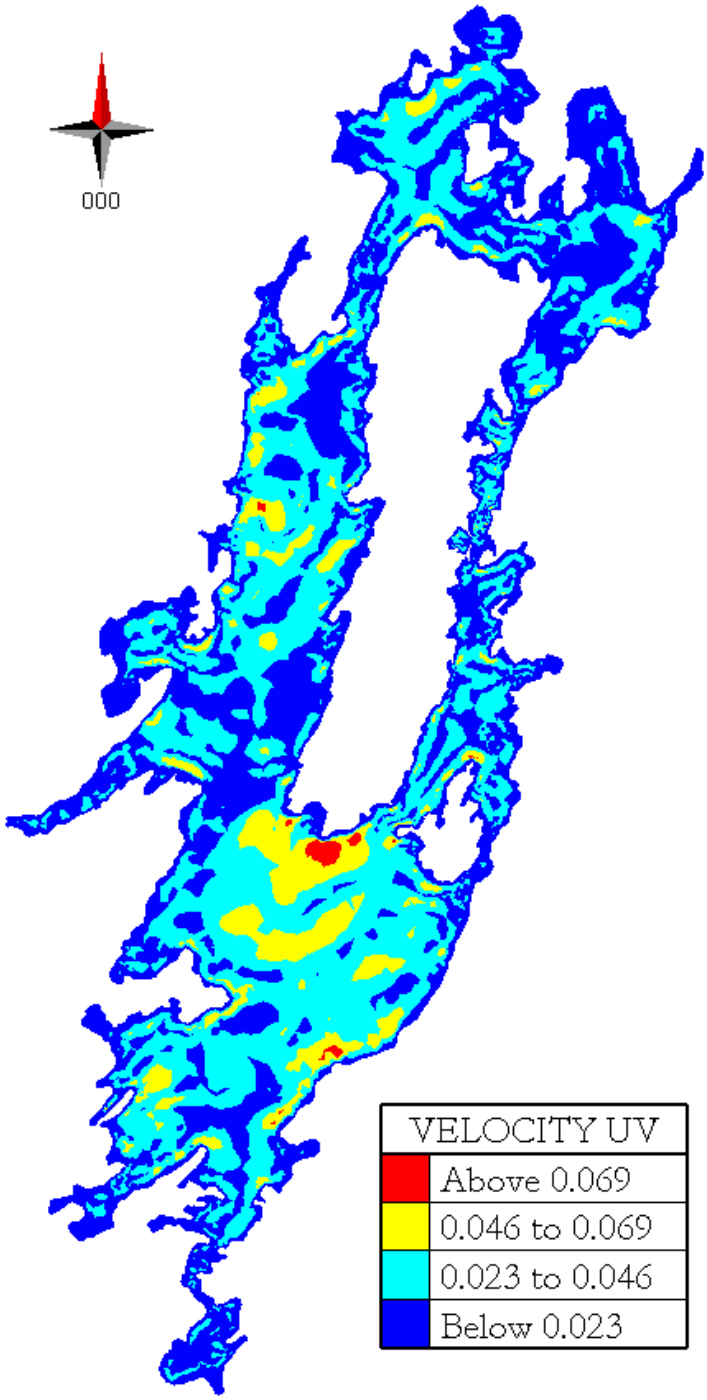

Figure A 6 Contour Scalar Velocity distribution (uv) for wind 10ms^{-1} from East Direction

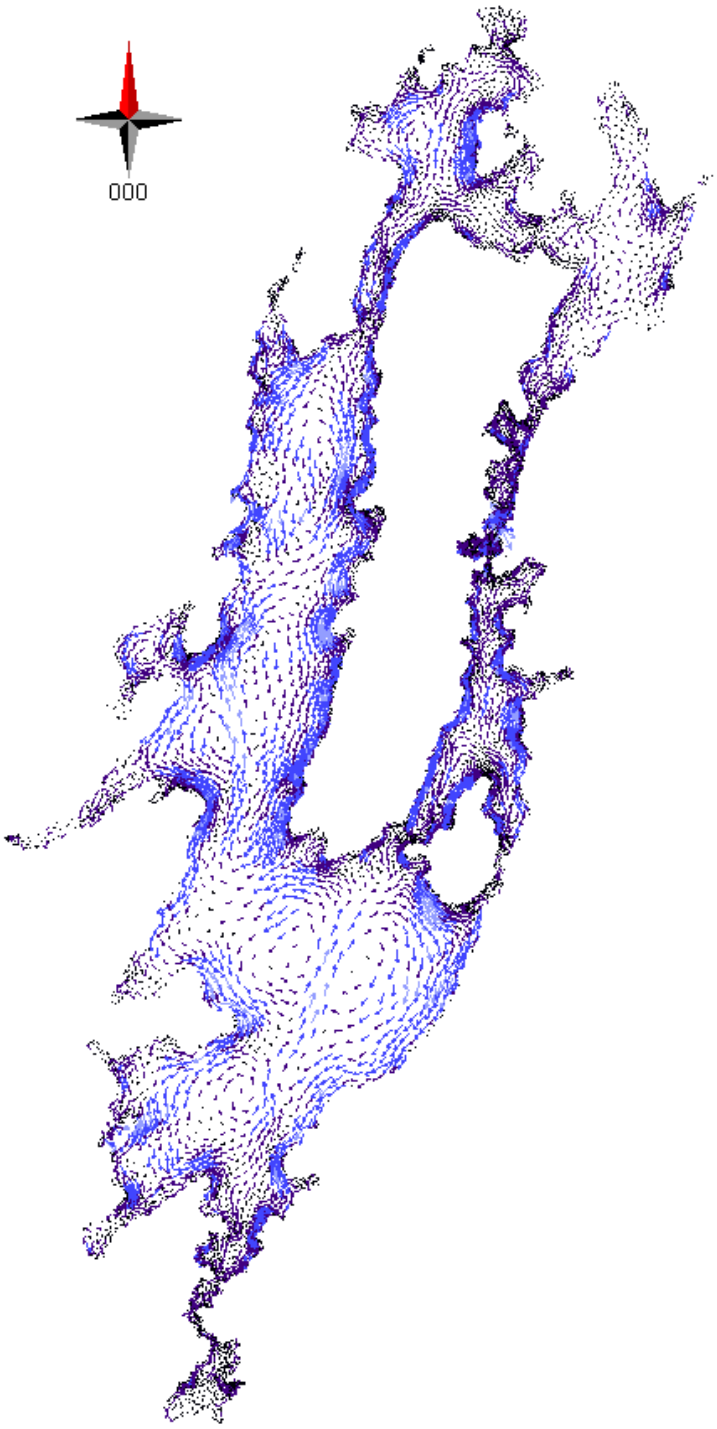

Figure A 7 Lake current patterns observed for simulating 10ms^{-1} wind from North

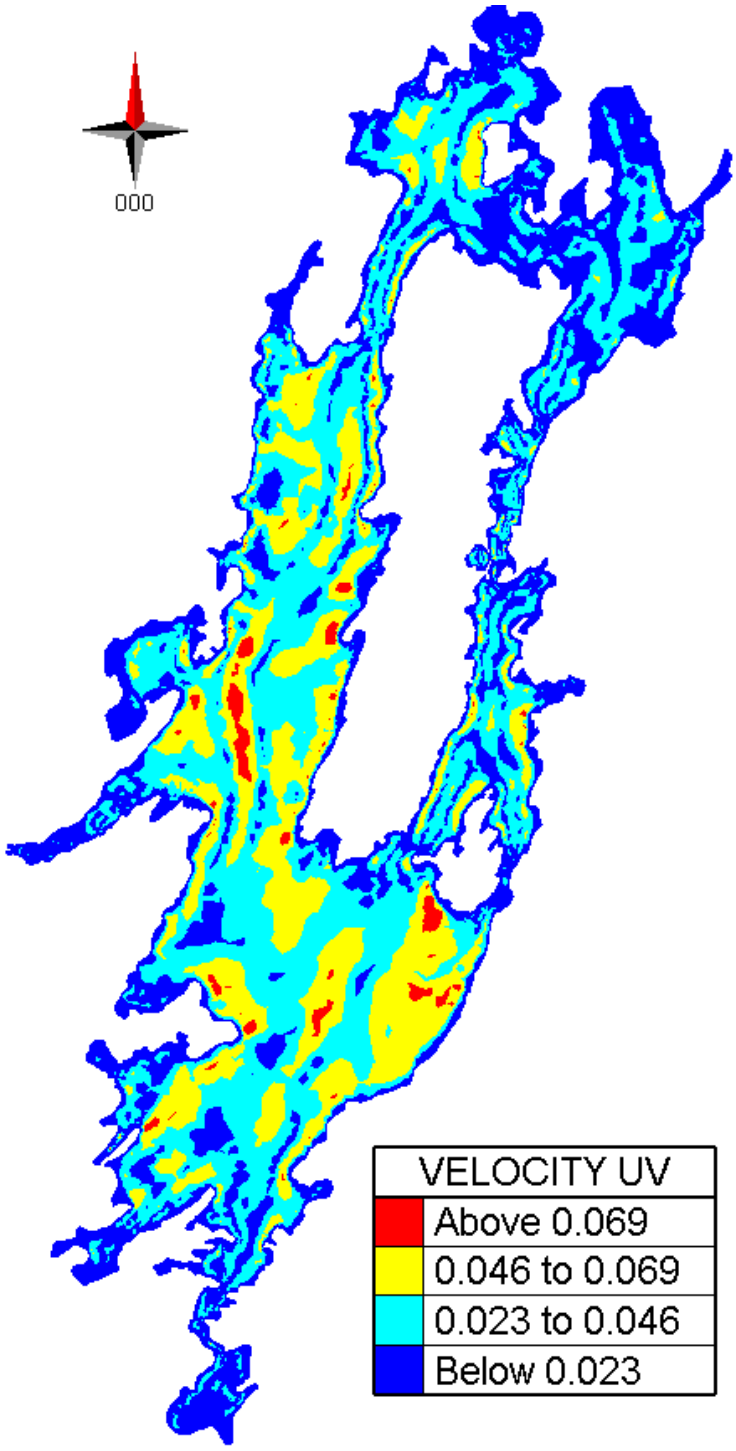

Figure A 8 Contour Scalar Velocity distribution (uv) for wind 10ms^{-1} from North Direction

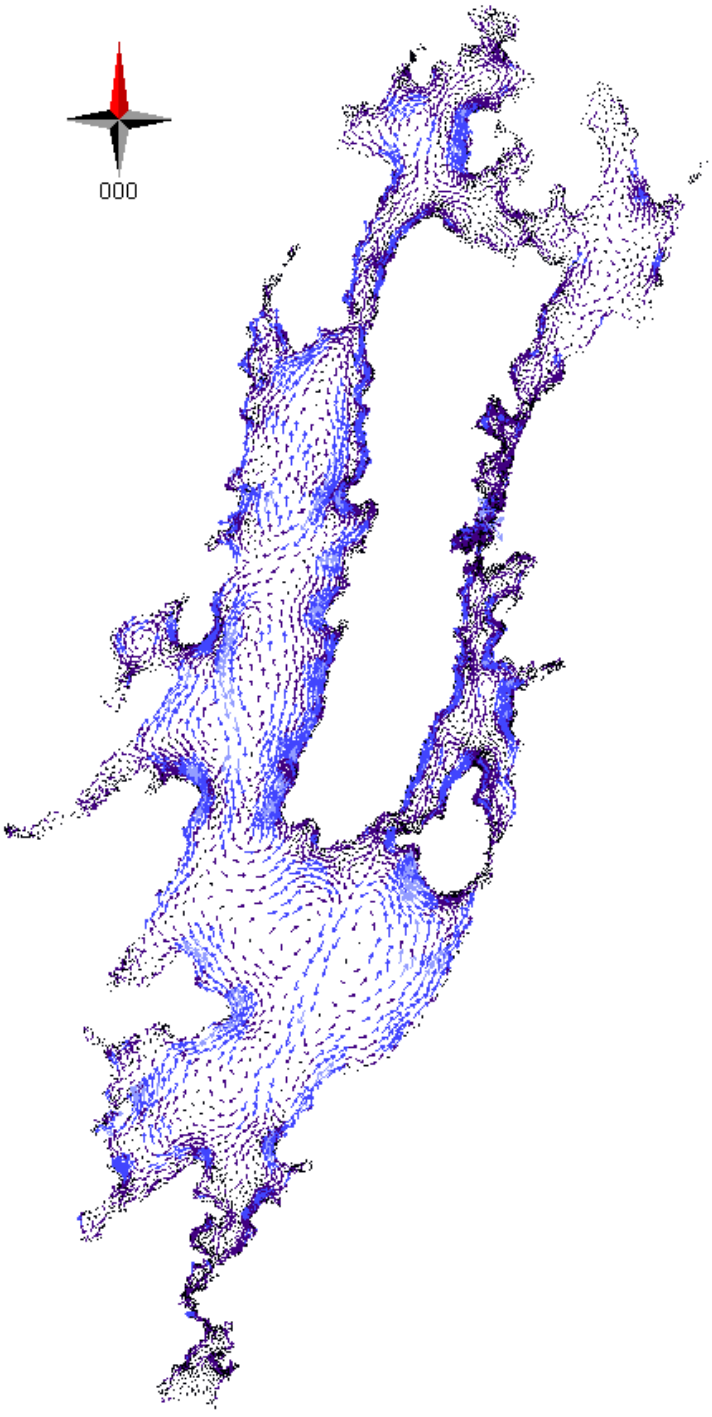

Figure A 9 Lake current patterns observed for simulating 10ms^{-1} wind from South

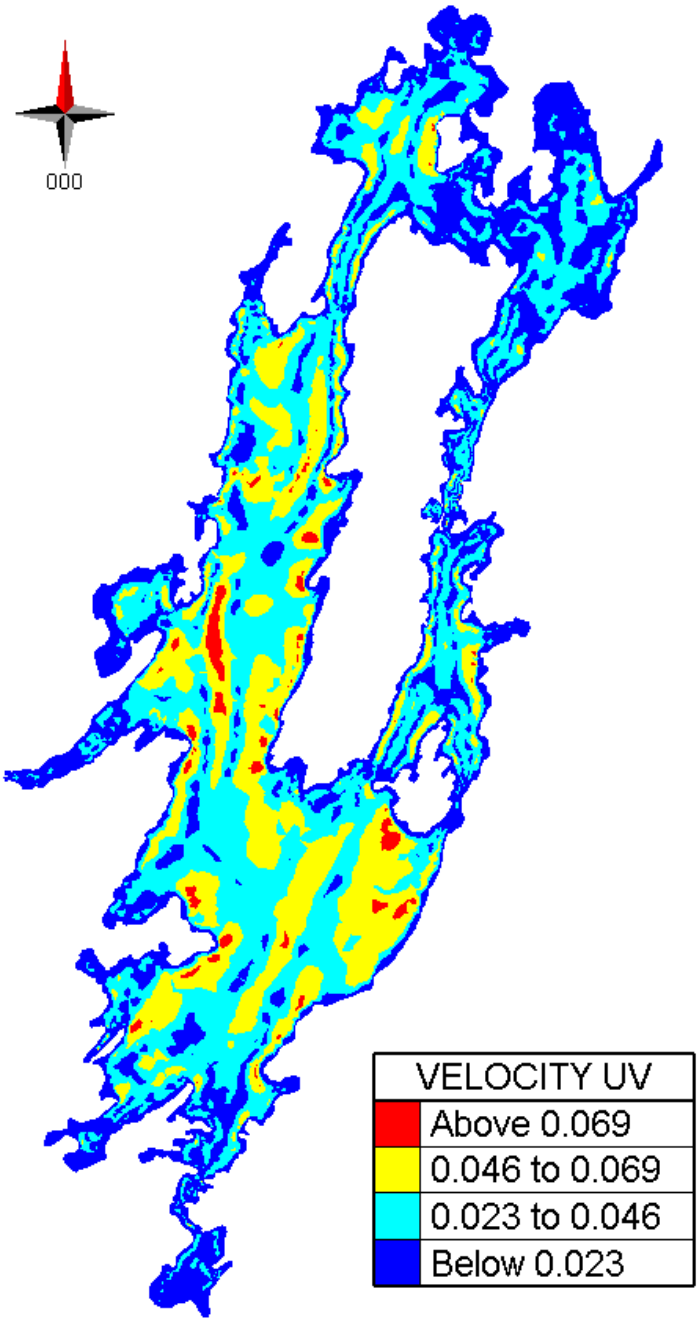

Figure A 10 Contour Scalar Velocity distribution (uv) for wind 10ms^{-1} from South Direction

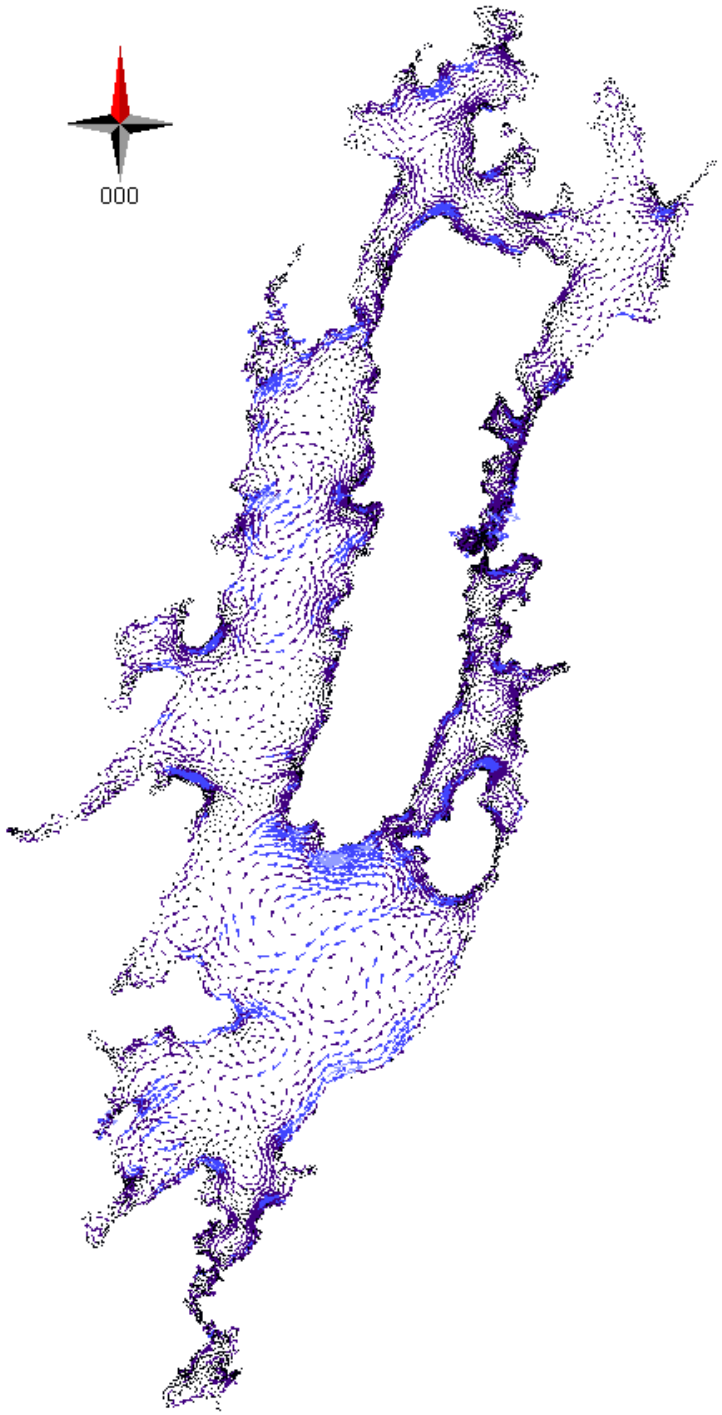

Figure A 11 Lake current patterns observed for simulating 10ms^{-1} wind from West

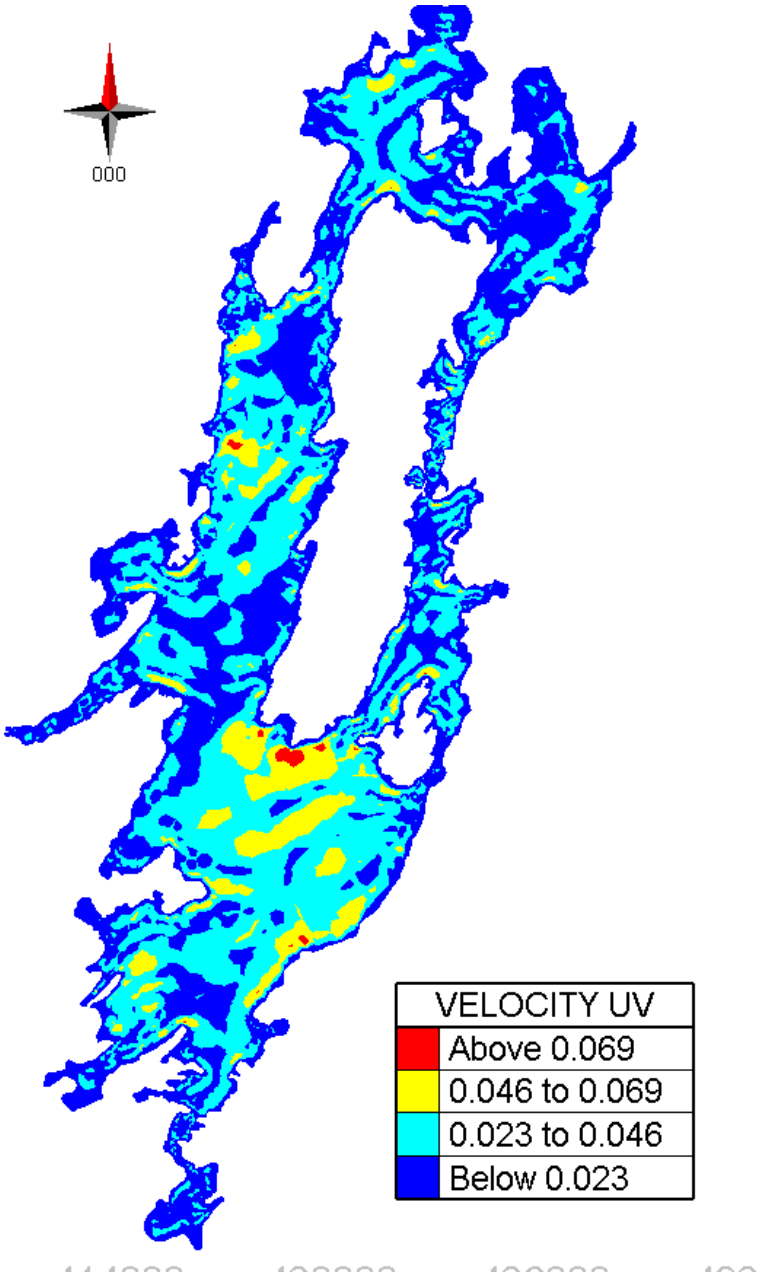

Figure A 12 Contour Scalar Velocity distribution (UV) for wind 10ms^{-1} from West Direction

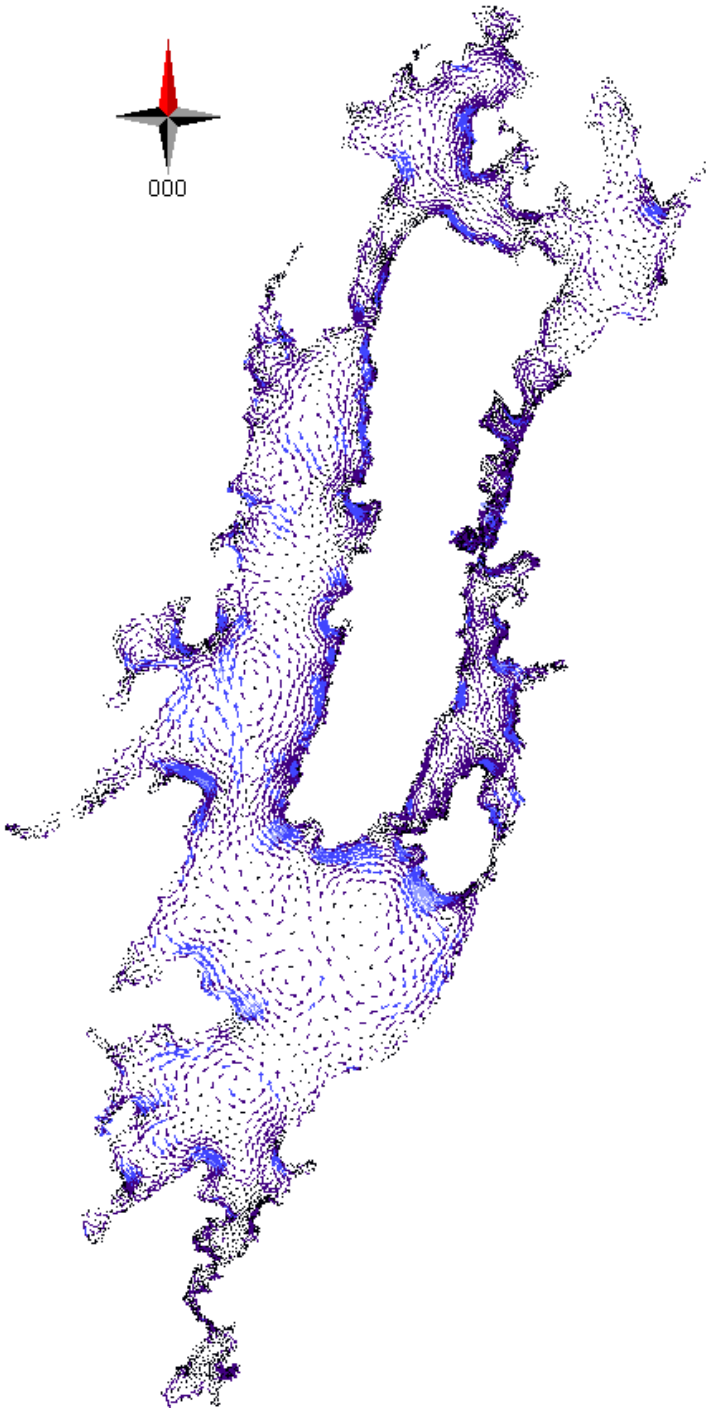

Figure A 13 Lake current patterns observed for simulating 10ms^{-1} wind from NorthWest

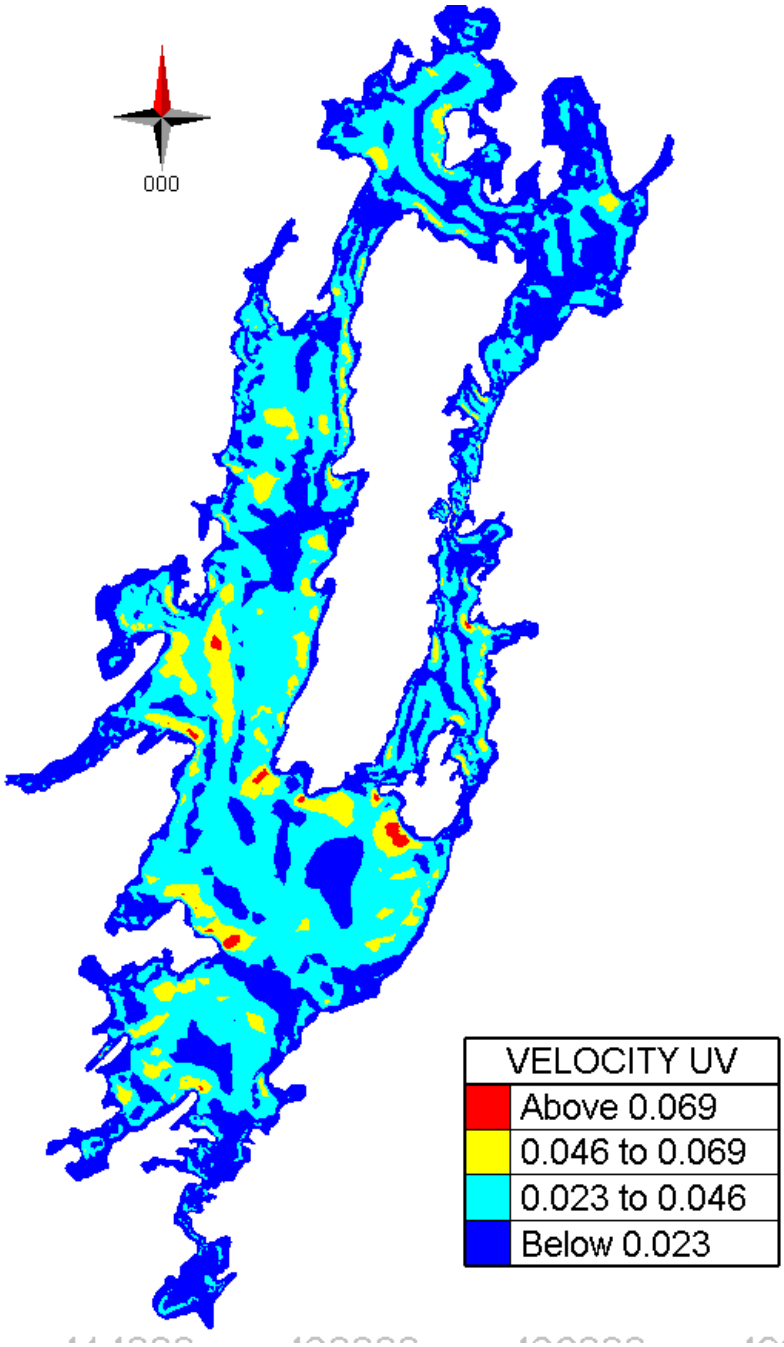

Figure A 14 Contour Scalar Velocity distribution (uv) for wind 10ms^{-1} from Northwest Direction

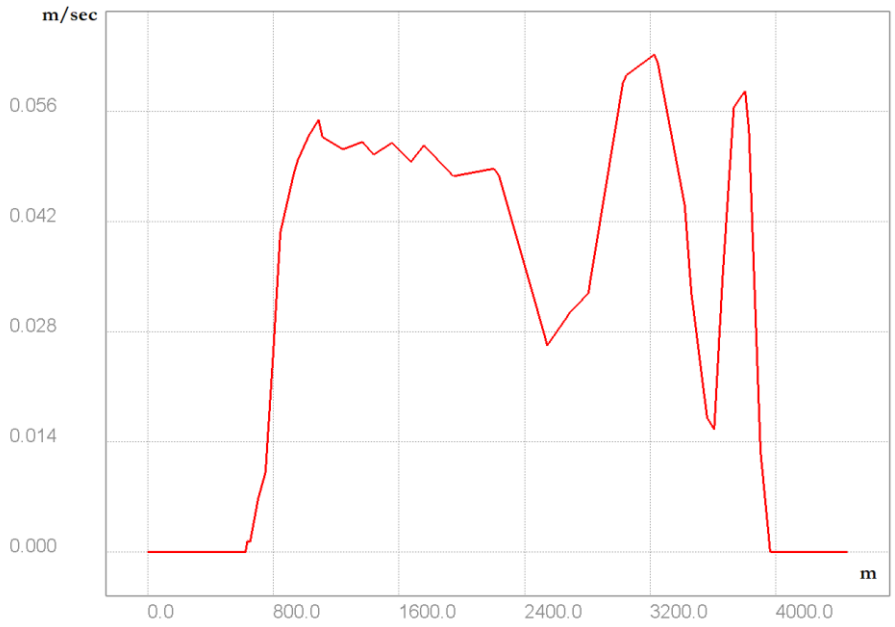

Figure A 15 Scalar velocity section profile A-A' for steady state wind 10ms^{-1} from southwest direction

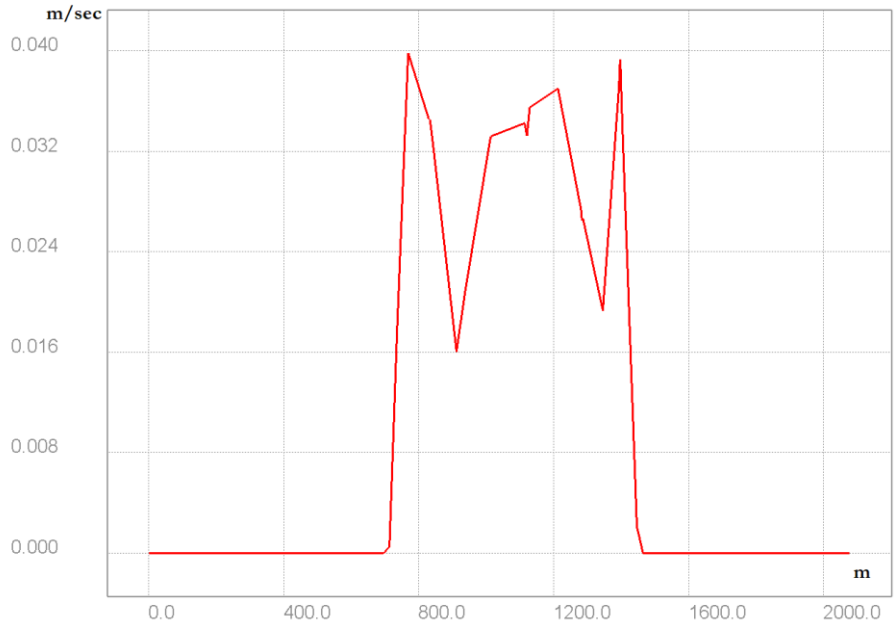

Figure A 16 Scalar velocity section profile B-B' for steady state wind 10ms^{-1} from southwest direction

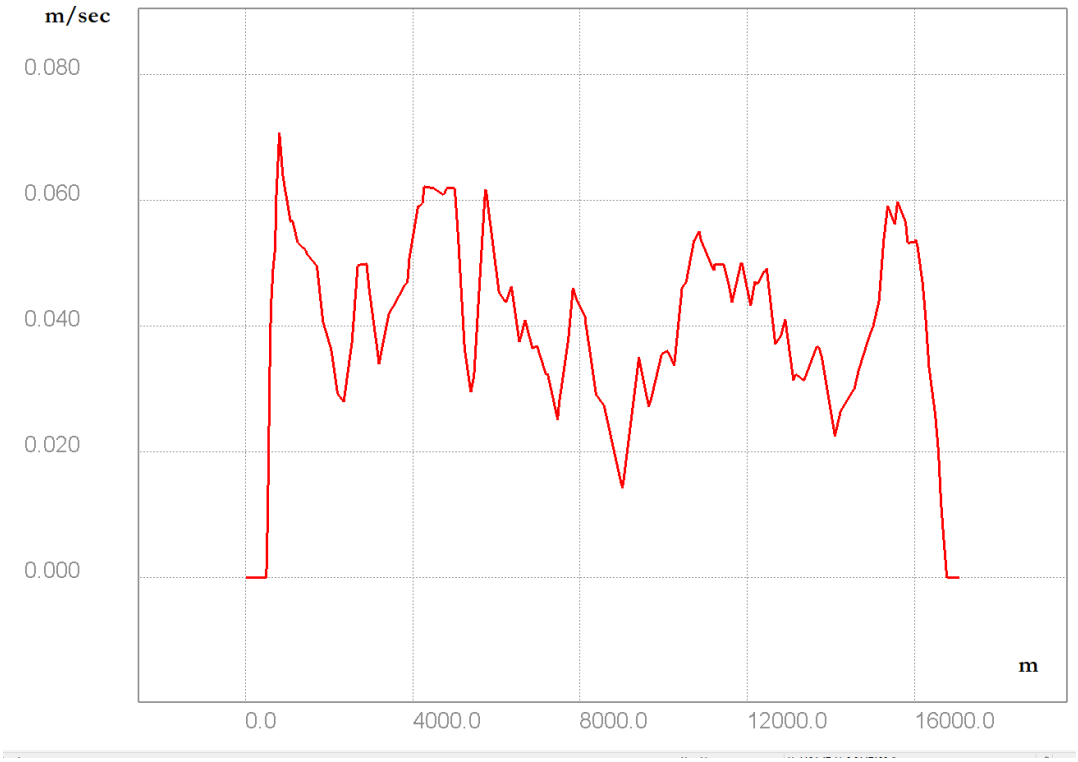

Figure A 17 Scalar velocity section profile E-E' for steady state wind 10m^{-1} from southwest direction

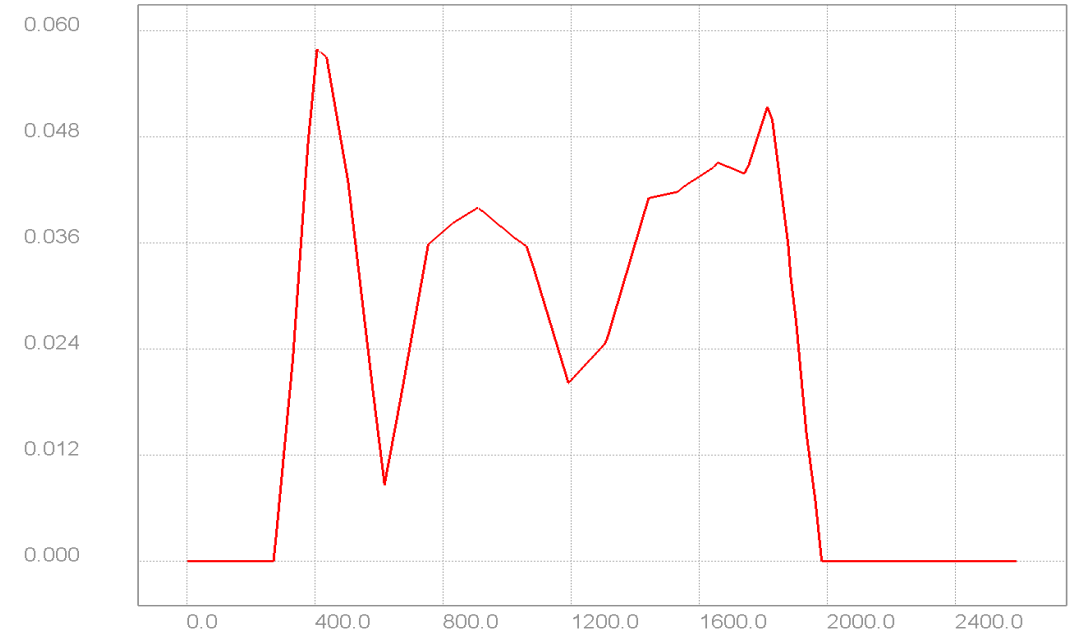

Figure A 18 Scalar velocity section profile C-C' for steady state wind 10ms^{-1} from south west direction

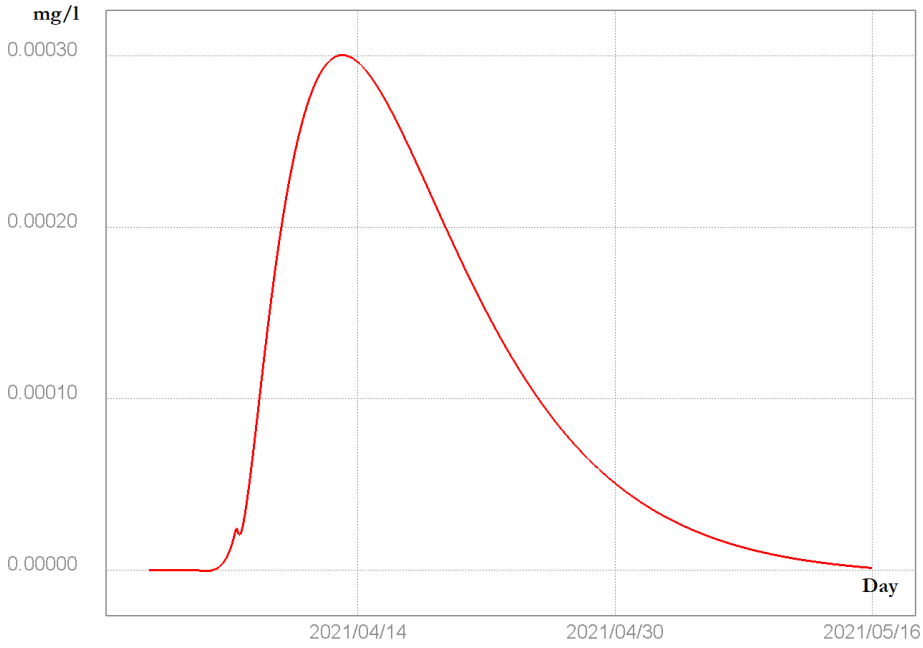

Figure A 19 Time series analysis for Tracer concentration at point 3 for the wind speed of 10ms^{-1} South West Direction

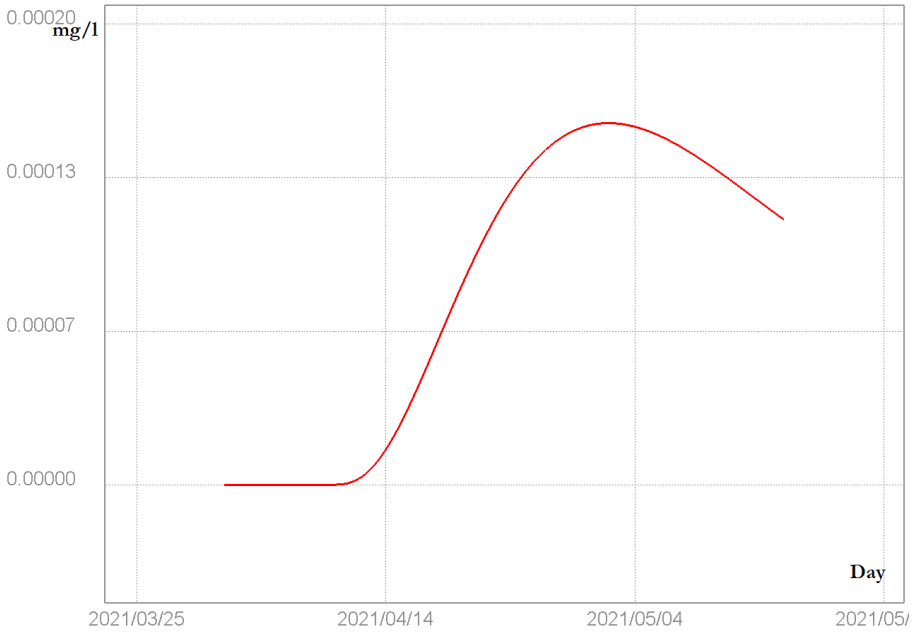

Figure A 20 Time series analysis for Tracer concentration at point 6 for the wind speed of 10ms^{-1} SouthWest Direction

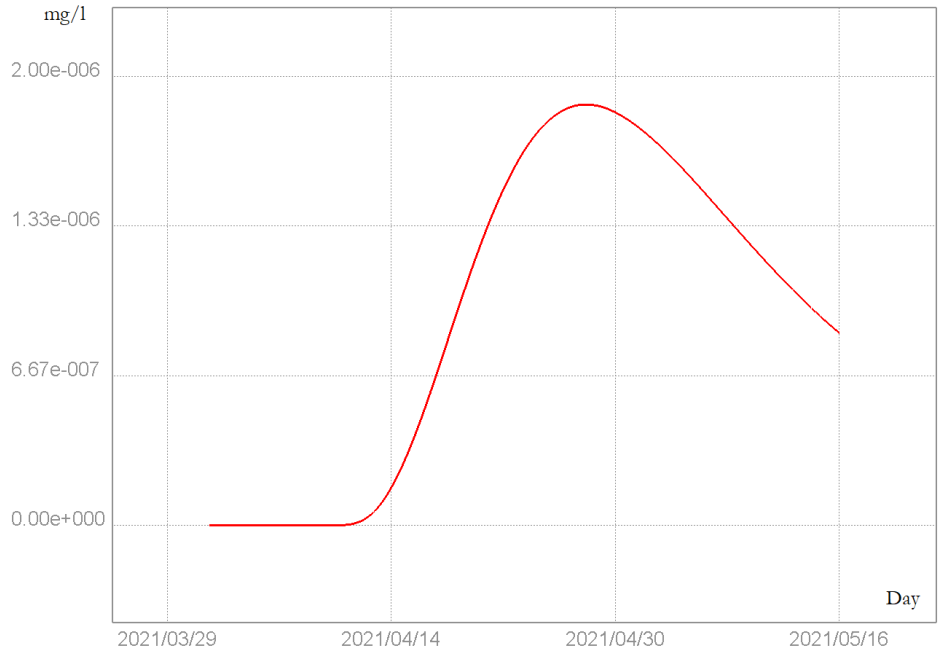

Figure A 21 Time series analysis for Tracer concentration at point 4 for the wind speed of 10ms^{-1} South West Direction

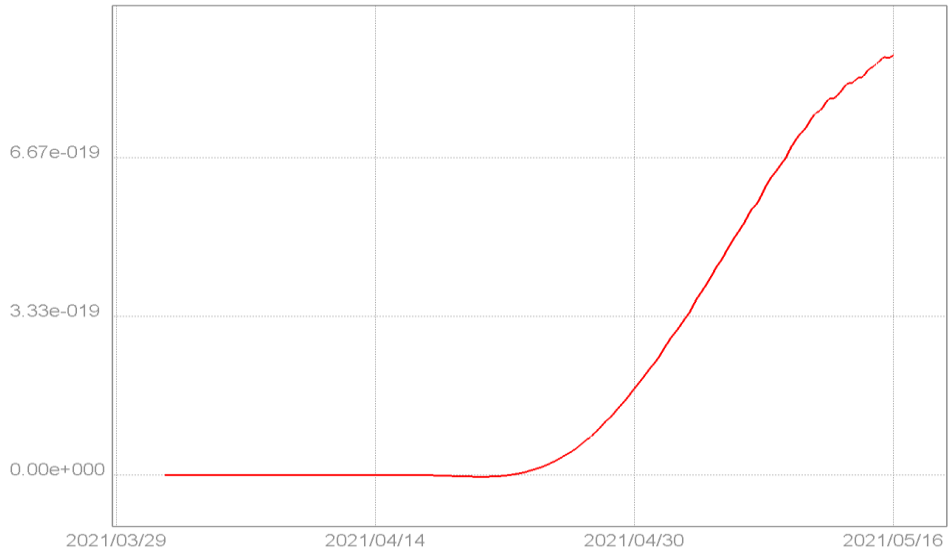

Figure A 22 Time series analysis for Tracer concentration at point 7 for the wind speed of 10ms^{-1} south-west Direction

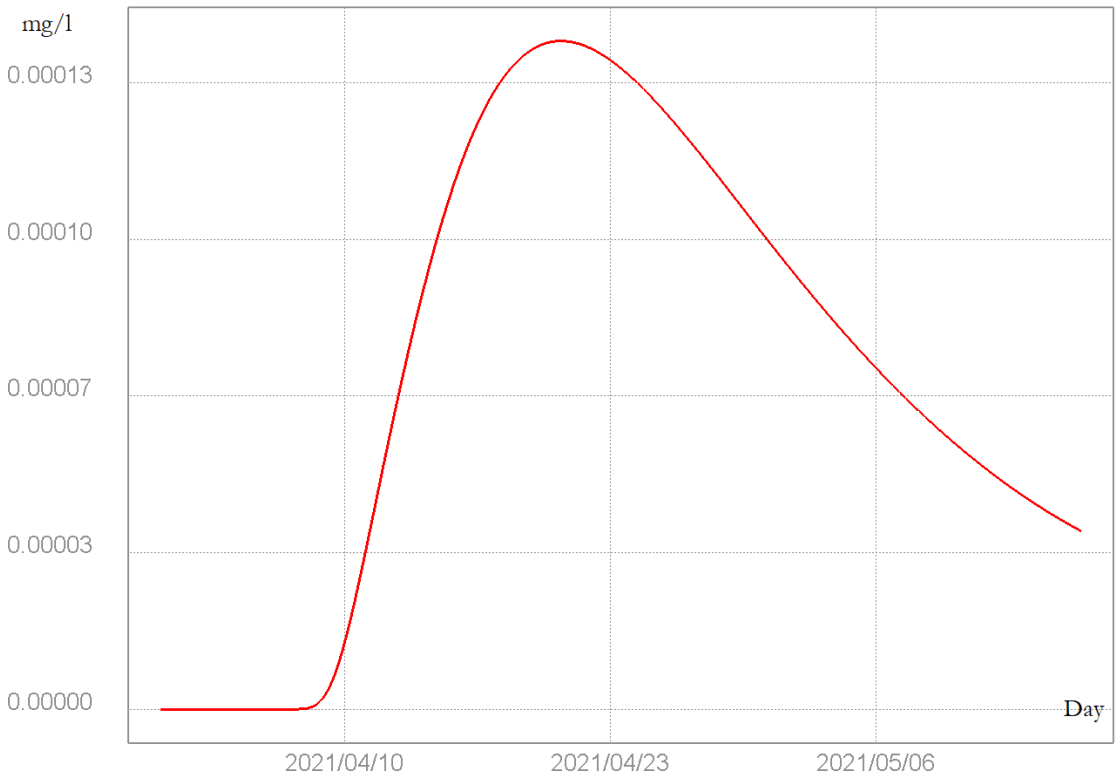

Figure A 23 Time series analysis for Tracer concentration at point 5 for the wind speed of 10ms^{-1} South West Direction

APPENDIX -C

SIMULATION RESULTS USING TELEMAC 2D FOR MAGNITUDE WIND VARIATIONS

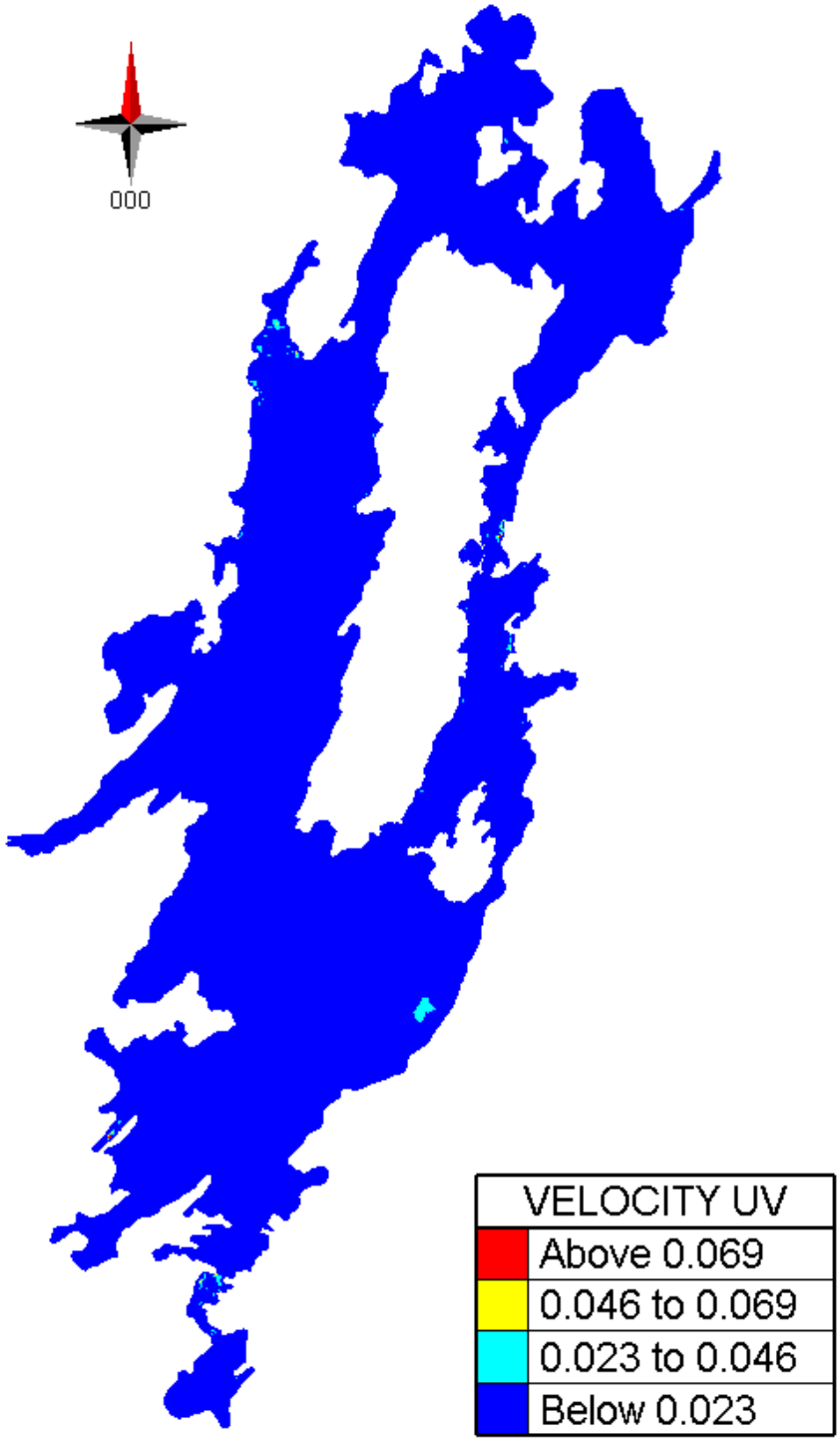

Figure A 24 Contour Scalar Velocity distribution (uv) for wind 2.5ms^{-1} from southwest Direction

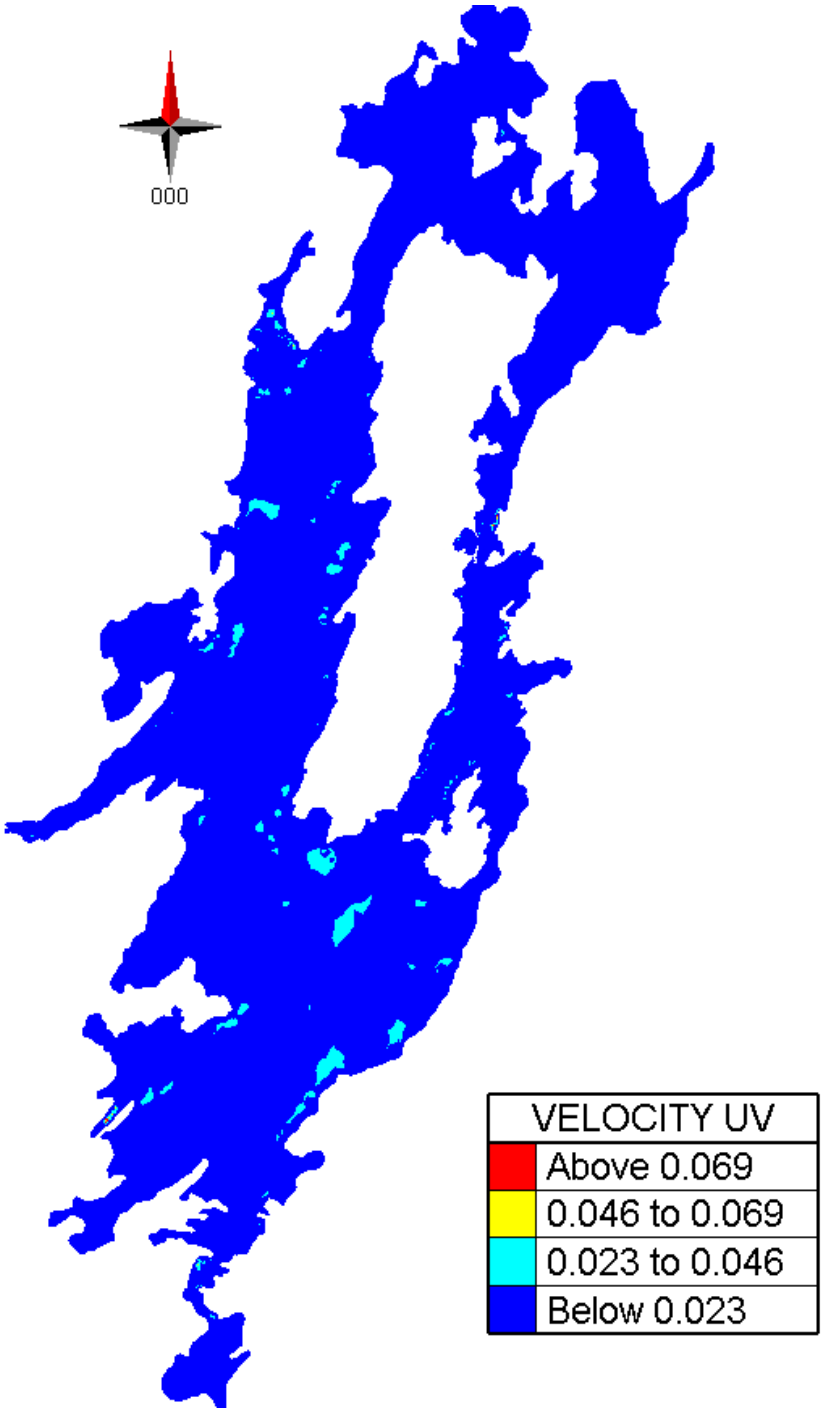

Figure A 25 Contour Scalar Velocity distribution (uv) for wind 5ms^{-1} from South West Direction

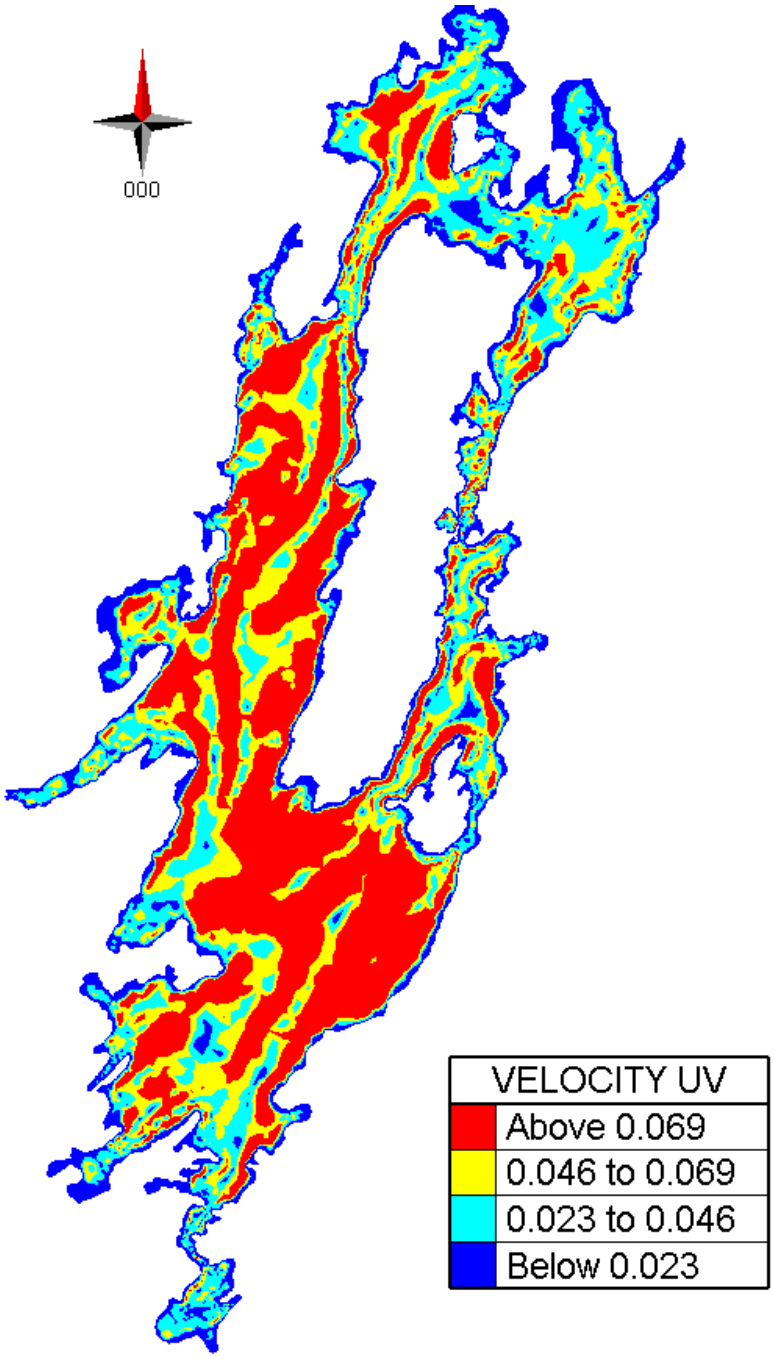

Figure A 26 Contour Scalar Velocity distribution (uv) for wind 15ms^{-1} from south-west Direction

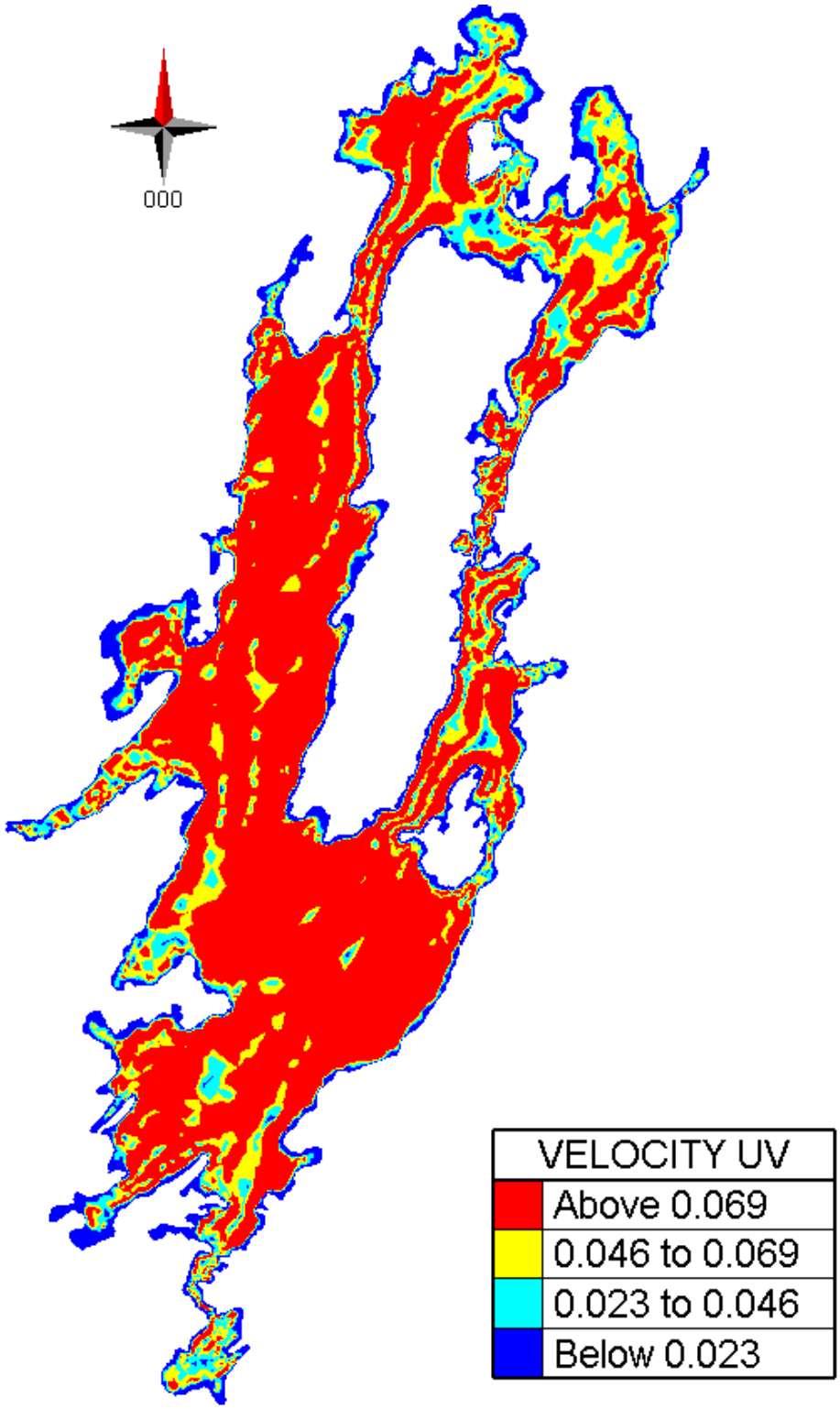

Figure A 27 Contour Scalar Velocity distribution (uv) for wind 20ms^{-1} from southwest Direction

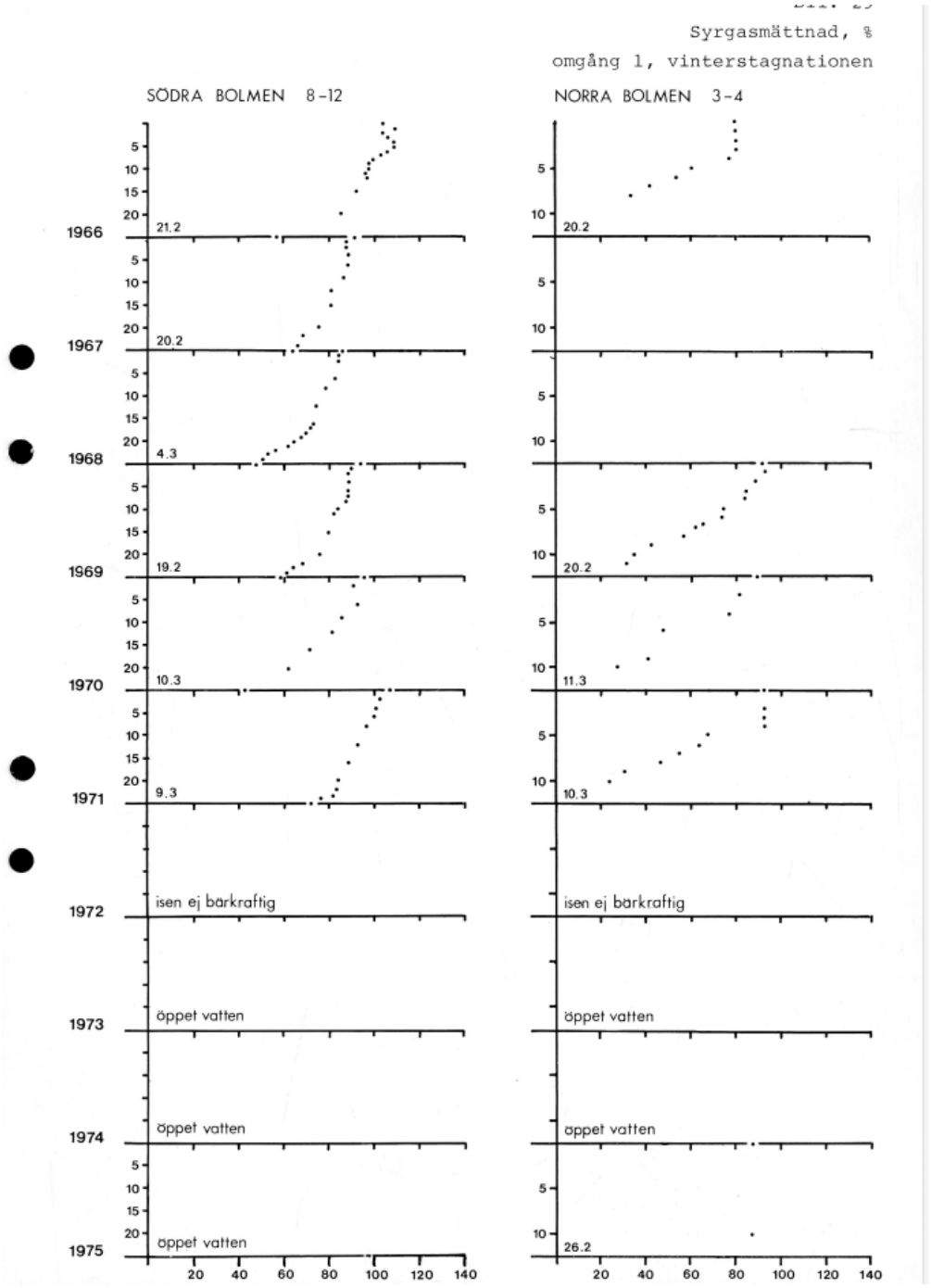

Figure A 28 Winter Stagnation in Lake Bolmen. The x-Axis is the water depth and the y-axis is the oxygen concentration in %. Source Hamrin, (1979)

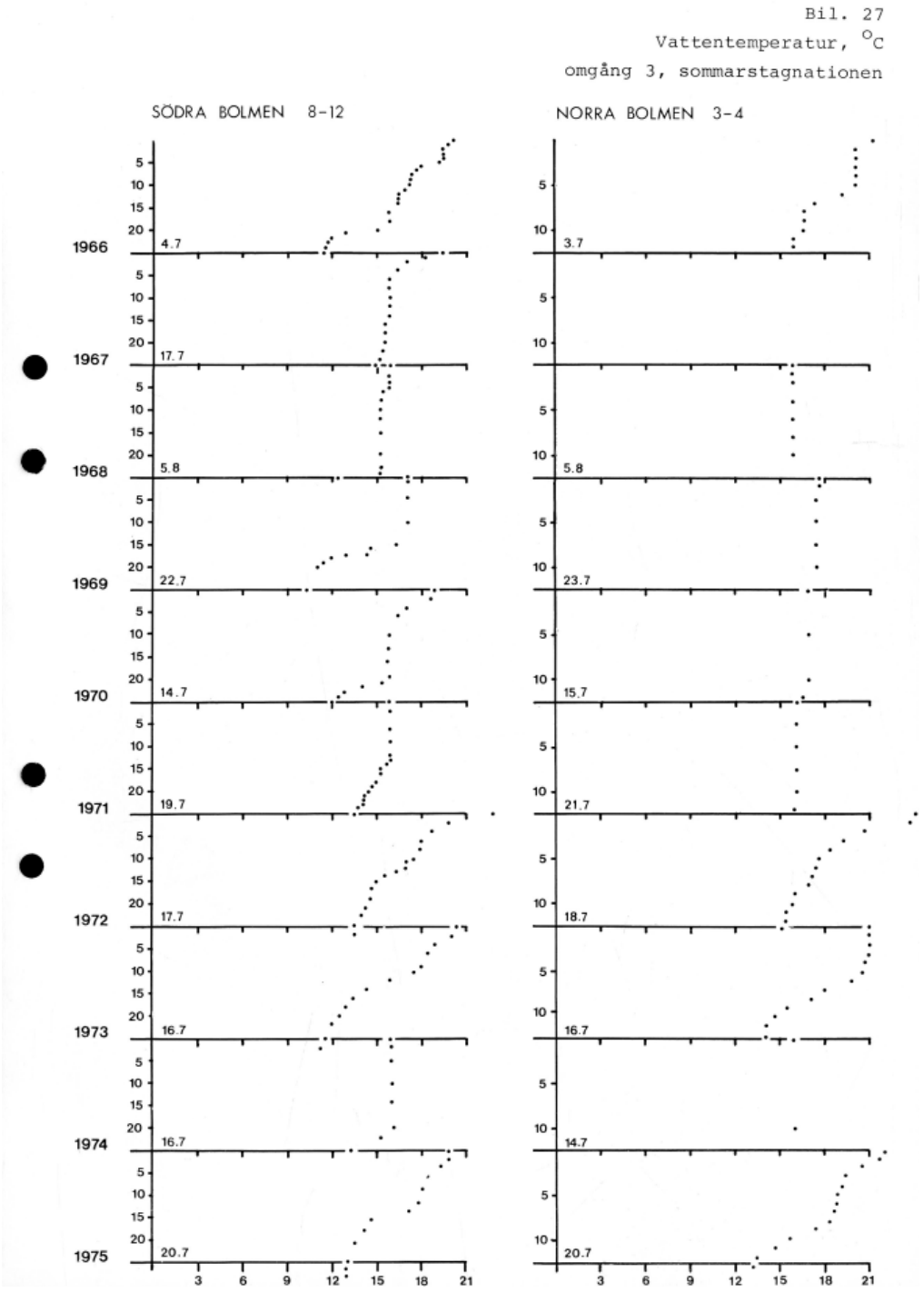

Figure A 29 Summer Stagnation in Lake Bolemn The x-Axis is the water depth and the y-axis is the degrees in C^0. Source Hamrin, (1979)